Synthesis of small-ring benzannulated triphospha-macrocycles by template methods

Wenjian Zhang

ProQuest LLC
789 East Eisenhower Parkway
P.O. Box 1346
Ann Arbor, MI 48106-1346

BINDING SERVICES
Tel +44 (0)29 2087 4949
Fax +44 (0)29 20371921
e-mail bindery@cardiff.ac.uk

Supervisor: Prof. Peter G. Edwards

Chapter 1

Introduction

Foreword

Phosphine ligands, especially tertiary phosphines, are one of the most common and important classes of ligand in organometallic and coordination chemistry.[1-6] Transition metal phosphine complexes have broad application in, for example, catalysis, biomedical imaging and medical therapy. The field of phosphine ligands and their metal complexes is still growing rapidly due to their academic and industrial importance as well as new insights which have been developed during previous decades, particularly on the basis of ligand design for the catalytic transformation of organic functional groups with high selectivity and activity. Some of the numerous applications include olefin metathesis, activation of small molecules such as CO and C-H bond activation.[7-14]

Phosphine ligands are known to stabilize metal centres over a range of oxidation states. The most common application of phosphines is as spectator ligands rather than their direct involvement in reactions as reagents.[15] One problem of using monophosphines in catalytic applications is dissociation of the phosphine from the metal centre which leads to decomposition. This is especially pronounced for the early transition metals since lability in these systems is commonly high. An interesting observation is that cyclopentadienyl complexes of the electropositive transition metals are now well known to form highly active alkene polymerisation catalysts whereas phosphine complexes of the same metals are inactive or poorly active. This inactivity appears to be related to excessive lability as discussed below. The mis-match of soft P donor and oxophilic hard metal centre contributes to the phosphine ligand lability under reaction conditions. As multidentate phosphine ligands have improved ligating ability over monophosphines, macrocycle

phosphine ligands should form more stable complexes than their monodentate analogues. Macrocycle phosphines however, have not been extensively studied due to synthetic difficulties in accessing such ligands and hence a lack of suitable examples for study.

1.1 General properties of phosphine ligands

1.1.1 Electronic factors

Two components of the bonding are of importance between phosphine ligands and metal centres (**Figure 1**). Phosphine ligands can form σ-type interactions with metals by donating the lone pair of the P atom into an empty metal orbital with proper symmetry. Phosphines are also known to act as π-acid ligands. The σ* orbital of the P-R bonds are believed to accept the electrons from electron rich metals (back-donation).[15-17]

Figure 1 Bonding between metals and phosphine ligands

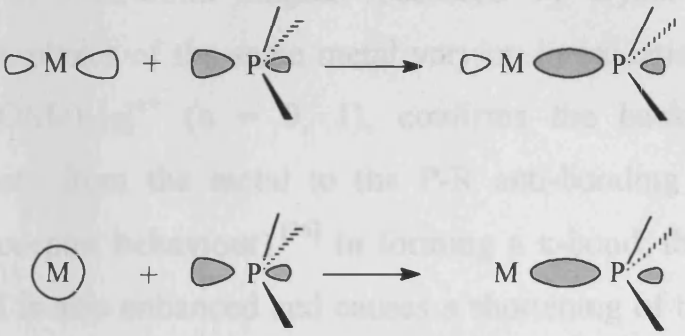

(a) σ bonding between metal and phosphine

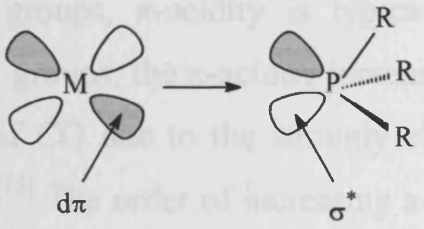

(b) π back-donation of electron density from metal to ligand orbital

The strength of σ bonding is influenced by the Lewis acidity and basicity of the metal and ligand respectively. 'Soft' P donor phosphines are generally used to coordinate soft later transition metals. The ability of phosphine ligands to donate the lone pair can generally be scaled *via* the pK_a value of the conjugated acid (**Eq. 1.1**), HPR_3^+, since there can only

be a σ-interaction involved in P-H bonding.[18,19] If the R groups of PR_3 are electron-donating, the basicity of phosphines is enhanced (**Table 1**).

$$HPR_3^+ \rightleftharpoons PR_3 + H^+ \qquad (1.1)$$

$$Ka = \frac{[H^+]\,[PR_3]}{[HPR_3]^+}$$

Table 1 pK_a values of selected phopshines

Phosphine	PH_3	PPh_3	$PPhMe_2$	PEt_3	PBu^t_3
pK_a	-14	2.73	6.5	8.69	11.40

The change of P-R bond lengths measured by crystallography for phosphine complexes of the same metal varying in oxidation states, $[\eta^3\text{-}(C_8H_{13})Fe\{P(OMe)_3\}_3]^{n+}$ (n = 0, 1), confirms the back-donation of electron density from the metal to the P-R anti-bonding orbitals (*i.e.* confirms π–acceptor behaviour).[16] In forming a π-bond, the strength of the M-P bond is also enhanced and causes a shortening of the M-P bond length.[20]

The degree of π-acidity is also influenced by the nature of the phosphine substituents. For alkyl groups, π-acidity is typically weak; for aryl, dialkylamino and alkoxy groups, the π-acidity increases. The π-acidity of PF_3 is as great as that of CO due to the strongly electron-withdrawing property of the F atoms.[15] The order of increasing π-acid character for a series of ligands is $PMe_3 \approx P(NR_2)_3 < PAr_3 < P(OMe)_3 < P(OAr)_3 < PCl_3 < CO \approx PF_3$.[15] The magnitude of this effect can be quantified by comparison of CO stretching frequencies in the IR spectrum of a series of complexes, $LNi(CO)_3$, L = phosphine ligand (**Table 2**).[21] The greater the π-acceptor ability of the phosphine ligand, the greater the competition for electron density from the metal, which reduces the available electron

density for back-donation to the π^* orbital of the CO ligands. This results in the strengthening of the C-O bond and a higher frequency for ν(CO).

Table 2 CO stretching frequencies of some $LNi(CO)_3$ complexes

Phosphine	ν(C=O) (cm^{-1})	phosphine (cm^{-1})	ν(C=O) (cm^{-1})
PCl_3	2104	$PPhMe_2$	2066
$P(OPh)_3$	2086	PMe_3	2064
$P(o\text{-}Tol)_3$	2072	PCy_3	2057
PPh_3	2069		

1.1.2 Steric factors

The steric properties of ligands also impose influences on the reactivity of metal complexes. The coordination sphere of a given metal contains a limited number of ligands. Bulky phosphine ligands generally stabilize coordinatively unsaturated metals and are commonly more labile. This allows small organic substrates to access the vacant site of activated species.

Steric bulk of PR_3 ligands on binding can be measured *via* Tolman's cone angle, the angle of a cone which encompasses the Van der Waals surface of the phosphine ligand substitutents with the apex at the metal and the R groups folding back as far as they are able in a space-filling model (**Figure 2**).[22] The cone angles of some phosphines are list in **Table 3**.

Figure 2 Definition of Tolman's cone angle with PMe_3 as an example

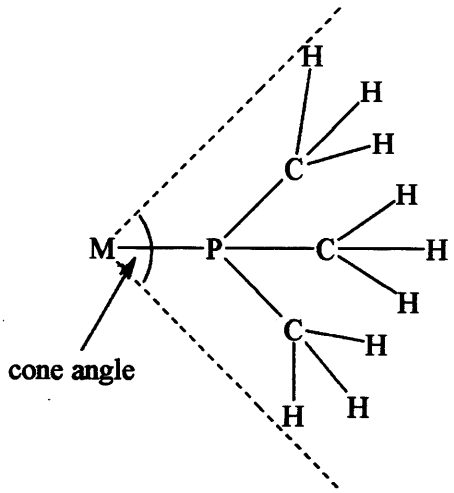

Table 3 Tolman's cone angle for selected phosphines*

Phosphine	Cone angle (°)	phosphine	Cone angle (°)
$PMes_3$	212	PPh_3	145
$P(o\text{-}Tol)_3$	194	PPr_3	132
PBu^t_3	182	PCl_3	124
PCy_3	170	PMe_3	118

* Tolman's original cone angle is measured from $R_3PNi(CO)_3$ complexes (*i.e.* where M-P = 2.24 Å)

1.2 Macrocycle ligands

Macrocycle ligands may be defined as cyclic organic compounds containing at least three heteroatom donors within a ring of at least nine atoms and with at least two carbon atoms (or dinuclear heteroatoms) between each adjacent pair of heteroatoms (**Figure 3**).[23a,b] This is the definition adopted in this thesis.

Figure 3 examples of N, O, S containing macrocycle

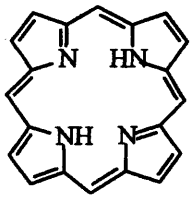

1.1 porphyrin

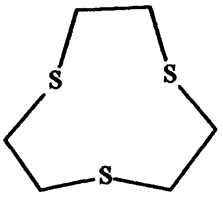

1.2 [9]aneS_3

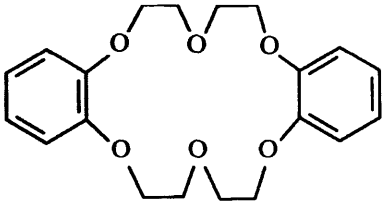

1.3 dibenzo-18-crown-6

Macrocycle complexes are widely involved as active centres for biological processes (*eg.* Fe complexes of porphyrin ring systems in electron transport). The synthesis of macrocycle ligands and their complexes, in order to mimic biological functions, is an important research topic.[23b] In addition, macrocylic ligands and related complexes have extensive application in areas of catalysis, clinical diagnosis, molecular recognition etc.[23] These properties are often based on the ability of macrocylic ligands to form very stable complexes and also their selectivity for different metals.[23a,b]

1.2.1 Chelate and macrocyclic coordination effects

Multidentate ligands form more stable chelate complexes than related monodentate ligands (*i.e.* with otherwise related structure) due to the chelate effect.[23a,b] The chelate effect is primarily entropic in origin. As illustrated in **Eq. 1.2,** the substitution of NH_3 for en results in an increased number of species released into solution, whereas the enthalpy remains approximately unchanged.[23a,b]

$$[M(NH_3)_6]^{2+} + 3en \rightleftharpoons [M(en)_3]^{2+} + 6NH_3 \qquad (1.2)$$

4 Species 7 Species

Macrocycle ligands generally bind metal ions into a cavity surrounded by donor atoms *via* three or more fused five, six or seven membered chelate rings. Macrocylic ligands usually form kinetically and thermodynamically more stable complexes with metal ions than do acyclic multidentate ligands due to the macrocyclic coordination effect.[23a,b] The origin of the macrocyclic coordination effect is based not only on entropy but also on enthalpy.[23a,b] For example, the data in **table 4** show the ΔG for the formation of the cyclic Ni(ii) complex with **1.4** is more negative than that for the formation of the acyclic complex with **1.5**.

Table 4 Thermodynamic data for the formation of Ni(ii) complexes at 298 K[23b]

ligand	Low-spin		High-spin	
	ΔH/kj mol^{-1}	$T\Delta S$/kJ mol^{-1}	ΔH/kJ mol^{-1}	$T\Delta S$/kJ mol^{-1}
1.4	-78.2	49.3	-100.8	24.3
1.5	-66.1	21.7	-80.3	10.9

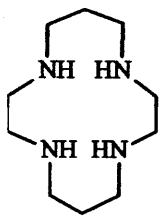

1.4

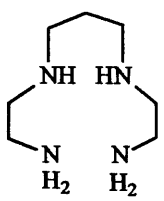

1.5

1.2.2 Selective Complexation of macrocycle ligands[23a-25]

The property of selective complexation of macrocycle ligands in terms of stability of the complexes depend on the composition and structure of the molecule. It is firstly based on the hardness of the donors in the macrocycle ring. Macrocycle ligands containing hard N or O donors show different complexation abilities to metal ions compared with ligands containing soft S donors. The architecture of macrocycle ligands also plays a role in the selective coordination to metal ions in several aspects. Firstly, an increased size of the chelate ring usually leads to a drop in complex stability, five-membered chelate rings are more stable than six (or more) membered chelate rings. This is due to the greater difficult in putting the dipoles and charges on donor atoms together and the increased steric strain as the size of chelate ring increases. Secondly, the different size of the macrocycle cavity can match different sizes of metal ions and influences the metal-ligand stability. A good match leads to a stable complex, mismatch to destabilization. Thirdly, the conformational flexibility of the macrocycle ring affects the fit of the metal ion to the ligand and the ability of the ligand to dissociate due to restricted degrees of freedom in bond rotation. For macrocycles with saturated aliphatic backbones that can form different conformers by rotation about single bonds, the ligand may be preorganized for various metal ion sizes. For macrocycles with more rigid aromatic backbones, conformational changes in the ligand are relatively restricted so that movement of the metal centre out of the preferred bonding configuration is then only possible by major distortions of the coordination sphere.

1.3 Triphosphamacrocycles

Phosphine macrocycles have been investigated for over three decades. Compared with well-known and extensively studied oxygen, nitrogen and sulfur containing macrocyles, reports on phosphorus macrocycles are quite rare. Most published work is still focused on ligand synthesis.[1,26-28] Some of the known phosphorus containing macrocycles are shown in **Figure 4**.

Figure 4 Some known phosphorus containing macrocycles[1,26-29]

(a) Triphosphamacrocycles with different ring sizes

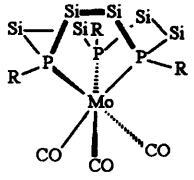

9 - membered

1.6

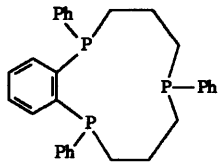

11 - membered

1.7

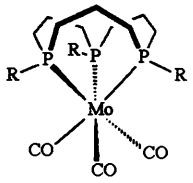

12 - membered

1.8

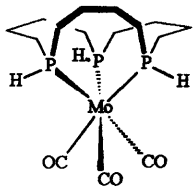

15 - membered

1.9

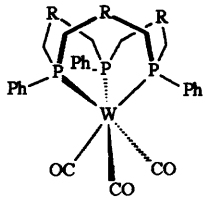

R = $(CH_2)_5CH{=}CH(CH_2)_5$

45 - membered

1.10

(b) Tetraphosphamacrocycles

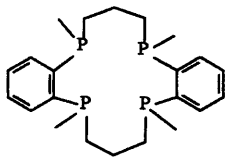

1.11

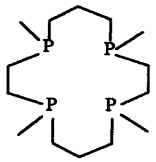

1.12

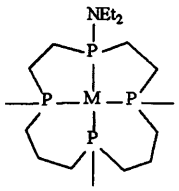

1.13

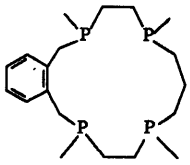

1.14

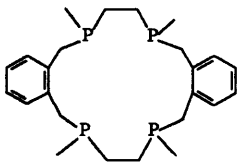

1.15

(c) Macrocycles with mixed N, O, S, P atoms

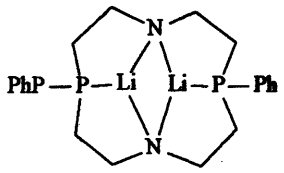

1.16

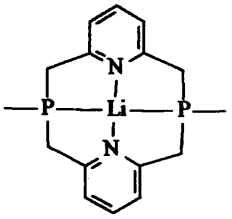

1.17

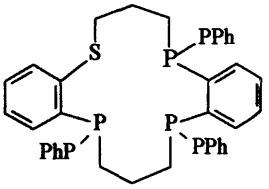

1.18

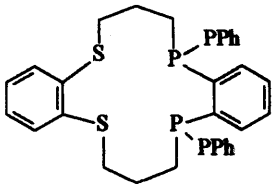

1.19

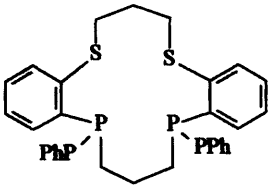

1.20

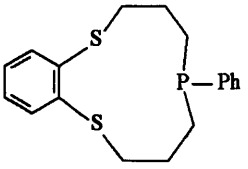

1.21

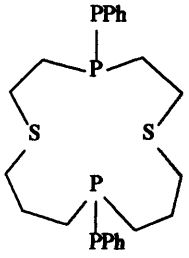

1.22

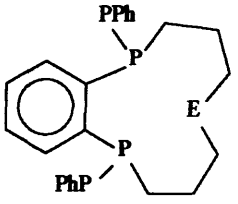

E = O, S, NR

1.23

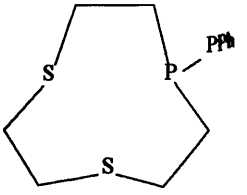

1.24

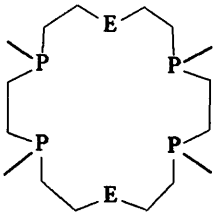

1.25

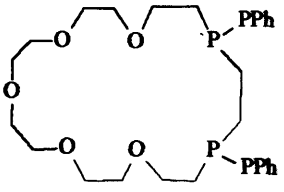

1.26

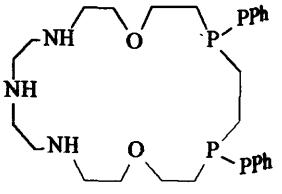

1.27

Of the known phosphorus containing macrocycles, triphospha-macrocycles (P_3 macrocycle) with three *syn,syn,syn*-P donors are of much interest due to their electronic analogy to η^5-Cp^- as tridentate $6e^-$ donors and structure character. P_3 macrocycles are facially capping ligands occupying three coordination sites (as η^5-Cp^- ligand) that can impose important structural influences on the metal centre (**Figure 5**). A primary and major influence is that they force the remaining reaction sites into a mutually *cis* arrangement. They may also cause shape distortions upon the coordination sphere with implications for modified reactivity. Due to their expected ligating ability as soft donor ligands, they may favour binding the more electronegative metals and those in low oxidation states. Enhanced stability due to the macrocyclic coordination effect may also allow access to new classes of complexes of electropositive metals and also stabilise active intermediates during catalytic reactions etc.

Figure 5 Coordination model of triphosphamacrocycles

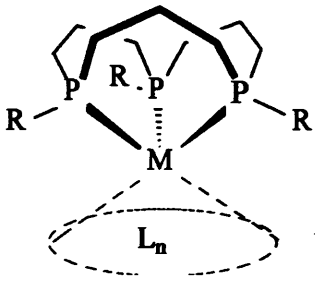

It is noteworthy that the development of single-site catalysts for olefin polymerisation is currently dominated by metallocene complexes.[30] The development of other non-metallocene complexes for catalytic olefin polymerisation has been of much interest during the last decade.[30,31] η^5-Cp^- analogous ligands, such as pyridine-diamide,[32] amidodiphosphine,[33] tris(pyrazolyl)borate[34] etc. ligands, have drawn much attention (**Figure 6**). Triphosphamacrocycles indeed also show intrinsic properties in this

application and it is of interest to note their similarities to cyclopentadienyl ligands as discussed above (see below).

Figure 6 Some tridentate capping ligands analogous to η^5-Cp^R as $6e^-$ donors

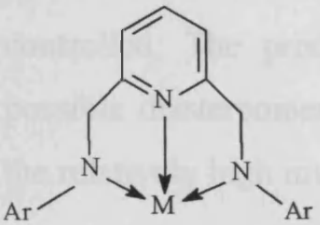

pyridine-diamide

1.28

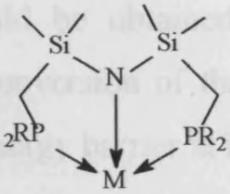

amidodiphosphine

1.29

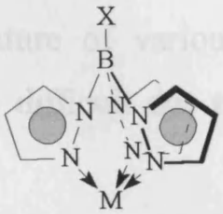

tris(pyrazolyl)borate

1.30

1.3.1 Synthetic aspects for the synthesis of triphospha-macrocycles

Despite the expectation that P_3 macrocycles will be of value in numerous applications, studies on P_3 macrocycles are somewhat limited due to the difficulties in synthesis. Two synthetic approaches for the synthesis of triphosphamacrocycles have been studied namely direct methods and template-directed methods.

Direct methods:

The phosphine precursors prior to ring closure are combined in dilute solution in a given ratio to yield the desired phosphine macrocycle. This method is less effective and has significant drawbacks.

A) The side reaction of polymerisation is hard to avoid even in highly dilute solution which causes the overall yields to be quite low and variable.

B) Handling the highly volatile, noxious, toxic and air-sensitive phosphine precursors and intermediates in large volumes of solvent is experimentally difficult and also leads to competing decomposition.

C) The stereochemistry of the phosphine macrocycle can not be controlled. The product would be obtained as a mixture of various possible diastereomers. Interconversion of these may be difficult due to the relatively high inversion energy barrier at P.

The first 11 membered triphosphamacrocycle (**1.7**) was prepared by Kyba using a direct method *via* reaction of a dilithium organophosphide with halogenophosphine under high dilution conditions (**Scheme 1**).[35] The reaction gave **1.7** as a mixture of stereoisomers that required subsequent separation. Overall chemical yields were moderate and yields of pure isomers correspondingly low.

Scheme 1 Synthesis of triphosphamacrocycle by direct method

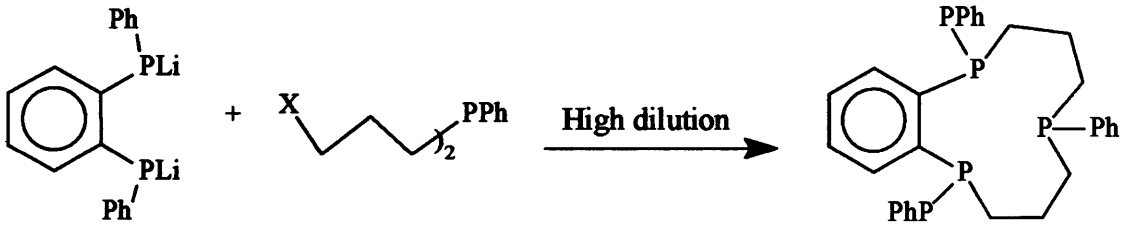

1.7

Template-directed methods

Phosphine precursors are coordinated to a metal centre followed by a series of intramolecular P-C coupling reactions leading to the desired phosphine macrocycle. The metal holds the phosphine precursors in close proximity to facilitate the ring closure reaction effectively and allow the formation of kinetic products, unlike the thermodynamic products produced by the direct method. The template-directed method produces phosphine macrocycles with controlled stereochemistry due to the P

precursors being preorganised. There are also disadvantages associated with the template method however.

A) Few suitable metal templates meet the conditions for the synthesis of phosphine macrocycles are few.

B) Once the phosphine macrocycle has been formed, the macrocycle complexes are typically kinetically inert and thermodynamically stable and may be resistant to demetallation.

The first 12-membered triphosphamacrocycle complex (1,5,9-triphosphacyclododecane, **1.8**) was prepared in high yield by Norman using the *fac*-$Mo(CO)_3$ fragment as a template *via* the radical-activated intramolecular hydrophosphination reaction of coordinated allylphosphine in high yield (**Scheme 2**).[36]

Scheme 2 Template Synthesis of {[12]ane-P_3H_3}$Mo(CO)_3$

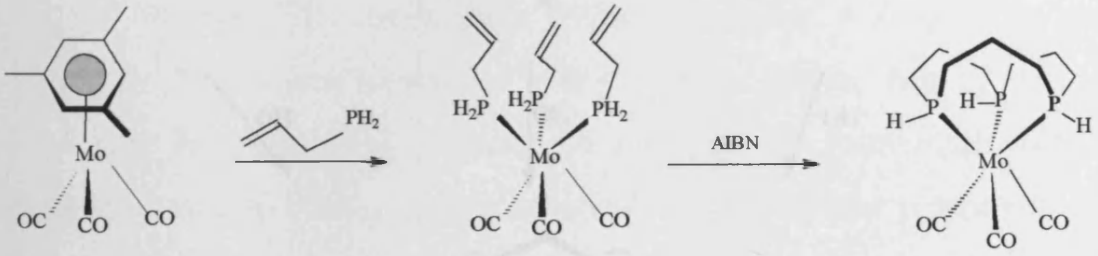

1.8

The liberation of free 1,5,9-triphosphacyclododecane (**1.31**) was achieved by oxidation of Mo^0 (d^6) to the more labile Mo^{II} (d^4) followed by hydrolysis with base in our laboratory (**Scheme 3**).[37] The synthesis and liberation can also be achieved using the alternative *fac*-$Cr(CO)_3$ or $CpFe^+$ templates.[38-40] A series of derivatives of 1,5,9-triphosphacyclododecane were prepared by alkylation of the secondary phosphines and related complexes have been investigated. These show interesting catalytic activity, particularly for olefin polymerization and olefin metathesis.[41,42]

Scheme 3 Functionalisation and liberation of [12]ane-P_3 macrocycles

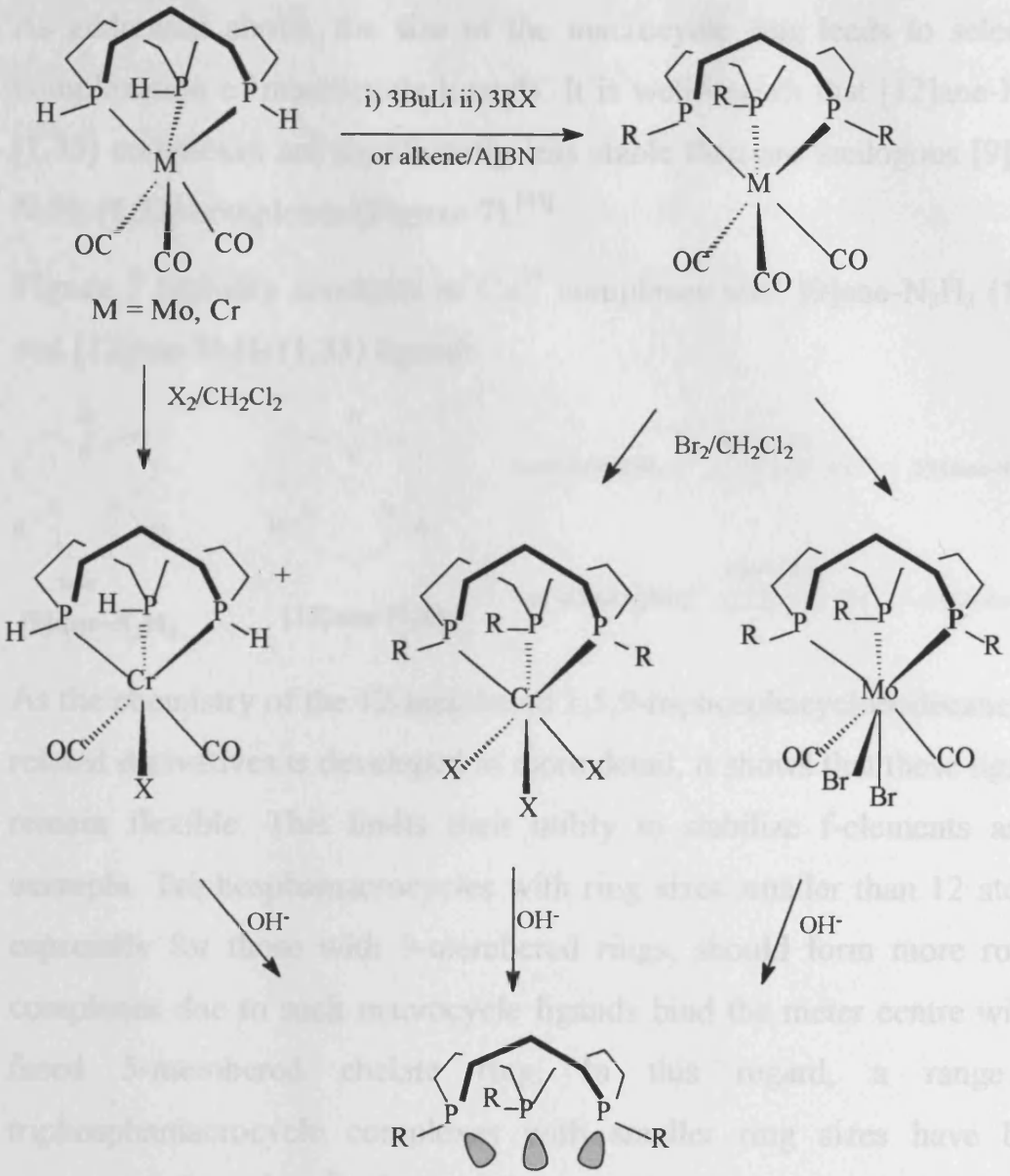

1.31

1.3.2 Triphosphamacrocycles with smaller ring sizes

As addressed above, the size of the macrocycle ring leads to selective complexation of macrocycle ligands. It is well known that [12]ane-N_3H_3 (**1.33**) complexes are significantly less stable than are analogous [9]ane-N_3H_3 (**1.32**) complexes (**Figure 7**).[43]

Figure 7 Stability constants of Cu^{2+} complexes with [9]ane-N_3H_3 (**1.32**) and [12]ane-N_3H_3 (**1.33**) ligands

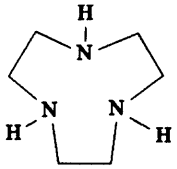

tacn

[9]ane-N_3H_3

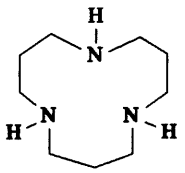

[12]ane-N_3H_3

$$Cu([9]ane\text{-}N_3H_3)_2^{2+} \xrightarrow{\log\beta = 31.5} Cu^{2+} + 2([9]ane\text{-}N_3H_3)$$

$$Cu([12]ane\text{-}N_3H_3)_2^{2+} \xrightarrow{\log\beta = 20.8} Cu^{2+} + 2([12]ane\text{-}N_3H_3)$$

As the chemistry of the 12-membered 1,5,9-triphosphacyclododecane and related derivatives is developed in more detail, it shows that these ligands remain flexible. This limits their utility to stabilize f-elements as an example. Triphosphamacrocycles with ring sizes smaller than 12 atoms, especially for those with 9-membered rings, should form more robust complexes due to such macrocycle ligands bind the meter centre with 3 fused 5-membered chelate ring. In this regard, a range of triphosphamacrocycle complexes with smaller ring sizes have been prepared using η^5-Cp^RFe^+ templates (R = H, alkyl) by the strategy of intramolecular hydrophosphination or dehydrofluorination.

A) Hydrophosphination

We have previously established the template promoted cyclisation of alkenyl phosphines on Cp^RFe^+ templates (**Scheme 4**). Phosphine precursors were introduced to the iron centre sequentially by replacing labile ligands (CH_3CN in the scheme) which are *trans* to the Cp^R ligand, followed by ring closure reactions. A range of triphosphamacrocycle

complexes with different ring sizes, including 9 (**1.34**,[44] **1.38**[45]), 10 (**1.35**,[46] **1.36**[47]) and 11(**1.37**[47]) membered rings, have been synthesised *via* this strategy by varying the phosphine precursors. Aromatic bridges can also be introduced into the macrocycle backbone (**1.38**).

Scheme 4 Synthesis of triphosphamacrocycles with small ring sizes by Cp^RFe^+ templates *via* hydrophosphination reactions

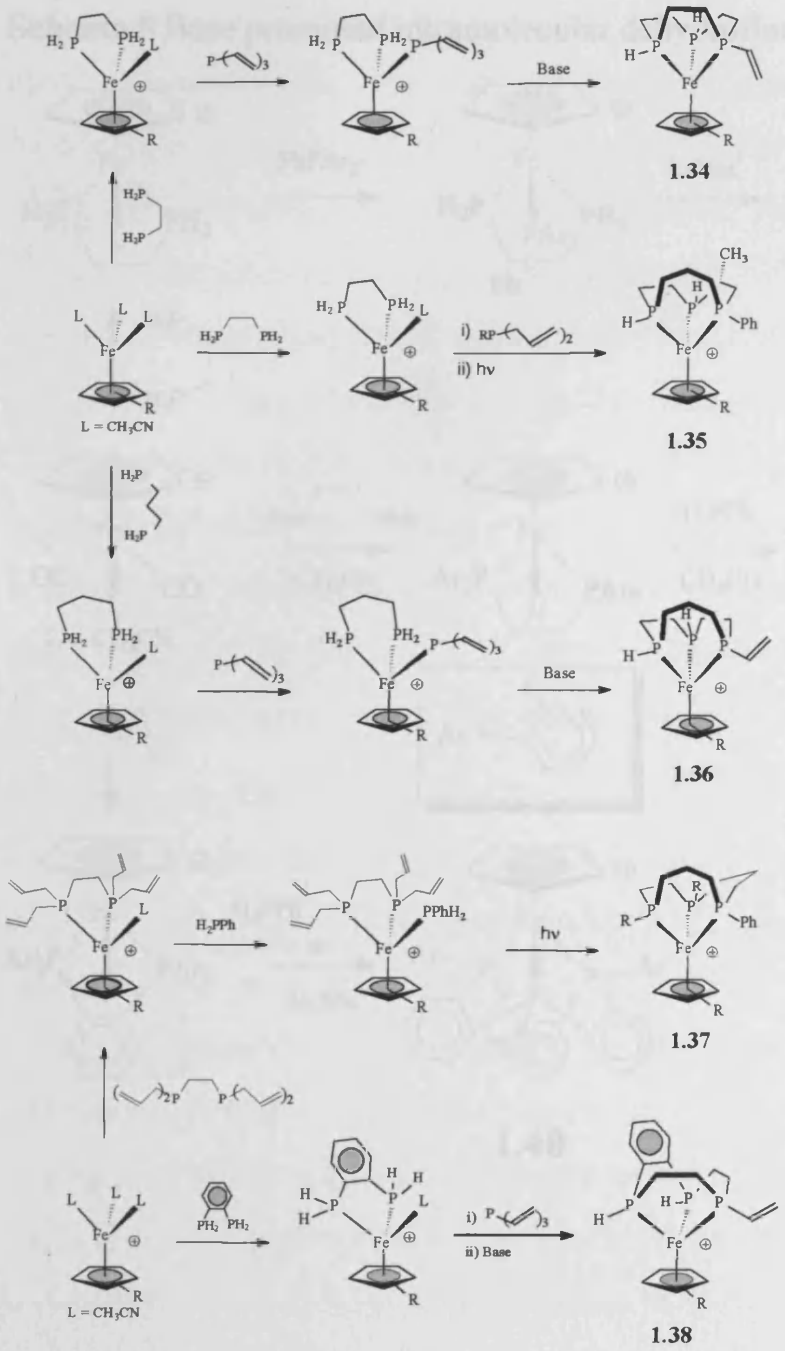

B) Dehydrofluorination

Cp^RFe^+ templates also support nucleophilic substitution of fluoride on adjacent aryl groups by coordinated phosphide. This allows the closure of very rigid 9-membered macrocycles bearing o-phenylene backbone functions (**1.39**, **1.40**, **1.41**)[48,49] as shown in **Scheme 5** below. Alternative donors eg. As, may also be incorporated using this route.[49]

Scheme 5 Base promoted intramolecular dehydrofluorination

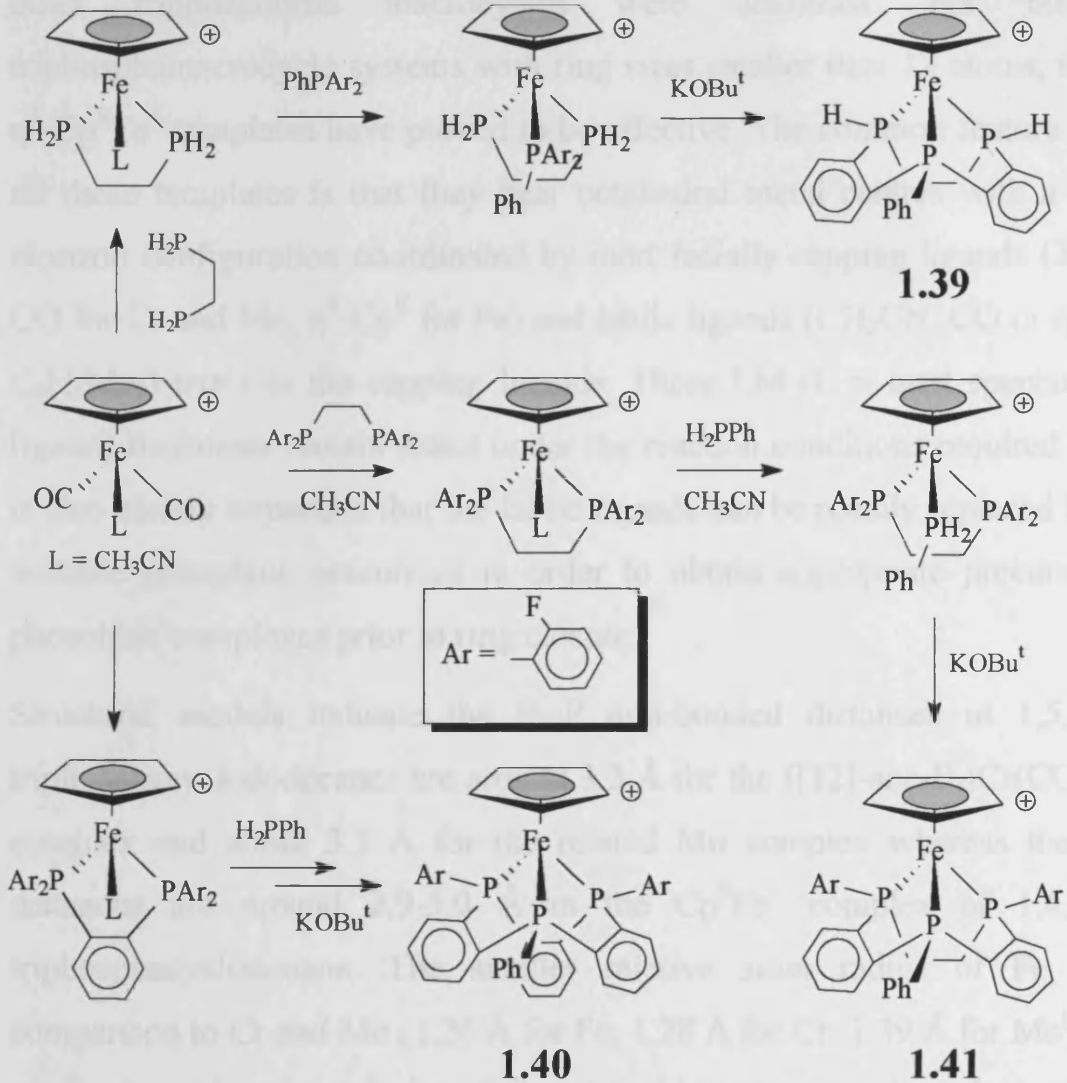

1.3.3 Template considerations for the synthesis of triphospha-macrocycles

For the synthesis of triphosphamacrocycles, the choice of suitable templates is important. Prior to our study of Cp^RFe^+ templates, the carbonyl complexes of group VI metals with a d^6 electron configuration are the only ones known for the synthesis of 1,5,9-triphosphacyclododecanes. Other than Kyba's 11-membered ring systems, other triphosphorus macrocycles were unknown. For other triphosphamacrocycle systems with ring sizes smaller than 12 atoms, the η^5-Cp^RFe^+ templates have proved to be effective. The common feature of all these templates is that they bear octahedral metal centres with a d^6 electron configuration coordinated by inert facially capping ligands (3 x CO for Cr and Mo, η^5-Cp^R for Fe) and labile ligands (CH_3CN, CO or η^6–$C_6H_3Me_3$) *trans* to the capping ligands. These LM (L = inert spectator ligand) fragments remain intact under the reaction conditions required. It is also clearly important that the labile ligands can be readily replaced by suitable phosphine precursors in order to obtain appropriate precursor phosphine complexes prior to ring closure.

Structural models indicate the P···P non-bonded distances in 1,5,9-triphosphacyclododecanes are around 3.3 Å for the ([12]-ane-P_3)$Cr(CO)_3$ complex and about 3.5 Å for the related Mo complex whereas these distances are around 2.9-3.0 Å in the Cp^RFe^+ complex of 1,4,7-triphosphacyclononane. The smaller relative atom radius of Fe in comparison to Cr and Mo (1.26 Å for Fe, 1.28 Å for Cr, 1.39 Å for Mo[50]) results in a closer proximity of the phosphine precursor ligands in the Fe^{2+} template complexes, which in turn facilitates the formation of shorter bridging links between the phosphines and hence smaller macrocycle ring sizes should be available. The longer Cr-P and Mo-P bond lengths (and

consequently P···P distances) limits the size of the ring system achievable on the Cr and Mo templates. In addition, for Cr and Mo, the remaining spectator ligands (3 x CO) are not sterically demanding and leave little steric influence in 'pushing' the phosphines closer together. In the Cp^RFe template however, the steric properties of the spectator (Cp^R) ligand may be modified to have a significant influence over the trans phosphines (*i.e.* compressing P-Fe-P angles) aiding closure of smaller ring sizes.

A advantage for the Cp^RFe^+ templates is that the phosphine precursors can be sequentially introduced into the Fe centre by the use of a range of cyclopentadienyl derivatives, giving access to a much wide range of precursor phosphine complexes and incorporation of functionality on the macrocycle backbones and substituents on the P atoms.

1.4 Aim of this thesis

Of all of the template systems investigated to date, the liberation of the free phosphorus macrocycle has only been achieved with the 12-membered 1,5,9-triphosphacyclododecane and its tertiary phosphine derivatives and only readily from Cr^0 or Mo^0 carbonyl templates. The synthesis of triphosphamacrocycles with smaller ring systems has been achieved by using η^5–Cp^RFe^+ templates. The complexes are however resistant to liberation of the macrocyle ($9aneP_3Et_3$ can only be liberated from the Fe centre by oxygen transfer oxidation to give the trioxide of $9aneP_3Et_3O_3$ which is resistant to reduction).[51] The smaller ring systems are of substantial interest in that they are expected to form very robust complexes indeed; they remain an important synthetic target.

In this thesis, the application of facially capping ligands to form robust metal-ligand fragments that will survive the necessary reaction conditions, and which will limit remaining reaction sites to mutually cis configurations as alternative templates for the synthesis of triphosphamacrocycles have been investigated. The aim of this study is also to allow ready access to the free (uncoordinated) macrocycles.

Of the robust metal-ligand fragments, piano-stool complexes with octahedral d^6 metal centres are promising as clearly demonstrated by the template-directed synthesis of 1,5,9-triphosphacyclododecane and 1,4,7-triphosphacyclononane. Examples are, however, few. In our laboratory, cyclopentadienyl complexes of cobalt, ruthenium and manganese, which are iso-structural and iso-electronic to the corresponding iron complexes have been investigated but have not led to new syntheses of macrocycles. In this thesis, tripodal complexes of trispyrazolylmethane, the cyclobutadienyl ligand and manganese carbonyl complexes were studied

as alternative templates with the aim of developing syntheses of new triphosphamacrocycles with small ring systems.

References:

1. C. A. McAuliffe, *Comprehensive Coodination Chemistry*, Vol. 2, Perganon Press, Oxford, **1987**, P989.
2. A. Pidcock, *Transition Metal Complexes of Phosphorus, Arsenic and Antimony Ligands*, Macmillan, London, **1973**, P3.
3. C. A. McAuliffe, W. A. Levason, *Phosphorus, Arsenic and Stibine Complexes of the transition Elements*, Elsevier, Amsterdam, **1979**.
4. T. Appleby, J. D. Woollins, *Coord. Chem. Rev.* 235, **2002**, 121-140.
5. H. A. Mayer, *Chem. Rev.* **1994**, 94, 1239-1272.
6. P. Braunstein; N. Boag, *Angew. Chem. Int. Ed.* **2001**, 40(13), 2427-2433.
7. T. Hayashi, *Acc. Chem. Res.* **2000**, 33(6), 354-362.
8. E. Milko, D. Milstein, *Chem. Rev.* **2003**, 103(5), 1759-1792.
9. H. H. Karsch; V. Graf; M. Reisky, *Phosphorus, Sulfur and Silicon and the Related Elements* **1999**, 144-146, 553-556.
10. U. Segerer; R. Felsberg; S. Blaurock; G. A. Hadi; E. Hey-Hawkins, *Phosphorus, Sulfur and Silicon and the Related Elements* **1999**, 144-146, 477-480.
11. H. Grutzmacher; C. Meyer; S. Boulmaaz; H. Schonberg; S. Deblon; J. Liedtke; S. Loss; M. Worle, *Phosphorus, Sulfur and Silicon and the Related Elements* **1999**, 144-146, 465-468.
12. K. V. L. Crepy; T. Imamoto, *Topics in Current Chemistry* **2003**, 229 (New Aspects in Phosphorus Chemistry III), 1-40.
13. T. Appleby; J. D. Woollins, *Coord. Chem. Rev.* **2002**, 235(1-2), 121-140.
14. D. Mingos; P. Michael, *Modern Coordination Chemistry* **2002**, 69-78.
15. R. H. Crabtree, *The Organometallic Chemistry of the Transition metals*, third edition, John Wiley & Sons, New York, 91-95, **2001**.
16. A. G. Orpen, *Chem. Commun.* 1310, **1985**
17. G. Pacchioni; P. S. Bagus, *Inorg. Chem.* 31, 4391, **1992**
18. C. A. Streuli, *Anal. Chem.*, **1960**, 82, 5791
19. T. Allman; R. G. Goel, *Can. J. Chem.*, **1982**, 60, 716
20. M. J. Wovkulich; J. L. Atwood, L. Canada, J. D. Atwood, *Organometallics*, **1985**, 4, 867
21. C. A. Tolman, *J. Amer. Chem. Soc.* **1970**, 92, 2953
22. C. A. Tolman, *Chem. Rev.*, **1977**, 77, 313

23. (a) L. F Lindoy. *The Chemistry of Macrocyclic Ligand Complexes* 1992, 269 pp Science. (b) E. C. Constable, *Coordination Chemistry of Marocyclic Compounds*, Oxford. **1999.** (c) D. Salvemini; D. P. Riley, *Cellular and Molecular Life Sciences* **2000**, 57(11), 1489-1492. (d) H. G. Jr. Richey, *Comprehensive Supramolecular Chemistry* **1996**, 1, 755-775.
24. P, Comba; W. Schiek, *Coord. Chem. Rev.* 238-239, **2003**, 21-29
25. R. D. Hancock; A. E. Martell, *Chem. Rev.* **1989**, 89, 1875-1914
26. W. Levason; G. Reid, *Comprehensive Coordination. Chemistry II*, **2004**, 1, 475-484.
27. O. Stelzer; K.-P. Langhans, *The Chemistry of Organophosphorus Compounds*, F. R. Hartley, Eds., Wiley, New York, **1990**, vol 1. Ch8, 192-254
28. A. Caminade; J. P. Majoral, *Chem. Rev.* **1994**, 94(5), 1183-213
29. S. Ekici; M. Nieger; R. Glaurn; E. Niecke, *Angew. Chem. Int. Ed.* **2003**, 42(4), 435-438
30. (a) W. Wang; L. Wang, *J. Poly. Mater.* **2003**, 20(1), 1-8. (b) G. G. Hlatky, *Coord. Chem. Rev.* **1999**, 181, 243-296.
31. G. J. P. Britovsek; V. C. Gibson; D. F. Wass, *Angew. Chem. Int. Ed.* **1999**, 38(4), 428-447.
32. F. Guérin; D. H. McConville; J. J. Vittal, *Organometallics* **1996**, 15, 5586-5590
33. M. D. Fryzuk; G. Giesbrecht; S. J. Rettig, *Organometallics* **1996**, 15, 3329-3336
34. S. Scheuer, J. Fisher, J. Kress, *Organometallics* **1995**, 14, 2627-2629
35. E. P. Kyba; A. M. John; S. B. Brown; C. W. Hudson; M. J. McPhaul; A. Harding; K. Larsen; S. Niedzwiecki; R. E. Davis, *J. Am. Chem. Soc.* **1980**, 102(1), 139-47.
36. B. N. Diel; R. C. Haltiwanger; A. D. Norman, *J. Am. Chem. Soc.* **1982**, 104(17), 4700-1.
37. S. J. Coles; P. G. Edwards; J. S. Fleming; M. B. Hursthouse; S. S. Liyanage, *Chem. Commun.* **1996**, (3), 293-4.
38. P. G. Edwards; J. S. Fleming; S. S. Liyanage, *Inorg. Chem.* **1996**, 35(16), 4563-4568.
39. P. G. Edwards; J. S. Fleming; S. S. Liyanage, *Dalton Trans.*, **1997**, (2), 193-197.
40. A. J. Price; P. G. Edwards, *Chem. Commun.* **2000** (11), 899-900.
41. R. J. Baker; P. G. Edwards, *Dalton Trans.* **2002**, (15), 2960-2965
42. R. J. Baker; P. G. Edwards; J. Gracia-Mora; F. Ingold; K. M. A. Malik, *Dalton Trans.* **2002**, (21), 3985-3992.

43. R. M. Smoth; A. E. Martell, *Critical Stability Constants*, Vols. 5 and 6, Plenum, **1989**
44. P. G. Edwards; P. D. Newman; K. M. A. Malik, *Angew. Chem. Int. Ed.* **2000**, 39(16), 2922-2924.
45. P. G. Edwards; M. L. Whatton; R. Haigh, *Organometallics* **2000**, 19(14), 2652-2654.
46. P. G. Edwards; P. D. Newman; D. E. Hibbs, *Angew. Chem. Int. Ed.* **2000**, 39(15), 2722-2724.
47. R. Haigh, *Doctoral Thesis*, **2002**, Cardiff University
48. T. Albers, *Doctoral Thesis*, **2001**, Cardiff University
49. J. Johnstone, *Doctoral Thesis*, **2004**, Cardiff University
50. J. G. Speight, *Lange's Handbook of Chemistry* 16th Ed. McGraw-Hill, New York 2005.
51. P. G. Edwards, P. D. Newman, Cardiff University; Unpublished results.

Chapter 2

Tripodal Tris-pyrazolylmethane Iron and Cobalt Complexes

Abstract

A series of cationic trispyrazolylmethane complexes of the general form $[Tm^RM(CH_3CN)_3]^{2+}$ (Tm = tris(pyrazolyl)methane, **2.1**, R = 3,5-Me_2, M = Fe; **2.2**, R = 3-Ph, M = Fe; **2.3**, R = 3,5-Me_2, M = Co; **2.4**, R = 3-Ph, M = Co) with 'piano-stool' structure were prepared by the reaction of the N_3 tripodal ligands (Tm^R) with $[(CH_3CN)_6M](BF_4)_2$ in a stoichiometric 1:1 ratio. Magnetic susceptibility measurements indicate that all four complexes with BF_4 counter anions are paramagnetic, high-spin systems in the solid state with μ_{eff} of 5.1 (**2.1**, S = 2), 5.1 (**2.2**, S = 2), 4.6 (**2.3**, S = 3/2) and 4.5 (**2.4**, S = 3/2) respectively. Comparisons of bond lengths from the metal centre to the Tm^R nitrogen donors, and from the metal centre to the acetonitrile nitrogen donors indicate that the neutral tripodal ligands appear to be more weakly coordinated to the metal centre than are the acetonitrile ligands. Reactions of these tripodal complexes with bidentate phosphine ligands, such as 1,2-diphosphinoethane or 1,2-bis(diallylphosphino)ethane leads to displacement of the tripodal ligand, or to the formation of more thermally stable bis-ligand complexes ML_2 {L = tris(3,5-dimethyl-1-pyrazoyl)methane}.

2.1 Introduction

We are interested in octahedral transition metal complexes stabilised by tripodal capping ligands, and which also contain labile monodentate ligands in a 'piano-stool' type of structure for the following reasons. These complexes may be potential templates for the synthesis of triphosphamacrocycles by replacing the labile monodentate ligands with phosphine presursors which may support intramolecular P-C bond formation by a range of suitable reactions as we have demonstrated for the synthesis of triphosphamacrocycles using the η^5-$Cp^RFeL_3^+$ (L = CH_3CN) class of complexes as templates (Chapter 1).

Current templates for the formation of triphosphorus macrocycles are either demetallated with difficulty, and/or with decomposition or not at all and templates stabilised by alternative tripodal capping ligand may be more amenable to liberation of the phosphorus macrocycle.

The tripodal nitrogen chelate ligands, tris(pyrazolyl)borate (Tp) and tris(pyrazolyl)methane (Tm) have been extensively investigated in inorganic, bioinorganic and organometallic chemistry, partly due to their close analogy to cyclopentadienyl ligands.[1-2] All these ligands are 6 electron donors (**Figure 1**) and occupy three coordination sites as capping ligands when binding a metal. These ligands form a variety of metal complexes that have counterparts in the classic cyclopentadienyl-iron systems.[2] The Tm or Tp ligands commonly form bis-ligand structures for octahedral metal ions in which the two tripodal ligands interdigitate, since the donors are held in a planar fashion roughly, in plane with the metal-donor bond. The parent tris(pyrazolyl)borate or tris(pyrazolyl)methane ligands can be modified by introducing substituents such as $-CH_3$, $-C_3H_7$, $-C_4H_9$ or $-C_6H_5$ in the 3- or 3,5-

positions of the pyrazole ring resulting in variations of steric bulk. These derivatives with controlled coordination behaviour may prevent formation of bis-ligand ML_2 complexes (L = Tp or Tm ligand).[2] The known tripodal complexes, $[Tp^RM(NCMe)_3]^+$ (Tp = hydrotrispyrazolyl-borate; M = Ni, Co), which are very labile in the solution absence of CH_3CN, were prepared by chloride abstraction from the corresponding chloro complexes, Tp^RM-Cl.[3] The related reported tripodal complex of $\{Fe[(3,5\text{-}Me_2pz)_3CH](H_2O)_3\}^{2+}$ shows less solubility in organic solvents.[4] This chapter will introduce the work of the direct and stoichiometric synthesis of piano-stool Fe/Co complexes of substituted tris-pyrazolylmethanes, their structural characterisation, magnetic properties and preliminary reactions with bis-phosphines.

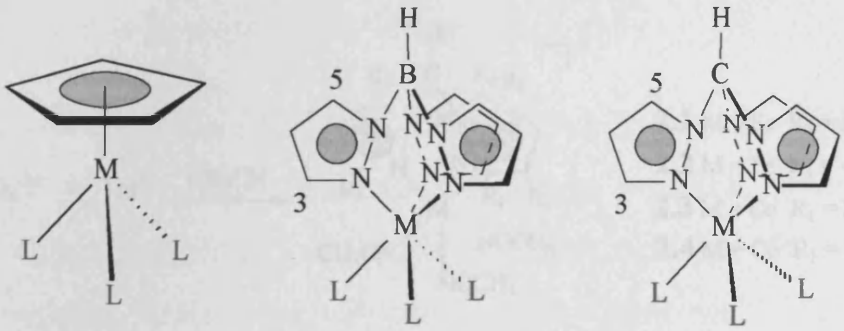

Figure 1 Analogy between Cp, tris(pyrazolyl)borate and tris(pyrazolyl)methane

2.2 Synthesis of tripodal complexes

The four tripodal complexes of $[Tm^{R}M(CH_3CN)_3](BF_4)_2$ (Tm = tris(pyrazolyl)methane; R=3-Ph, 3,5-Me_2; M = Fe, Co) were directly prepared by reactions of tripodal Tm^{R} ligands with one equivalent of $[(CH_3CN)_6M](BF_4)_2$ in acetonitrile solvent (**Scheme 1**). The products are conveniently crystallised directly from the reaction mixture and are isolated as colourless (Fe) or orange/red (Co) crystals. IR spectra of these complexes confirm the existence of three terminal CH_3CN ligands. The compounds are all air- and moisture- sensitive as the solids or in solution.

Scheme 1 Preparation of tripodal trispyrazolylmethane iron and cobalt complexes, $[(TM^{R})M(CH_3CN)_3]^{2+}$

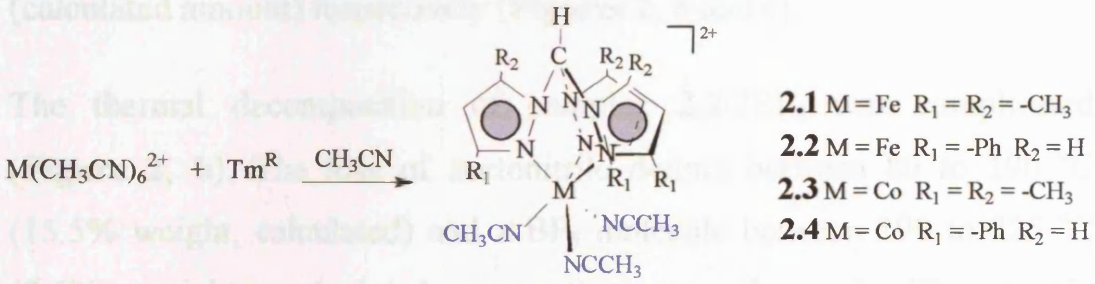

The thermally stable bis-ligand complexes, $[ML_2]^{2+}$ (M = Fe, Co; L = Tm^{R}), were avoided due to coordination control through the steric hindrance introduced by substituents in the 3, 5 positions of the pyrazole ring. The ratio of the two reagents in the reaction is also very important in order to limit formation of the bis-ligand complexes. In the mass spectra of the iron and cobalt complexes **2.1** to **2.4**, the highest ion observed corresponds to the $[Tm^{R}M]^{2+}$ fragment (m/z = 354, 498, 357, 501 amu for **2.1** to **2.4** respectively) except when the compound is admitted as a methanol solution in which case complex ions corresponding to the formula, $[Tm^{R}M(CH_3CN)_2(CH_3OH)]^{2+}$ were observed (m/z = 468, 612, 471, 615 amu for **2.1** to **2.4** respectively) in all cases. Crystalline samples

of compounds **2.1** and **2.2** are colourless, which is consistent with a paramagnetic high-spin (HS) state for iron complexes at room temperature.[5] In the NMR spectra of these four tripodal complexes in solution, only broad non-diagnostic resonances are observed due to them being paramagnetic.

Thermal analyses (TGA) indicated three decomposition steps for complexes **2.1**·$2BF_4$ and **2.3**·$2BF_4$ corresponding to loss of coordinated acetonitrile ligands between 80-190 °C with weight losses of 18.9% and 18.8% (calculated amount) respectively followed by loss of one molecule of BF_3 between 190 to 240 °C with weight losses of 10.4% and 10.3% (calculated amount) respectively, then loss of tris(3,5-dimethyl-pyrazoyl)methane up to 400 °C, with weight losses of 45.7% and 45.5% (calculated amount) respectively (**Figures 2, a** and **c**).

The thermal decomposition of complex **2.2**·$2BF_4$ was complicated (**Figure 2, b**). The loss of acetonitrile donors between 80 to 190 °C (15.5% weight, calculated) and a BF_3 molecule between 190 to 225 °C (8.5% weight, calculated amount) were observed. The tris(3-phenylpyrazoyl)methane ligand probably begins to be decomposed at around 300 °C.

For complex **2.4**·$2BF_4$·CH_3CN, multi decomposition steps were involved upon heating (**Figure 2,** d). The steps of losing the co-crystallised acetonitrile and the three coordinated acetonitrile ligands between 60-190 °C (19.5% for the four CH_3CN, calculated amount) were not well-separated. The loss of BF_3 (8.0% weight, calculated amount) was observed between 190 to 250 °C. From 250 to 550 °C, an observed total weight loss of 41% was assigned to the decomposition of the tris(3-phenylpyrazoyl)methane ligand (52.6%, calculated amount).

Figure 3 TGA diagrams of complexes **2.1**·$2BF_4$ (**a**), **2.2**·$2BF_4$ (**b**), **2.3**·$2BF_4$ (**c**), and **2.4**·$2BF_4$·CH_3CN (**d**)

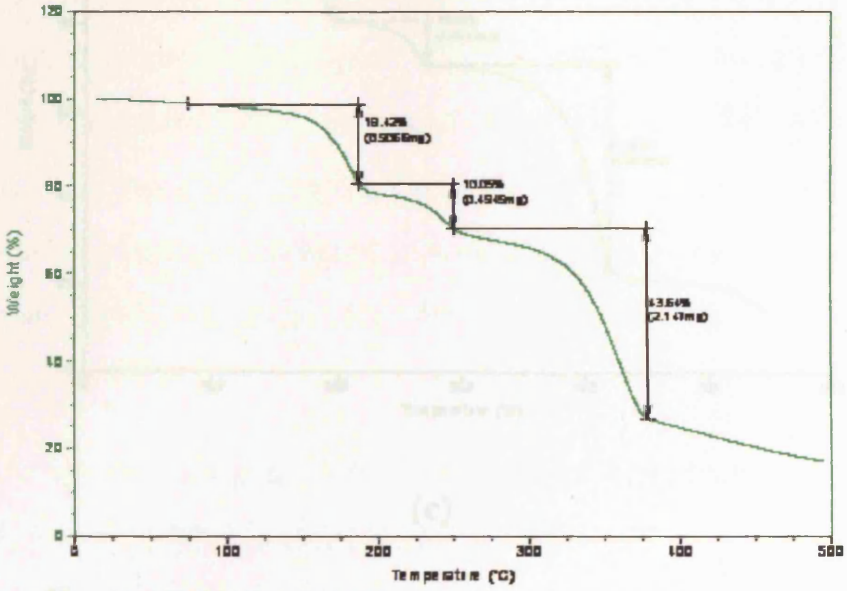

(**a**)

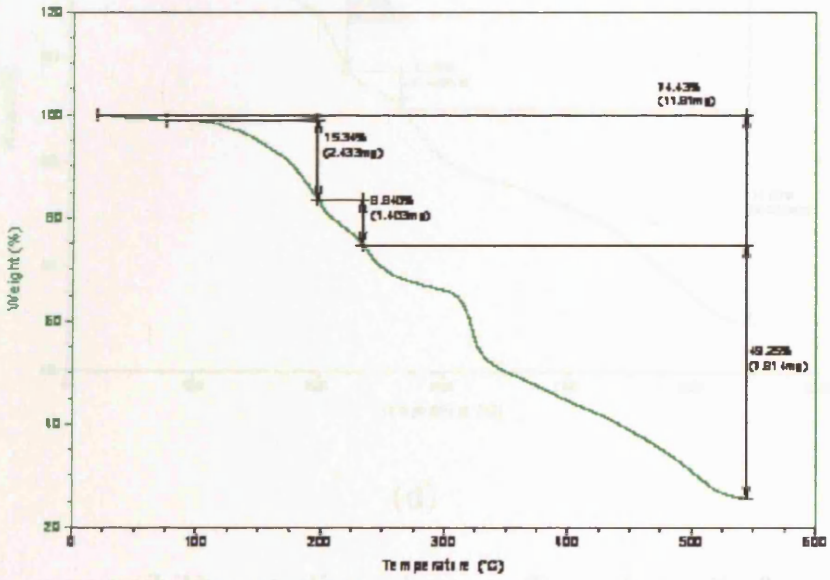

(**b**)

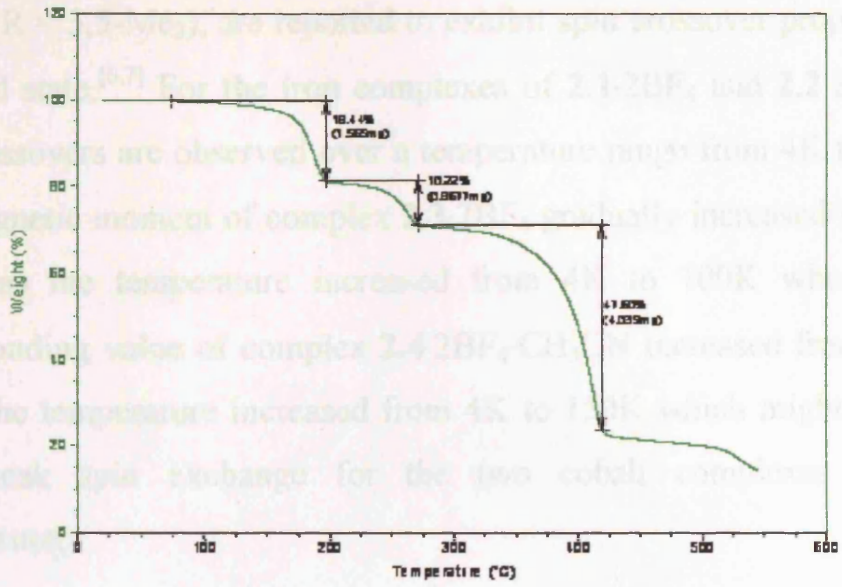

(c)

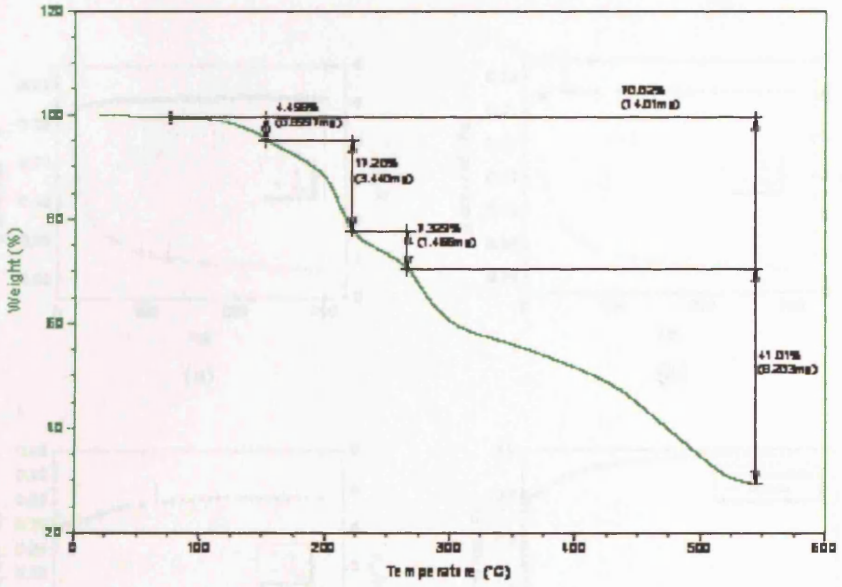

(d)

Magnetic susceptibility studies also confirm that all four tripodal complexes with BF_4^- counter anions are high-spin paramagnetic complexes with μ_{eff} of 5.1 (**2.1**, S = 2), 5.1 (**2.2**, S = 2), 4.6 (**2.3**, S = 3/2) and 4.5 (**2.4**, S = 3/2) respectively in the solid state (**Figure 3**) at room temperature. The bis-ligand Fe(II)/Co(II) complexes, $(Tm^R)_2M(BF_4)_2$ (M=

Fe, Co; R = 3,5-Me_2), are reported to exhibit spin crossover properties in the solid state.[6,7] For the iron complexes of **2.1**·2BF_4 and **2.2**·2BF_4, no spin crossovers are observed over a temperature range from 4K to 300K. The magnetic moment of complex **2.3**·2BF_4 gradually increased from 4.2 to 4.6 as the temperature increased from 4K to 100K whereas the corresponding value of complex **2.4**·2BF_4·CH_3CN increased from 3.4 to 4.4 as the temperature increased from 4K to 150K which might suggest very weak spin exchange for the two cobalt complexes at low temperature.

Figure 3 Magnetic susceptibility diagrams of complexes **2.1**·2BF_4 (a), **2.2**·2BF_4 (b), **2.3**·2BF_4 (c) and **2.3**·2BF_4·CH_3CN (d)

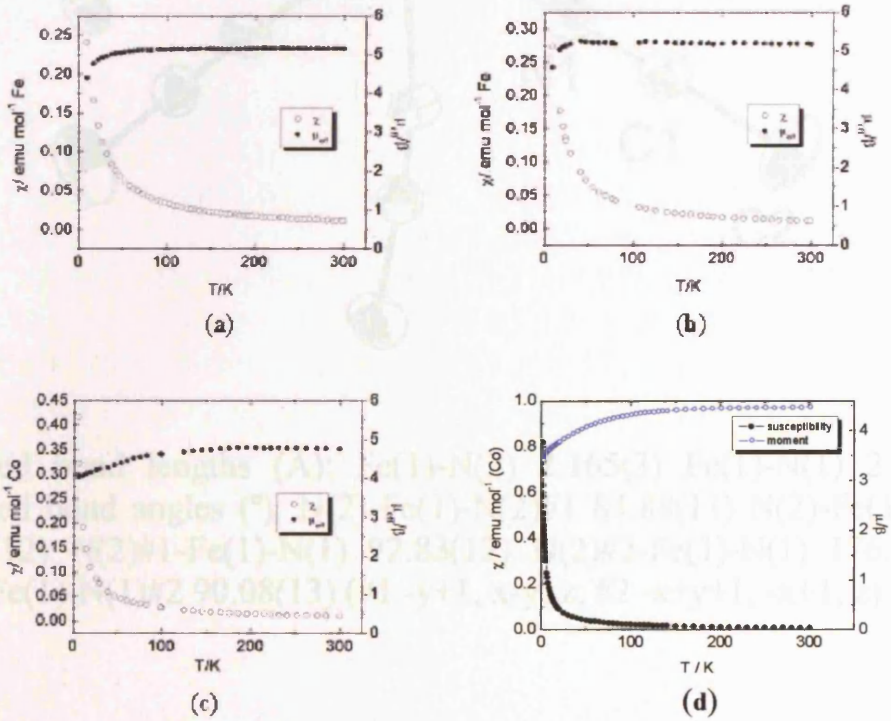

The structures of complexes **2.1** to **2.4** were characterized by X-ray diffraction studies as well. Their crystal structures are illustrated in **Figures 4**, **5**, **6** and **7** respectively. Table 1 gives selected structural parameters for the four tripodal complexes.

Figure 4 ORTEP plot (30% probability level) of **2.1** (H atoms omitted)

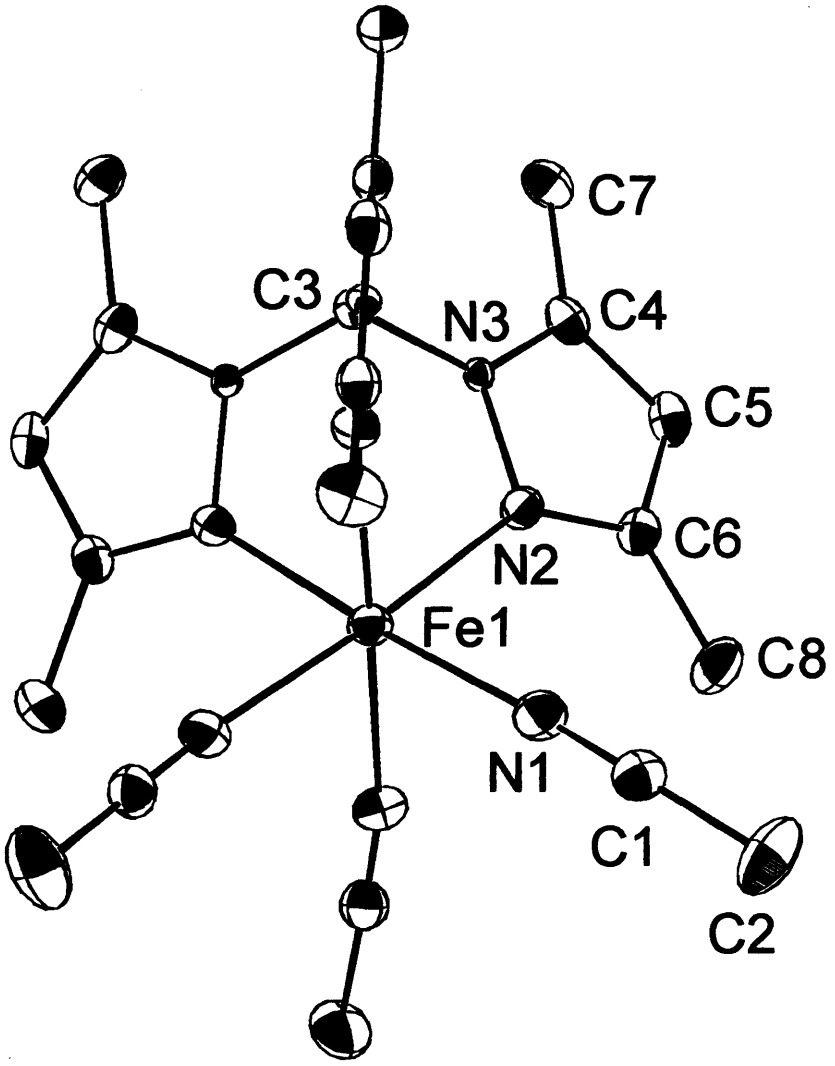

Selected bond lengths (Å): Fe(1)-N(2) 2.165(3) Fe(1)-N(1) 2.165(3) Selected bond angles (°): N(2)-Fe(1)-N(2)#1 84.88(11) N(2)-Fe(1)-N(1) 92.11(12) N(2)#1-Fe(1)-N(1) 92.83(12) N(2)#2-Fe(1)-N(1) 176.36(12) N(1)-Fe(1)-N(1)#2 90.08(13) (#1 -y+1, x-y, z; #2 -x+y+1, -x+1, z)

Figure 5 ORTEP plot (30% probability level) of **2.2** (H atoms omitted)

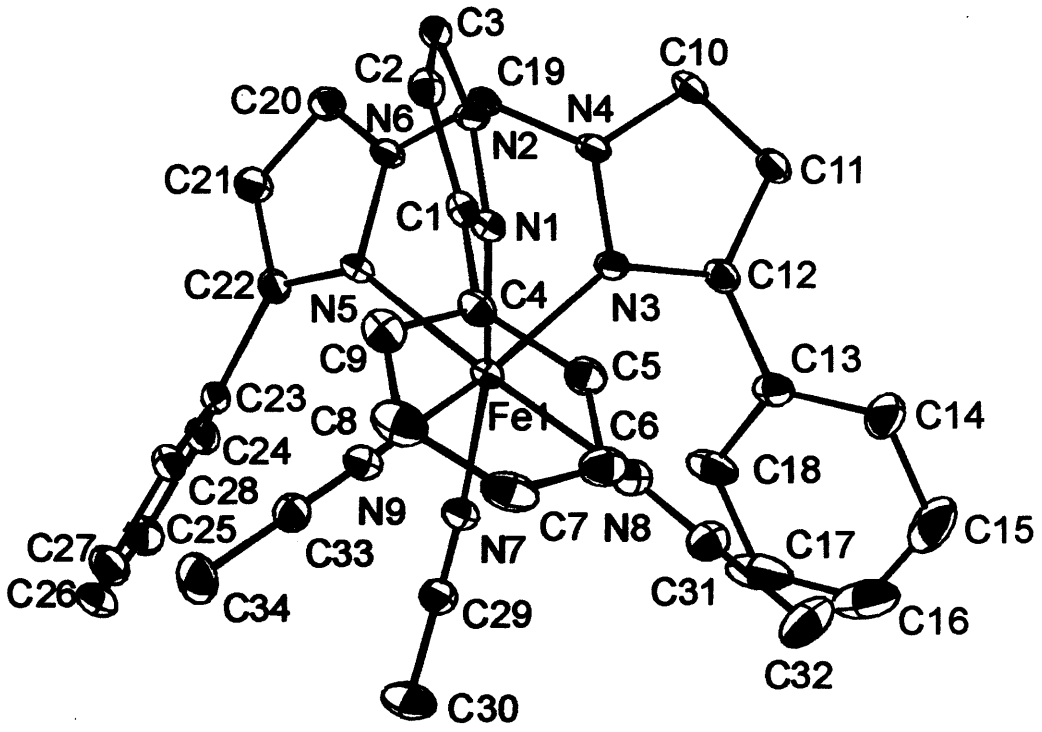

Selected bond lengths (Å): Fe1-N1 2.199(2) Fe1-N3 2.196(2) Fe1-N5 2.205(2) Fe1-N7 2.131(3) Fe1-N8 2.156(3) Fe1-N9 2.165(3) Selected **bond angles (°):** N(7)-Fe(1)-N(8) 86.37(10) N(7)-Fe(1)-N(9) 87.64(10) N(8)-Fe(1)-N(9) 90.29(10) N(7)-Fe(1)-N(3) 101.57(9) N(8)-Fe(1)-N(3) 89.59(10) N(9)-Fe(1)-N(3) 170.76(9) N(7)-Fe(1)-N(1) 172.21(10) N(8)-Fe(1)-N(1) 98.78(10) N(9)-Fe(1)-N(1) 86.50(9) N(3)-Fe(1)-N(1) 84.40(9) N(7)-Fe(1)-N(5) 89.86(9) N(8)-Fe(1)-N(5) 171.10(10) N(9)-Fe(1)-N(5) 97.61(9) N(3)-Fe(1)-N(5) 83.27(9) N(1)-Fe(1)-N(5) 85.84(9) C(1)-N(1)-N(2) 104.6(2)

Figure 6 ORTEP plot (30% probability level) of **2.3** (H atoms omitted)

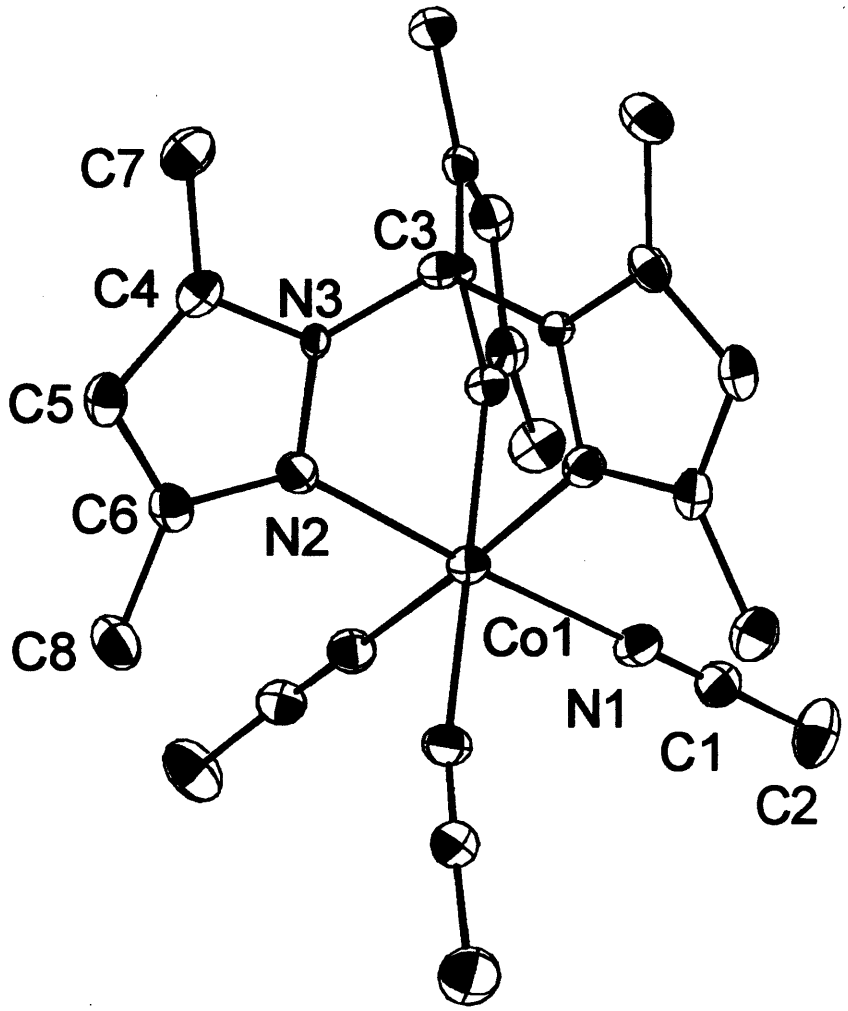

Selected bond lengths (Å): Co(1)-N(1) 2.122(5) Co(1)-N(2) 2.125(4) **Selected bond angles** (°): N(1)-Co(1)-N(1)#1 89.15(18) N(1)-Co(1)-N(2)#2 92.42(17) N(1)#1-Co(1)-N(2)#2 92.96(17) N(1)#2-Co(1)-N(2)#2 177.39(16) N(2)#2-Co(1)-N(2)#1 85.42(17) (#1 -y+1, x-y, z; #2 -x+y+1, -x+1, z)

Figure 7 ORTEP plot (30% probability level) of **2.4** (H atoms omitted)

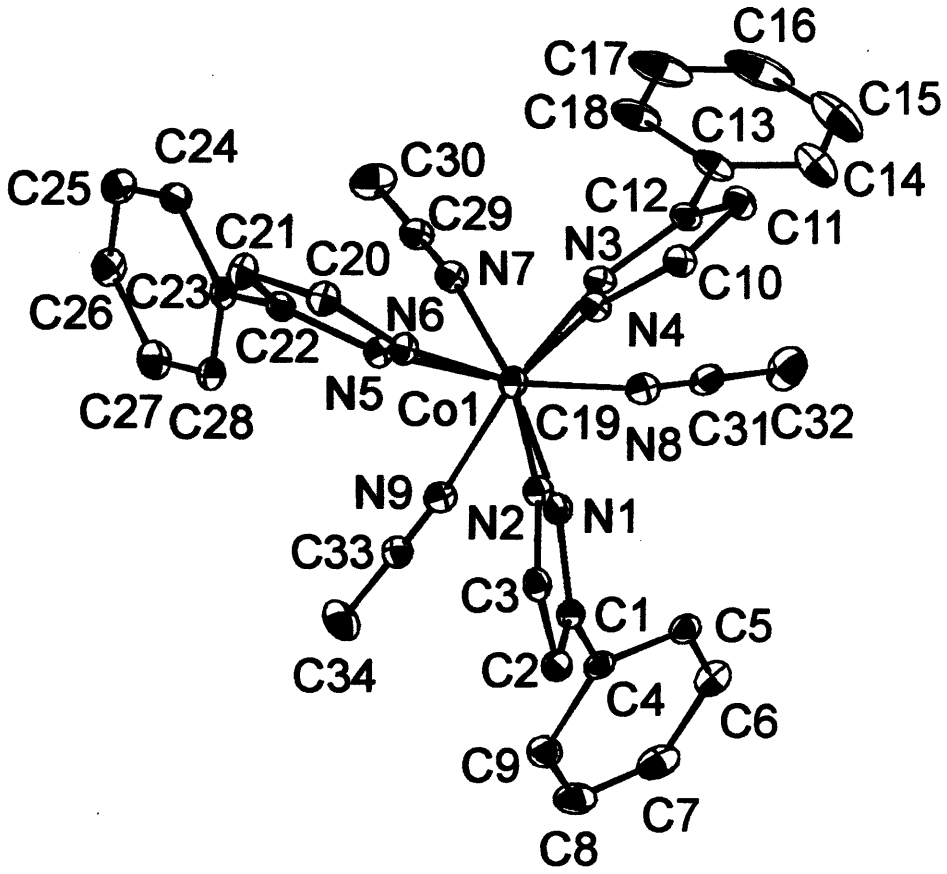

Selected bond lengths (Å): Co1-N1 2.169(2) Co1-N3 2.167(2) Co1-N5 2.172(2) Co1-N7 2.091(2) Co1-N8 2.117(2) Co1-N3 2.129(2) Selected **bond angles (°):** N(7)-Co(1)-N(8) 85.68(9) N(7)-Co(1)-N(9) 86.64(8) N(8)-Co(1)-N(9) 89.25(8) N(7)-Co(1)-N(3) 101.46(8) N(8)-Co(1)-N(3) 90.14(8) N(9)-Co(1)-N(3) 171.81(8) N(7)-Co(1)-N(1) 172.34(8) N(8)-Co(1)-N(1) 98.56(8) N(9)-Co(1)-N(1) 87.04(8) N(3)-Co(1)-N(1) 84.98(8) N(7)-Co(1)-N(5) 90.42(8) N(8)-Co(1)-N(5) 171.84(8) N(9)-Co(1)-N(5) 97.69(8) N(3)-Co(1)-N(5) 83.60(8) N(1)-Co(1)-N(5) 86.13(8)

The ideal molecular symmetry for these complexes is C_{3v} with a 3-fold axis (**2.1** and **2.3**) or pseudo 3-fold axis (**2.2** and **2.4**) which passes through the metal centre and the apical C atom which links the three pyrazole rings. All four tripodal complexes have a similar structure bearing a distorted octahedral metal centre which is coordinated by tris-pyrazolylmethane ligand in tridentate facially capping model and three acetonitrile supporting ligands *trans* to the Tm^R N donors. The metal centres are sandwiched by two roughly parallel nitrogen planes, one defined by the Tm^R nitrogen donors and the other by the acetonitrile nitrogen donors. The average Fe-N bond lengths in **2.1** {2.165(3) Å} and **2.2** {2.175(3) Å} are consistent with the high-spin configuration of the Fe centre in both complexes at 150K. Average bond lengths of ca 1.97 Å are typically observed in low-spin (LS) octahedral FeN_6 complexes.[5,7] The Tm^R ligands chelate the metal centre *via* three fused 6-membered rings which restricts the average M-N-N angles to 84.88(11)°, 84.50(9)°, 85.42(17)° and 84.90(8)° for complexes **2.1** to **2.4** respectively.

The Fe-N bond length between Fe and the Tm^R N donors in **2.1** {2.165(3) Å} is shorter than that in **2.2** {aver. 2.200(2) Å}, and the corresponding Co-N bond lengths in **2.3** {2.125(3) Å} are also shorter than that in **2.4** {aver. 2.169(2) Å}. These M-N bond length changes are consistent with the variation in the steric bulk of the Tm ligand as a function of the substituents (R = phenyl, methyl) on the pryazole ring. The Co-N bond lengths between Co and Tm^R N donors in **2.3** and **2.4** are both longer than those {2.150(4) Å} in the known $[Tp^RCo(CH_3CN)_3]^+$ (Tp = hydrotrispyrazolylborate, R = 3-Ph, 5-Me).[3] This implies that the anionic Tp^R ligand coordinates more tightly to the metal centre than does the neutral Tm^R ligand in complexes **2.3** and **2.4**.

In **2.1** and **2.3**, the M-N(Tm^R) value is almost the same as that of the M-$NCCH_3$ value. In **2.2** and **2.4**, the M-N(Tm^R) values are both much larger than the M-N(CH_3CN) values. The distances of the metal to the N_3 plane centroid (constituted by Tm^R nitrogen donors) for these complexes are also longer than the distances of the metal to the N_3 plane centroid constituted by the acetonitrile nitrogen donors. These values imply that the neutral tripodal ligand coordinates relatively weakly to the metal in comparison to the acetonitrile ligands. This may be due to the steric bulk of the 3-substituent on the pyrazole ring.

Table 1 Selected structural parameters for complexes **2.1**, **2.2**, **2.3** and **2.4**

Complex	**2.1**	**2.2**	**2.3**	**2.4**
M-N(Tm^R) (Å)	2.165(3)	2.199(2) 2.196(2) 2.205(2) aver. 2.200	2.125(3)	2.169(2) 2.167(2) 2.172(2) aver. 2.169
M-N(CH_3CN) (Å)	2.165(3)	2.156(3) 2.131(3) 2.165(3) aver. 2.150	2.122(4)	2.091(2) 2.117(2) 2.129(2) aver. 2.112
Aver. M-N (Å)	2.165(3)	2.175(3)	2.123(4)	2.140(2)
N-M-N(Tm^R) (°)	84.88(11)	84.40(9) 83.27(9) 85.84(9) aver. 84.50	85.41(14)	84.98(8) 83.60(8) 86.13(5) aver. 84.90
Distance of M to N_3 plane of Tm^R (Å)	1.356(3)	1.386(2)	1.322(3)	1.359(2)
Distance of M to N_3 plane of CH_3CN (Å)	1.248(3)	1.282(3)	1.243(4)	1.277(2)

2.3 Reactions of tripodal complexes with phosphine reagents

As a potential template for the synthesis of triphosphamacrocycles, the tripodal metal-ligand fragments need to be stable when treated with phosphine ligands whereas the labile monodentate ligands *trans* to the tripodal ligand within the coordination sphere, need to be replaced sequentially by phosphine ligands. Consequently the tripodal complexes **2.1** to **2.4** were reacted with 1 equivalent of the bidentate phosphine ligands, 1,2-diphosphinoethane (dpe) and 1,2-bis(diallylphosphino)-ethane (tape) (**Scheme 2**) respectively.

Scheme 2 Reactions of complex **2.1** to **2.4** with bidentate phosphine ligands

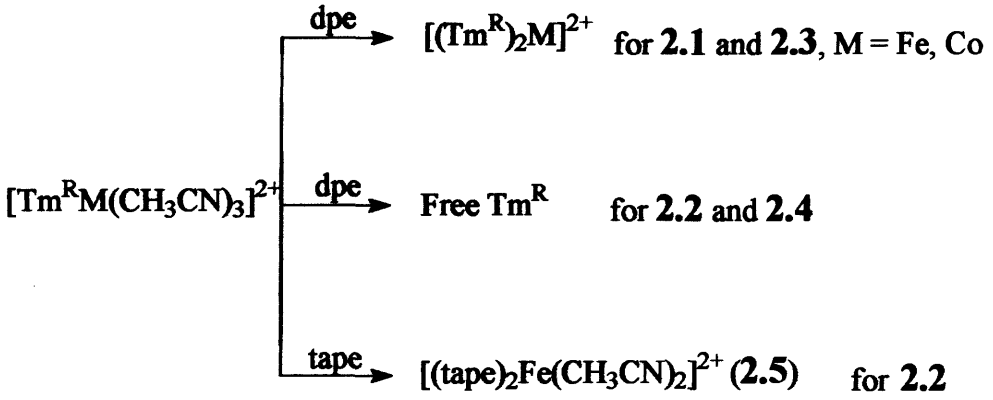

Reactions with the diphosphines did not produce the expected complexes, but resulted in displacement of the tripodal Tm^R ligands. It is likely that the generally weaker binding between the Tm^R ligands and the metal centre (in part due to the steric bulk of the 3-substituent on the pyrazole ring) leads to lability and the displacement of the Tm^R ligands from the metal centre when complexes **2.1** to **2.4** were treated with dpe in solution. The tris(pryazolyl)methane ligands behave as bidentate ligands in complexes $\{M(PMe_3)_2(CO)(COMe)[\eta^2\text{-}(3,5\text{-}Me_2pz)_3CH]\}^+$ (M = Fe, Ru; pz = pyrazolyl ring) may confirms the labile coordination model of such

ligands.[8] In the case of complexes **2.2** and **2.4**, the free tripodal Tm^R ligand was isolated as white powders and identified by NMR spectroscopy and melting point determination. For complexes **2.1** and **2.3** with the less sterically hindered (3,5-dimethyl-pyrazoyl)methane ligand, the bis-tripodal complexes $[(Tm^R)_2M]^{2+}$ (M = Fe, Co) were isolated in low yield (confirmed crystallographically).

The reaction of complex **2.2** with 1,2-bis(diallylphosphino)ethane (**tape**) gives complex **2.5** which has been characterized by X-ray diffraction. **Figure 8** provides the ORTEP diagram of complex **2.5** with selected bond lengths and bond angles. As the structure shows, complex **2.5** does not include the tripodal ligands. The iron centre, with pseudo-octahedral geometry is located on a crystallographic inversion centre coordinated by two bidentate tape ligands in the equatorial plane and two acetonitrile ligands in axial positions.

Figure 8 ORTEP plot (30% probability level) of **2.5** (H atoms omitted)

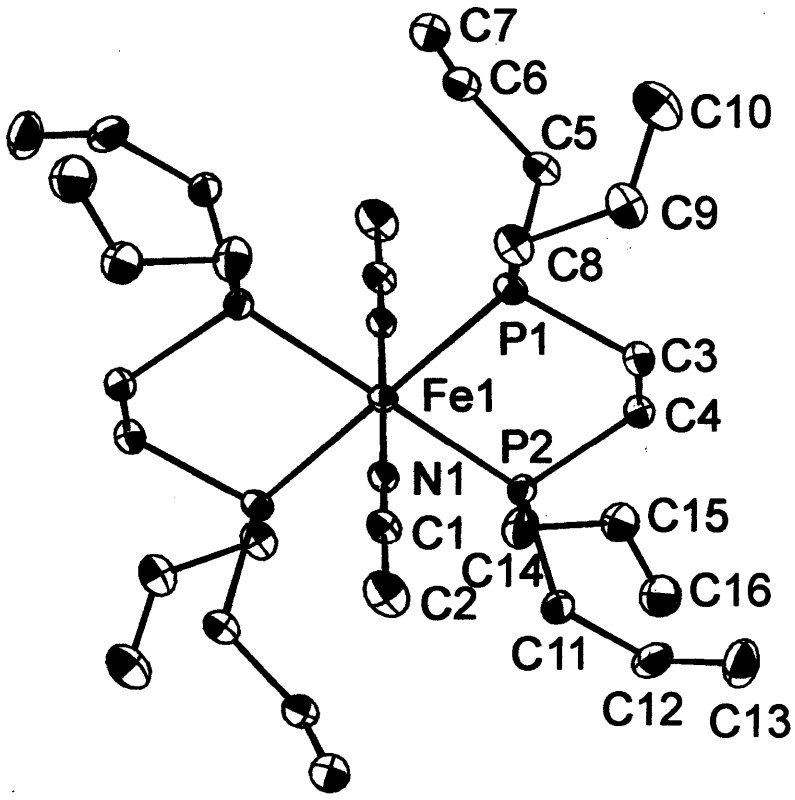

Selected bond lengths (Å): Fe1-N1 1.905(3) Fe1-P1 2.3032(9) Fe1-P2 2.2911(9) Selected bond angles (°): N(1)-Fe(1)-N(1)#1 180.00 N(1)-Fe(1)-P(2)#1 88.72(9) N(1)-Fe(1)-P(2) 91.28(9) N(1)-Fe(1)-P(1) 89.33(9) N(1)-Fe(1)-P(1)#1 90.67(9) P(2)-Fe(1)-P(1) 84.03(3) P(2)-Fe(1)-P(1)#1 95.97(3) P(2)#1-Fe(1)-P(2) 180.00 P(1)-Fe(1)-P(1)#1 180.00 (#1 -x, -y, -z)

2.4 Conclusions

Novel tripodal trispyrazolylmethane complexes of Fe(II)/Co(II) with piano-stool structures supported by acetonitrile ligands have been prepared and characterised. The preliminary investigation of substitution reactions of these complexes with phosphine ligands showed that the LM ($L = Tm^R$) fragment is not resistant enough to displacement, to limit the remaining reaction to sites to be *trans* to the tripodal ligand. Reactions with bis-phosphines lead instead however to substitution of the tripodal ligand. This results in the formation of the more thermally stable bis-ligand ML_2 complex. The removal of the tripodal ligand from the metal centre illustrates the flexiblility of the bonding between the tripodal ligand and the metal in these complexes. Thus these tripodal metal-ligand fragments are not suitable as templates for the synthesis of P_3 marocycles.

2.5 Experimental Section

General experimental information: All reactions were performed under a nitrogen atmosphere with standard Schlenk glassware, vacuum or Glovebox techniques unless otherwise noted. The solvents were dried and degassed by refluxing over standard drying agents and distilled immediately prior to use. Infrared spectra were recorded on a Perkin Elmer 1600 spectrometer using KBr pellets for solid samples. Mass spectra were carried out on a VG Platform II Fisons mass spectrometer. Magnetic susceptibility measurements were performed with a Quantum Design MPMS2 SQUID magnetometer in collaboration with Prof. Andrew Harrison in Edinburgh. TGA measurements were performed on a SDT Q600 thermal analyzer. Elemental analyses were performed by Warwick Analytical Service. X-ray diffraction data collections were carried out on a Bruker Kappa CCD diffractometer at 150(2) K with Mo $K\alpha$ irradiation (graphite monochromator). Empirical absorption corrections were performed using equivalent reflections. For the solution and refinement of the structures, the program package SHELXL 97 was employed.[9] H atoms were placed into calculated positions and included in the last cycles of refinement. Crystal structure and refinement data are collected in **Appendix A** and supplementary CD.

Materials: Tris(3,5-dimethyl-pyrazoyl)methane,[10] tris(3-phenylpyrazoyl)methane,[10] $[M(CH_3CN)_6](BF_4)_2$ (M = Fe, Co),[11] 1,2-diphosphinoethane(dpe),[12] 1,2-bis(diallylphosphino)ethane(tape)[13] were prepared according to literature methods. All other chemicals were obtained from commercial sources and, where appropriate, dried over molecular sieves and degassed by repeated freeze-thaw degassing.

$[Tm^{R}Fe(CH_3CN)_3](BF_4)_2$ (2.1·$2BF_4$, R = 3,5-Me_2)

0.20 g (0.5 mmol) of tris(3,5-dimethyl-pyrazolyl)methane in 10 ml CH_2Cl_2 was gradually added to a solution of 0.22 g (0.50 mmol) $[Fe(CH_3CN)_6](BF_4)_2$ in 20 ml CH_3CN with stirring at room temperature. The solvents were evaporated and 20 ml CH_3CN added to dissolve the solid residue. The solution was filtered and concentrated. Colourless crystals of **2.1**·$2BF_4$ were obtained by vapour diffusion of diethyl ether into the filtrate. M.S.(APCI): 354 {$[Tm^{R}Fe]^{2+}$, in CH_3CN solution}, 468 {$[Tm^{R}Fe(CH_3CN)_2(CH_3OH)]^{2+}$, in CH_3OH solution}. IR (KBr): 2313 (ν_{CN}), 2283 (ν_{CN}). Anal. Calcd for $C_{22}H_{31}N_9B_2F_8Fe_1$ (651.2 $gmol^{-1}$) C, 40.59; H, 4.80; N, 19.36. Found: C, 39.68; H, 4.67; N, 18.85.

$[(Tm^{R})Fe(CH_3CN)_3](BF_4)_2$ (2.2·$2BF_4$, R = 3-Ph)

0.20 g (0.5 mmol) of tris(3-phenylpyrazolyl)methane in 10 ml CH_2Cl_2 was gradually added to a solution of 0.22 g (0.50 mmol) $[Fe(CH_3CN)_6](BF_4)_2$ in 10ml CH_3CN with stirring at room temperature. After half an hour, the volatiles were removed in *vacuo* and 10 ml CH_3CN added to dissolve the solid residue. The solution was filtered and concentrated by evaporating some of the solvent under vacuum. Colourless crystals of **2.2**·$2BF_4$ were obtained by vapour diffusion of diethyl ether into the filtrate. M.S.(APCI): 498 {$[Tm^{R}Co]^{2+}$, in CH_3CN}, 612 {$[Tm^{R}Co(CH_3CN)_2(CH_3OH)]^{2+}$, in CH_3OH}. IR (KBr): 2310 (ν_{CN}), 2282 (ν_{CN}). Anal. Calcd for $C_{34}H_{31}N_9B_2F_8Fe_1$ (795.2 $gmol^{-1}$): C, 51.31; H, 3.93; N, 15.85 Found: C, 50.88; H, 3.85; N, 15.64.

$[(Tm^{R})Co(CH_3CN)_3](BF_4)_2$ (2.3·$2BF_4$, R = 3,5-Me_2)

0.20 g (0.5 mmol) of tris(3,5-dimethylpyrazolyl)methane in 10 ml CH_2Cl_2 was gradually added to a pink solution of 0.22 g (0.50 mmol) $[Co(CH_3CN)_6](BF_4)_2$ in 20 ml CH_3CN with stirring at room temperature.

Tthe solvents were removed and 20 ml CH_3CN added to dissolve the pink solid residue. The solution was filtered and concentrated. Yellow crystalline **2.3**·$2BF_4$ were obtained by vapour diffusion of diethyl ether into the filtrate. M.S.(APCI): 357 {$[Tm^RFe]^{2+}$, in CH_3CN}, 471 {$[Tm^RFe(CH_3CN)_2(CH_3OH)]^{2+}$, in CH_3OH}. IR (KBr): 2316 (ν_{CN}), 2287 (ν_{CN}). Anal. Calcd for $C_{22}H_{31}N_9B_2F_8Co_1$ (654.2 $gmol^{-1}$) C, 40.40; H, 4.78; N, 19.27. Found: C, 39.36; H, 4.84; N, 18.54.

$[(Tm^R)Co(CH_3CN)_3](BF_4)_2$ (2.4·$2BF_4$, R = 3-Ph)

The complex was prepared in an analogous fashion to **2.3**·$2BF_4$. 0.20 g (0.5 mmol) of tris(3-phenylpyrazolyl)methane in 10 ml CH_2Cl_2 was gradually added to a pink solution of 0.22 g (0.50 mmol) $[Co(CH_3CN)_6](BF_4)_2$ in 20 ml CH_3CN with stirring at room temperature. The solvent were removed and 20 ml CH_3CN added to dissolve the pink solid residue. The solution was filtered and concentrated. Red-orange crystals of **2.4**·$2BF_4$·CH3CN were obtained by vapour diffusion of diethyl ether into the filtrate. M.S.(APCI): 501 {$[Tm^RCo]^{2+}$, in CH_3CN}, 615 {$[Tm^RFe(CH_3CN)_2(CH_3OH)]^{2+}$, in CH_3OH}. IR (KBr): 2318 (ν_{CN}), 2291 (ν_{CN}). Anal. Calcd for $C_{36}H_{34}N_{10}B_2F_8Co_1$ (**2.4**·$2BF_4$·CH_3CN, M = 839.28 g mol^{-1}): C, 51.48; H, 4.08; N, 16.69. Found: C, 51.24; H, 4.04; N, 16.44.

$[(tape)Fe(CH_3CN)_2](BF_4)_2$ (2.5·$2BF_4$)

0.7 ml of 10% 1,2-bis(diallylphosphino)ethane(tape) (0.27 mmol) in THF was added dropwise to a solution of **2.2**·$2BF_4$ (0.21 g, 0.25 mmol) in 20 ml CH_2Cl_2 with stirring in room temperature. The colour of reaction mixture changed to pale brown. The volatiles were removed in *vacuo* and the solid residue dissolved in CH_2Cl_2. The solution was filtered and concentrated. Red crystals of **2.5**·$2BF_4$ were obtained by vapour diffusion of diethyl ether into the filtrate.

References

1. S. Trofimenko, *Chem. Rev.* **1993**, 93, 943.
2. H. R. Bigmore; S. C. Lawrence; P. Mountford; C. S. Tredget, *J. Chem. Soc., Dalton Trans.*, **2005**, 635-651.
3. K, Uehara; S, Hikichi; M, Akita, *J. Chem. Soc., Dalton, Trans.*, **2002**, 3529-3528.
4. D. L. Reger; C. A. Little; G. J. Long, et al. *Inorg. Chim. Acta*, **2001**, 316, 65-70.
5. (a) P. Gütlich, in Mössbauer *Spectroscopy Applied to Inorganic Chemistry* (Ed.: G. J. Long), Plenum: New York, **1984**; Vol. 1, P287; (b) P. Gütlich, A. Hauser, H. Spiering, *Angew. Chem. Int. Ed. Engl.* **1994**, 33, 2024-2044; (c) O. Kaln, J. Martinez, *Science* **1998**, 279, 44-68.
6. D. L. Reger; C. A Little; M. D. Smith, *Inorg. Chem.* **2002**, 41, 4453-4460.
7. (a) D. L. Reger; C. A Little; G. J. Long *et al*, *Eur. J. Inorg. Chem.* **2002**, (5), 1190-1197;
8. A. Macchioni, G. Bellachioma, G. Cardaci, *Organometallics* **1997**, 16, 2139-2145.
9. G. M. Sheldrick, *SHELXTL97, Program for the refinement of Crystal Structures*, University of Goettingen, Germany, **1997**.
10. D. L. Reger; T. C. Grattan *et al J. Organomet. Chem.* 607, **2000**, 120-128.
11. (a) B.J. Hathaway, A.E. Underhill, *J. C. S.* **1960**, 3705-3711; (b) B.J. Hathaway, A.E. Underhill, *J. C. S.* **1962**, 2444-2449.
12. L. Maier, *Helv. Chim. Acta* **1966**, 49, 842.
13. N. P. Cooper, Doctoral thesis, **1991**, Cardiff University

Chapter 3

Cyclobutadienylcobalt Template Complexes

Abstract

The cationic solvated complex (tetramethylcyclobutadienyl)cobalt-(trisacetonitrile), $[Cb^*Co(NCCH_3)_3]^+$ ($Cb^* = \eta^4$-C_4Me_4) (**3.1**), allows the stepwise introduction of suitable phosphine precursors to the Cb^*Co^+ fragment by replacement of the labile acetonitrile ligands. These reactions give rise to the piano-stool complexes, $[Cb^*Co(dppe)(NCCH_3)]^+$ (**3.2**), $[Cb^*Co(dppe)(PH_2Ph)]^+$ (**3.3**), $[Cb^*Co(dfppb)(NCCH_3)]^+$ (**3.4**) and $[Cb^*Co(dfppb)(PH_2Ph)]^+$ (**3.5**), where dfppb = 1, 2-bis(di-2-fluorophenyl-phosphino)benzene and dppe = 1,2-bis(diphenylphosphino)ethane. Selected examples behave as alternative templates for the synthesis of P_3 macrocycle complex, $[Cb^*Co\{1,4\text{-bis}(2\text{-fluorophenyl})\text{-}7\text{-phenyl-}[b,e,h]\text{tribenzo-}1,4,7\text{-triphosphacyclononane}\}]^+$ (**3.6**), promoted by $KOBu^t$ in almost quantitative yield. The ring-methyl of the teramethylcyclobutadienyl ligand of the macrocycle complex (**3.6**) can be activated with concomitant coupling to the *ortho* position of a PC_6H_4 group of the macrocycle by intramolecular dehydrofluorination to give the hybrid phosphorus-carbon donor complex, $\{\eta^4, \kappa P, \kappa P, \kappa P\text{-}Me_2C_4\text{-}[1,4\text{-bis}(2\text{-}CH_2C_6H_4)\text{-}7\text{-}C_6H_5\text{-}[b,e,h]\text{tribenzo-}1,4,7\text{-triphosphacyclo-nonane}]\text{-}1,2\}Co^+$ (**3.7**), in which the P_3 macrocycle bears two 2-methylphenyl bridges to the cyclobutadienyl function.

3.1 Introduction

As mentioned previously, formation of P_3 macrocycles with smaller than 12-membered ring-sizes has required the use of the η^5-Cp^RFe^+ (R = H or alkyl) template complexes instead of the $(CO)_3Cr$ or $(CO)_3Mo$ template fragments. The recent availability of the piano-stool complex, (tetramethylcyclobutadienyl)cobalt-trisacetonitrile,[1] $[Cb^*Co(NCCH_3)_3]^+$ ($Cb^* = \eta^4$-C_4Me_4), prompted us to investigate the potential application of this complex fragment as an alternative template for the synthesis of small ring P_3 macrocycles for several reasons. Firstly, these $Cb^*CoL_3^+$ species are isoelectronic and isostructural with the successful template precursors $Cp^RFeL_3^+$, $(CO)_3CrL_3$, and $(CO)_3MoL$. All have d^6 metal centres with a pseudo octahedral configuration with inert capping ligands (3 x CO for Cr and Mo, Cp^R for Fe, Cb^* for Co) occupying three facial positions and the other three positions are occupied by labile monodentate ligands (*eg.* 3 x CH_3CN or η^6-aryl for Mo). In practice, this arrangement should enable the introduction of phosphine precursors to the metal centre through replacement of the labile ligands allowing subsequent formation of P_3 macrocycles by a range of P-C bond forming methods. And with low-spin d^6 metal centre the reactions can be easily monitored by NMR spectroscopy. Secondly, Co(III) has a smaller radius then Fe(II) (covalent, 1.28 Å for Co and 1.26 for Fe[2]) and the steric bulk imposed by the Cb^* ligand may help force the phosphine precursor into a close proximity which facilitates the formation of smaller ring P_3 macrocycles through intramolecular P-C bond formation reactions. Thirdly, the monocationic Cb^*Co^+ fragment should enhance solubilities of intermediates and P_3 macrocycle complex products in most polar solvents. The importance of solubility is highlighted by $[Cp^*Co(NCCH_3)_3]^{2+}$ (Cp^* = C_5Me_5) which has been previously

investigated in our laboratory as a template for the synthesis of phosphorus macrocycles.[3] In this case, solubility problems of the phosphine precursor complexes in most suitable solvents prevented ring closure to form the target complexes. Fourthly, the predicted instability of the Cb* moiety (relative to Cp^R complexes), which can be reduced by lithium metal,[4] oxidised[5] or attacked by both nucleophiles[6,7] or electrophiles[8] may enhance the potential to liberate any P_3 macrocycles formed on this template.

The preparation of $[Cb^*Co(NCCH_3)_3]^+$ according to literature[1,9] methods is presented in **Scheme 1** below.

Scheme 1 Preparation of $[Cb^*Co(NCCH_3)_3]^+$ and related complexes

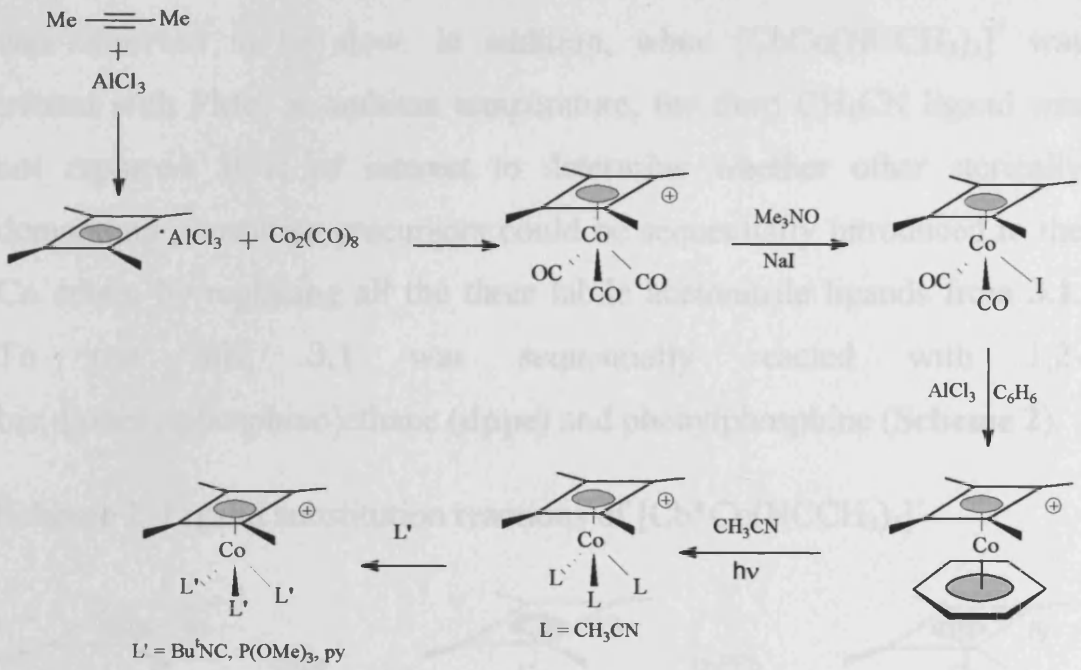

The reaction of 2-butyne with aluminium chloride gives rise to the cocyclodimerization complex, η^1-$C_4Me_4AlCl_3$. This was reacted with octacarbonyldicobalt affording $[Cb^*Co(CO)_3]^+$ which was isolated as a PF_6^- salt. The salt was then converted to $Cb^*Co(CO)_2I$ by reaction with Me_3NO (to abstract CO) and NaI. The arene complex, $[Cb^*Co(benzene)]^+$, was formed by refluxing the iodo complex in

benzene in the presence of $AlCl_3$ as a Lewis acid catalyst. The target complex, $[Cb^*Co(NCCH_3)_3]^+$, was finally obtained by either photolysis of the arene complex or thermal ligand exchange in acetonitrile.

3.2 Ligand substitution reactions of $[Cb^*Co(NCCH_3)_3]^+$

Although $[Cb^*Co(NCCH_3)_3]^+$ (**3.1**) has a close steric and electronic analogy to $[Cp^RFe(NCCH_3)_3]^+$, differences between the two species are apparent. The Co(III) centre has a smaller radius and is a harder Lewis acid than Fe(II). According to the literature,[1] when $[Cb^*Co(NCCH_3)_3]^+$ was treated with excess $P(OMe)_3$, the substitution of the third CH_3CN was observed to be slow. In addition, when $[CbCo(NCCH_3)_3]^+$ was treated with PMe_3 at ambient temperature, the third CH_3CN ligand was not replaced. It is of interest to determine whether other sterically demanding phosphine precursors could be sequentially introduced to the Co centre by replacing all the three labile acetonitrile ligands from **3.1.** To test this, **3.1** was sequentially reacted with 1,2-bis(diphenylphosphino)ethane (**dppe**) and phenylphosphine (**Scheme 2**).

Scheme 2 Ligand substitution reactions of $[Cb^*Co(NCCH_3)_3]^+$

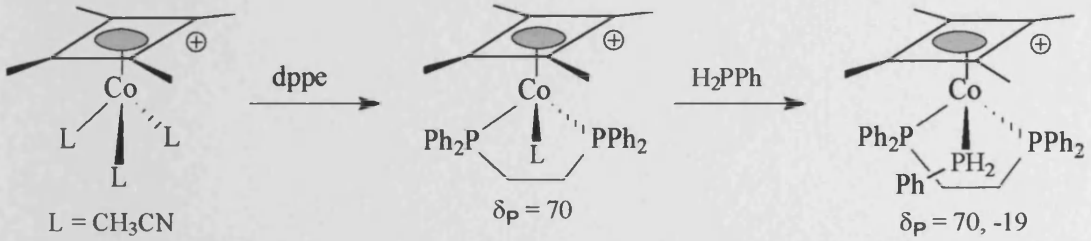

L = CH_3CN — **3.1**

$\delta_P = 70$ — **3.2**

$\delta_P = 70, -19$ — **3.3**

Treatment of **3.1** in acetonitrile with a molar equivalent of **dppe** causes the rapid displacement of two CH_3CN ligands affording the

bisphosphine-monoacetonitrile complex **3.2**, $[Cb^*Co(dppe)(NCCH_3)]^+$, which shows a resonance at δ 70.2 ppm in the ^{31}P NMR spectrum. The chemical shift is consistent with a 5-membered chelate ring.[10] The replacement of the third CH_3CN ligand was carried out by reacting **3.2** with another molar equivalent of phenylphosphine in CH_2Cl_2 to give the bisphosphine-monophosphine complex **3.3**, $[Cb^*Co(dppe)(PH_2Ph)]^+$. In the $^{31}P\{^1H\}$ NMR spectrum of **3.3**, the resonances of coordinated **dppe** and coordinated phenylphosphine are observed at δ 70.2 ppm and δ -18.6 ppm (with $^1J_{H,P}$ = 336 Hz in the ^{31}P NMR spectrum) respectively.

Complexes **3.2** and **3.3** were crystallized as PF_6^- salts and characterized by X-ray crystallography. Their structures are shown in **Figure 1** and **Figure 2** respectively.

Figure 1 ORTEP plot (30% probability level) of **3.2** (H atoms omitted)

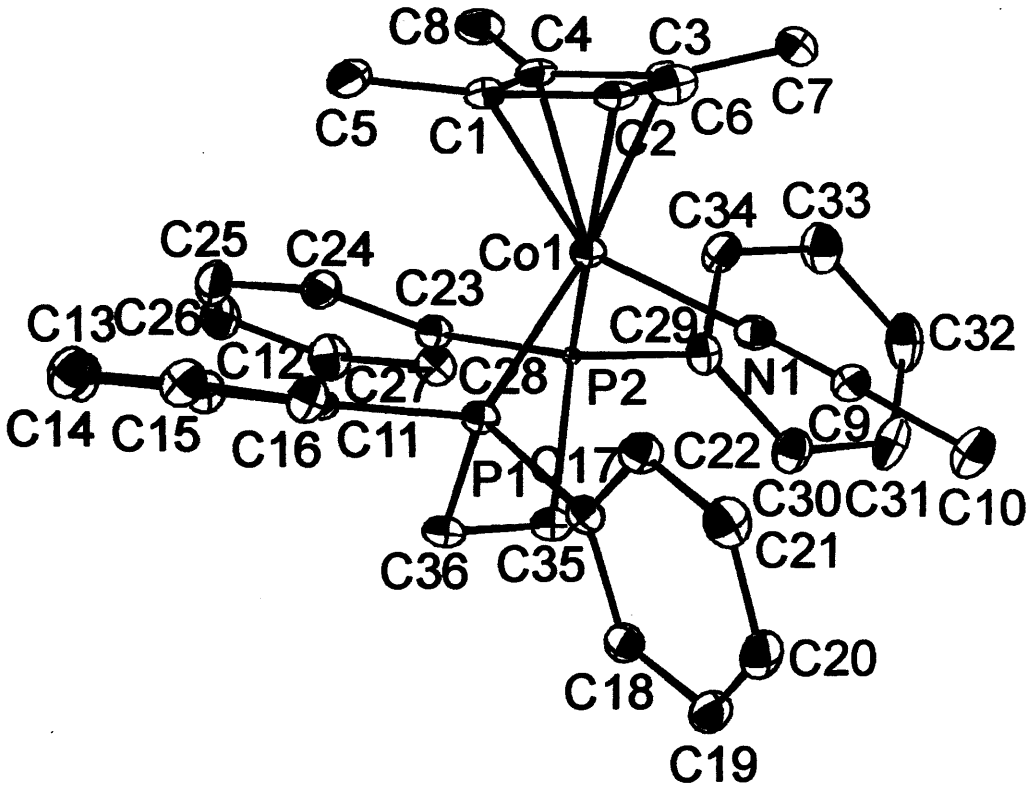

Selected bond lengths (Å): Co1-N1 1.930(3) Co1-P1 2.2400(9) Co1-P2 2.2086(9) Co1-C1 2.047(3) Co1-C2 2.013(3) Co1-C3 2.010(3) Co1-C4 2.057(3) **Selected bond angles (°):** N1-Co1-P1 91.98(8) N1-Co1-P2 90.92(8) P1-Co1-P2 87.15(3)

Figure 2 ORTEP plot (30% probability level) of **3.2** (H atoms on phenyl and methyl groups omitted)

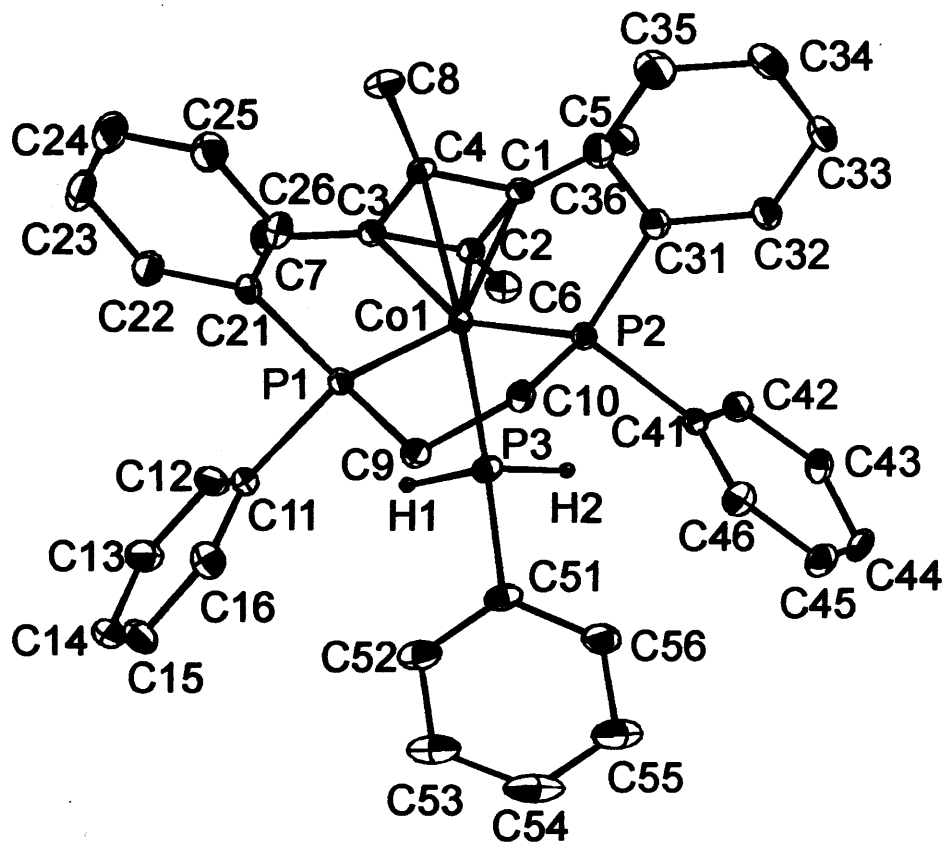

Selected bond lengths (Å): Co1-P1 2.2043(7) Co1-P2 2.2116(7) Co1-P3 2.2196(8) Co1-C1 2.065(2) Co1-C2 2.088(2) Co1-C3 2.044(2) Co1-C4 2.027(2) Selected bond angles (°): P1-Co1-P2 89.88(3) P1-Co1-P3 96.18(3) P2-Co1-P3 98.58(3)

The structures of **3.2** and **3.3** confirm the sequential replacement of labile CH_3CN ligands from the starting material, $[Cb^*Co(NCCH_3)_3]^+$. Both complexes **3.2** and **3.3** have three-legged piano-stool geometries about pseudooctahedral cobalt. The η^4-tetramethylcyclobutadiene ligand coordinates in a facial fashion to the Co(III) centre by occupying three coordination sites. Bidentate **dppe** occupies two *cis* coordination sites as expected with the last coordination site being occupied by CH_3CN in **3.2** or phenylphosphine in **3.3**. The distance of Co to the plane defined by the cyclobutadiene carbons (plane C_4) is 1.752(3) Å for **3.2** and 1.782(2) Å for **3.3** which are both larger than that in **3.1** {1.670(10) Å}. This is presumably due to the relatively weak π–acceptor/good σ-donor properties of acetonitrile ligands in **3.1** which allows for a stronger Co-Cb* interaction compared to that in **3.2** and **3.3**.[1] There is also expected to be a larger repulsion between the phosphine ligands (in **3.2** and **3.3**) and Cb* than between acetonitrile and Cb* (in **3.1**). The average Co-P bond length in **3.2** is 2.224(1) Å, while the Co-N bond length of 1.930(3) Å is less than the average value of 1.950(7) Å in **3.1**. In **3.3**, the plane defined by the P atoms (plane P_3) is roughly parallel to the C_4 plane with a deviation of 3.2°. The distance of Co to the centre of the P_3 plane is 1.161(1) Å; the Co-PH_2Ph bond length of 2.219(1) Å is similar to those between Co centre and chelate P donors {aver. 2.207(1) Å} in **3.3**.

3.3 Synthesis of tribenzannulated 9-membered triphospha-macrocycles based on tetramethylcyclobutadienyl templates

We have demonstrated above that both bisphosphine and monophosphine ligands may be sequentially incorporated into the Cb^*Co^+ fragment by replacing the labile acetonitriles from **3.1**. Thus the Cb^*Co^+ fragment appears suitable for pre-organising the phosphine precursors, placing them in close proximity. If **dppe** in **3.3** can be replaced by other bisphosphines bearing an appropriate functionality, e.g. *o*-F aryl, intramolecular ring closure may be encouraged to occur.

Our strategy for the synthesis of tribenzannulated triphospha-cyclononanes is outlined in **Scheme 3**, and is based upon the methodology established in our laboratory using the Cp^RFe^+ template.[11]

Scheme 3 Synthesis of tetramethylcyclobutadienylcobalt(III)-1,4-bis(2-fluorophenyl)-7-phenyl-[b,e,h]tribenzo-1,4,7-triphosphacyclononane.

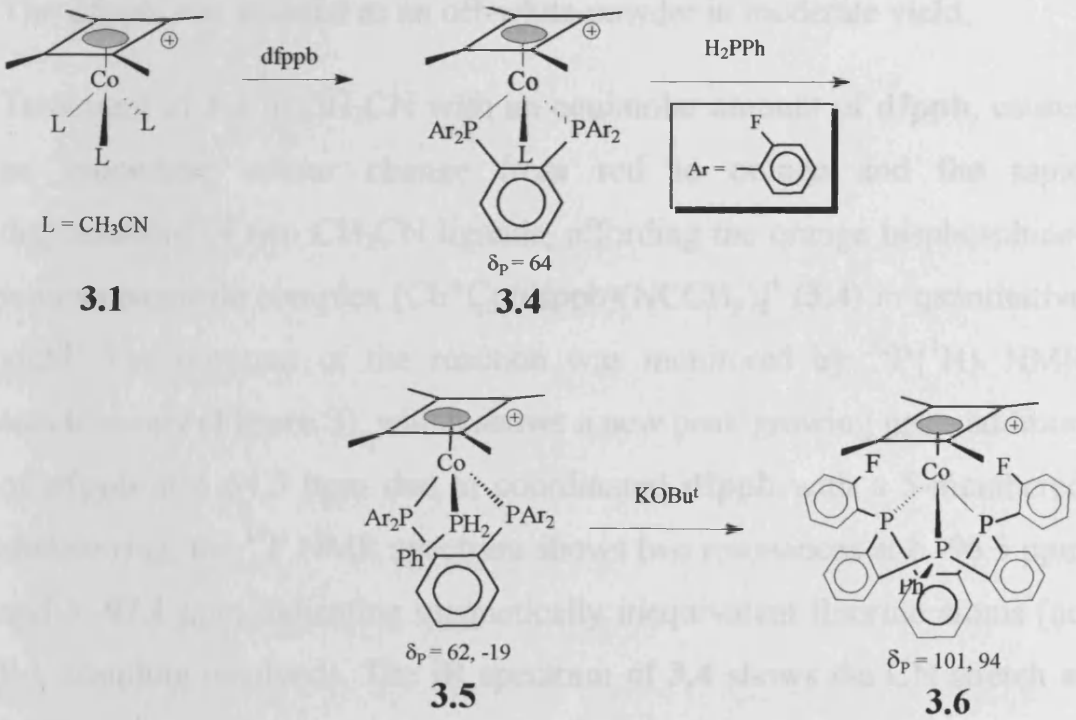

The bisphosphine ligand, 1,2-bis(di-2-fluorophenylphosphino)benzene (**dfppb**) (**Scheme 4**) was recently prepared in our laboratory and it was successfully used in the synthesis cyclopentadienyl-Iron(II)-1,4-bis(2-fluorophenyl)-7-phenyl-[b,e,h]tribenzo-1,4,7-triphosphacyclo-nonane.[10,11]

Scheme 4 Preparation of 1,2-bis(dichlorophosphino)benzene

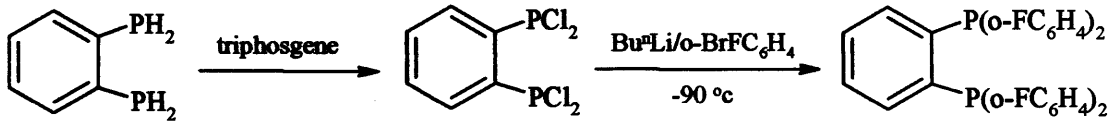

In a modification of the procedure by Kyba,[12] substituting phosgene by triphosgene, 1,2-bis(dichlorophosphino)benzene was prepapred by reaction of 1,2-diphosphinobenzene and triphosgene. The fluoroaryl derivative **dfppb** was subsequently prepared by addition of 1,2-bis(dichlorophosphino)benzene to a solution of Li[*o*-F-C_6H_4], formed by addition of Bu^nLi to 2-bromofluorobenzene in diethyl ether at -100 °C. The **dfppb** was isolated as an off-white powder in moderate yield.

Treatment of **3.1** in CH_3CN with an equimolar amount of **dfppb**, causes an immediate colour change from red to orange and the rapid displacement of two CH_3CN ligands, affording the orange bisphosphine-monoacetonitrile complex $[Cb^*Co(dfppb)(NCCH_3)]^+$ (**3.4**) in quantitative yield. The progress of the reaction was monitored by $^{31}P\{^1H\}$ NMR spectroscopy (**Figure 3**), which shows a new peak growing upon addition of **dfppb** at δ 64.3 ppm due to coordinated **dfppb** with a 5-membered chelate ring; the ^{19}F NMR spectrum shows two resonances at δ -96.5 ppm and δ -97.1 ppm indicating magnetically inequivalent fluorine atoms (no P-F coupling resolved). The IR spectrum of **3.4** shows the CN stretch at 2269 cm^{-1}.

Figure 3 $^{31}P\{^{1}H\}$ NMR spectrum of **3.4**

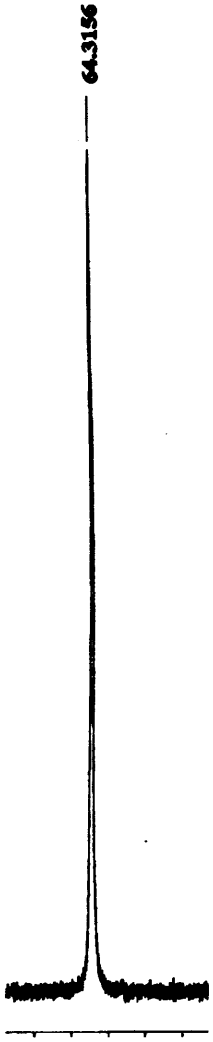

The CH_3CN ligand in **3.4** is labile enough to be exchanged by another equimolar amount of phenylphosphine which affords the bis(phosphine)-mono(phosphine) complex $[Cb^*Co(dfppb)(PH_2Ph)]^+$ (**3.5**). No obvious colour change (following addition of phenylphosphine) was observed, however, a new resonance at δ -19.6 ppm in the $^{31}P\{^{1}H\}$ spectrum confirms coordination of phenylphosphine ($^{1}J_{H,P}$ = 339 Hz in the ^{31}P NMR spectrum); and the coordinated **dfppb** is observed at δ 61.7 ppm (**Figure 4**). The ^{19}F NMR spectrum shows two resonances at δ -96.3 ppm and δ -97.2 ppm (no P-F coupling resolved). The IR spectrum of

compound **3.5** shows the absence of band due to CN group indicating loss of CH_3CN; the PH bond stretches appear at 2304 and 2335 cm^{-1}.

Figure 4 ^{31}P NMR spectrum of **3.5**

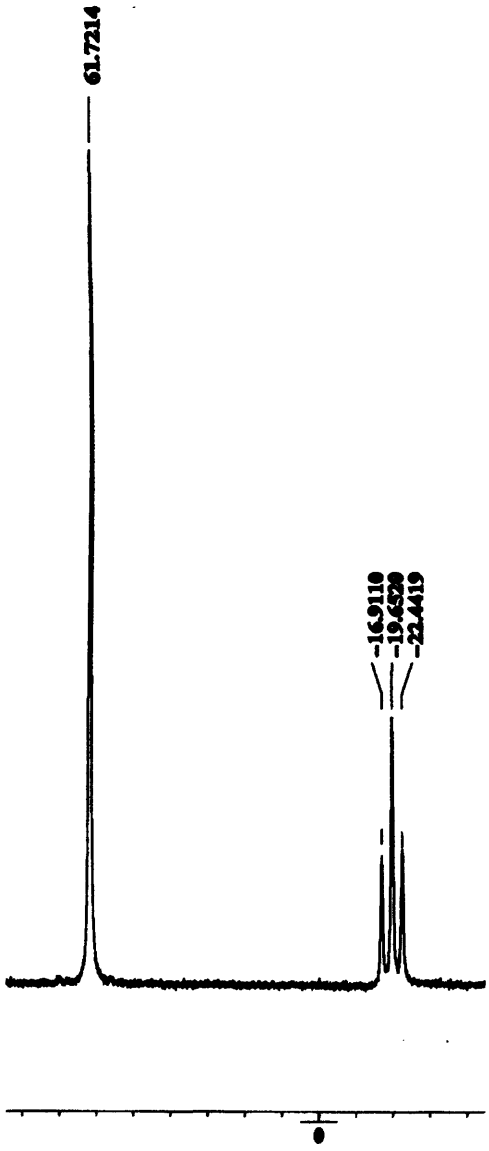

The cyclisation reaction producing the macrocycle complex [Cb*Co{1,4-bis(2-fluorophenyl)-7-phenyl-[b,e,h]tribenzo-1,4,7-triphosphacyclono-nane}]$^+$ (**3.6**) was performed by addition of $KOBu^t$ to a solution of complex **3.5** in THF. The mechanism is presumed to involve base deprotonation of the coordinated phenylphosphine to produce the phosphide anion, which then acts as a nucleophile substituting the

fluorine on the adjacent -P(*o*-F-$C_6H_4)_2$, and resulting in ring-closure (**Scheme 5**).

Scheme 5: Base promoted substitution of *ortho*- fluoride

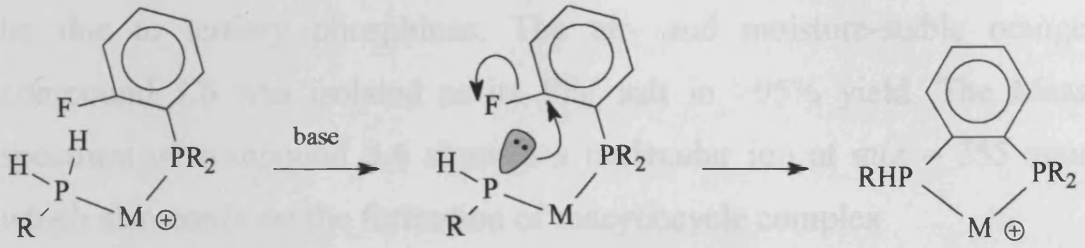

1) Coordinated phosphine and electron withdrawing metal activates arylfluoride to facile substitution.
2) Coordinated phosphide must remain nucleophilic after deprotonation, *i.e.* require 18 electron complexes.
3) The metal centre holds the phosphide nucleophile and *ortho* fluoro-phenyl group in close proximity.

For the phosphide to remain nucleophilic, the template complex should be coordinatively saturated (i.e. an 18 electron complex) to avoid the phosphide acting as a base to other metal centre. The overall process may be described as an intramolecular dehydrofluorinative P-C coupling reaction *via* nucleophilic aromatic substitution promoted by base. The substitution will also be assisted if the phosphine is *ortho* to the leaving group since it will be coordinate to an electron-withdrawing metal favouring the S_NAr reaction.

After addition of 2 mol equivalents of $KOBu^t$ to a solution of **3.5** in THF, the colour of the solution immediately changed from orange to red, then back to orange again in less than one minute, the red colour is interpreted as due to the intermediate phosphide complex. The ^{31}P NMR spectrum of the reaction solution was recorded, the chemical shifts of the coordinated

primary phosphine and diphosphine disappeared simultaneously with the growth of two new peaks significantly downshifted to δ 100.9 ppm and δ 94.8 ppm and with relative intensities of 1:2 respectively (AB_2 pattern) (**Figure 5**). No P-H coupling was observed indicating these resonances to be due to tertiary phosphines. The air- and moisture-stable orange compound **3.6** was isolated as its PF_6^- salt in >95% yield. The Mass spectrum of compound **3.6** showed a molecular ion at m/z = 755 amu which also confirms the formation of macycocycle complex.

Figure 5 $^{31}P\{^1H\}$ NMR spectrum of complex **3.6**

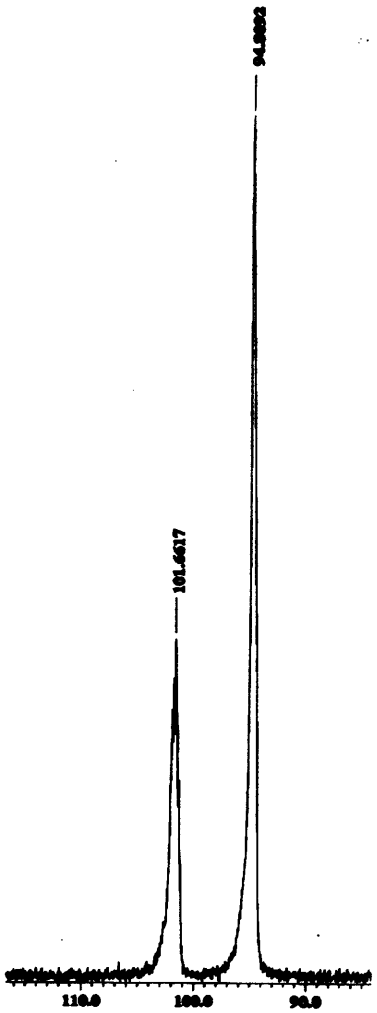

$^{31}P\{^1H\}$ and $^{19}F\{^1H\}$ NMR spectra of compound **3.6** appear as complicated AB_2XX' (A, B = P, X = F) spin systems. The P-F coupling and P-P coupling could not be resolved. The $^{19}F\{^1H\}$ spectrum of **3.6** is temperature dependent suggesting fluxional processes arising from sterically hindered rotation of the *o*-fluorophenyl group around the P-C_{ipso} bonds (**Figure 6**). The hindered rotation and conformational dynamics in solution renders the F atoms inequivalent. At room temperature, $^{19}F\{^1H\}$ NMR spectra recorded in $(CD_3)_2SO$ show four broad singlets. At elevated temperature (70 °C), the fluorophenyl rotation becomes fast and only two averaged lines are observed. At low temperature, $^{19}F\{^1H\}$ NMR spectra recorded in CD_2Cl_2 also show four broad singlets. The presence of two peaks in the high temperature spectrum suggests another magnetically distinct species (isomer) in solution. This might due to the conformatiom of the backbone residing in an inverted position with two aryl group pointing away from the metal. This system needs further study to resolve this issue.

Figure 6 Variable temperature $^{19}F\{^1H\}$ NMR spectra of **3.6**

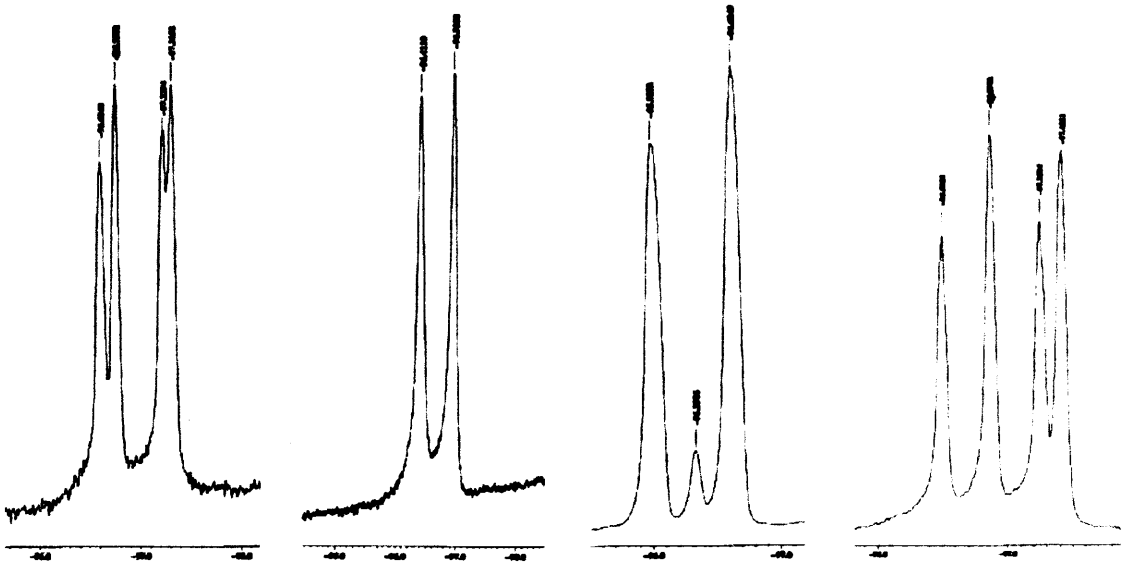

20 °C, D_6-DMSO (a) 70 °C, D_6-DMSO (b) 20 °C, CD_2Cl_2 (c) -50 °C, CD_2Cl_2 (d)

Complexes **3.4, 3.5** and **3.6** were crystallized as PF_6^- salt and characterized by X-ray crystallography. Their structures are shown in **Figures 7, 8** and **9** respectively.

Figure 7 ORTEP plot (30% probability level) of $[Cb^*Co(dfppb)(CH_3CN)]^+$ **(3.4)** (H atoms omitted)

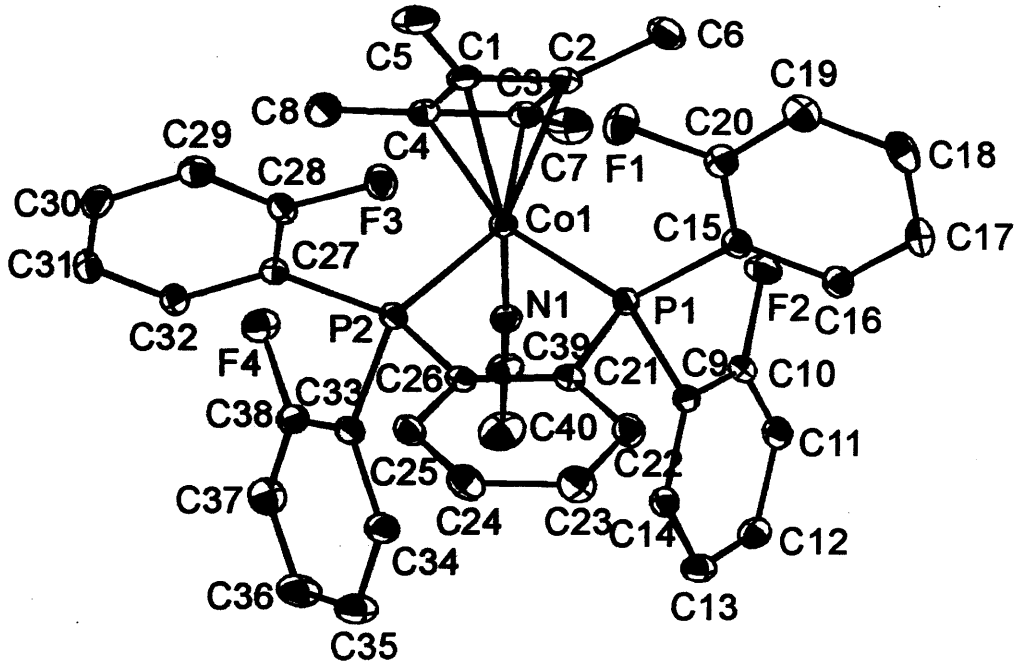

Selected bond lengths (Å): Co1-N1 1.934(2) Co1-C1 2.032(3) Co1-C2 2.087(3) Co1-C3 2.060(3) Co1-C4 2.015(3) Co1-P1 2.2241(8) Co1-P2 2.2260(8) Selected bond angles (°): N1-Co1-P1 95.79(7) N1-Co1-P2 94.46(8) P1-Co1-P2 85.85(3)

Figure 8 ORTEP plot (30% probability level) of $[Cb^*Co(dfppb)(PH_2Ph)]^+$ **(3.5)** (H atoms on phenyl and methyl groups omitted)

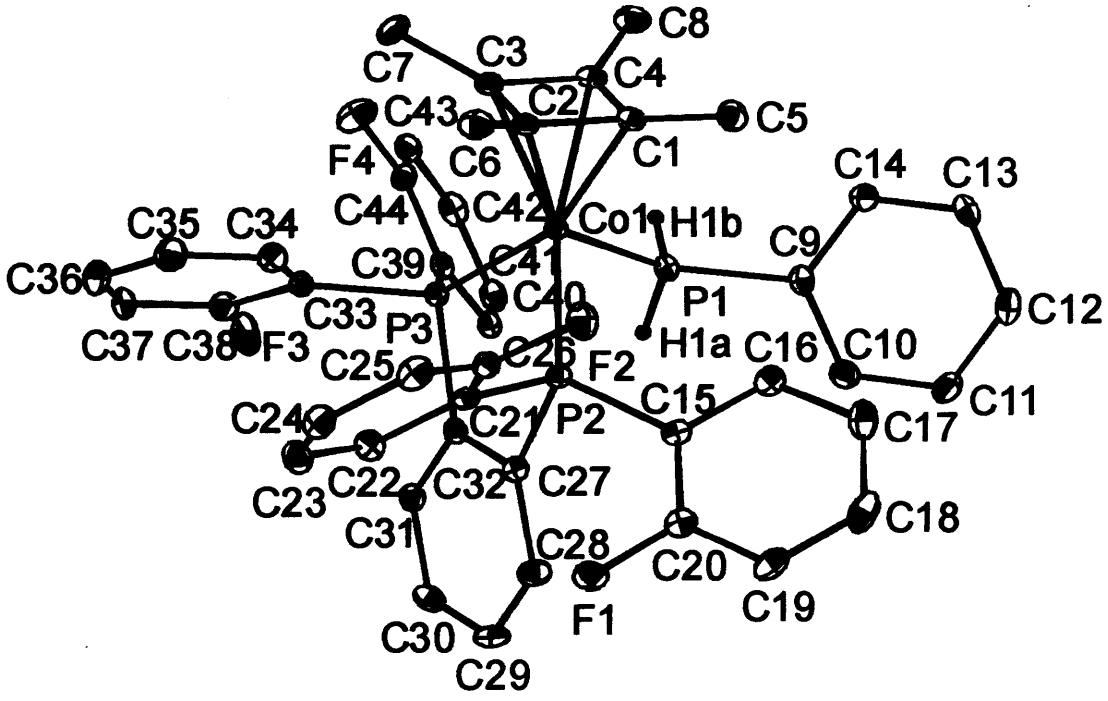

Selected bond lengths (Å): Co1-C1 2.023(3) Co1-C2 2.078(3) Co1-C3 2.104(3) Co1-C4 2.053(3) Co1-P1 2.2190(8) Co1-P2 2.2139(8) Co1-P3 2.2125(7) Selected bond angles (°): P1-Co1-P2 97.79(3) P1-Co1-P3 88.86(3) P2-Co1-P3 86.90(3)

Figure 9 ORTEP plot (30% probability level) of **3.6** (H atoms omitted, F1A and F1B are disordered in a ratio of 0.6:0.4.)

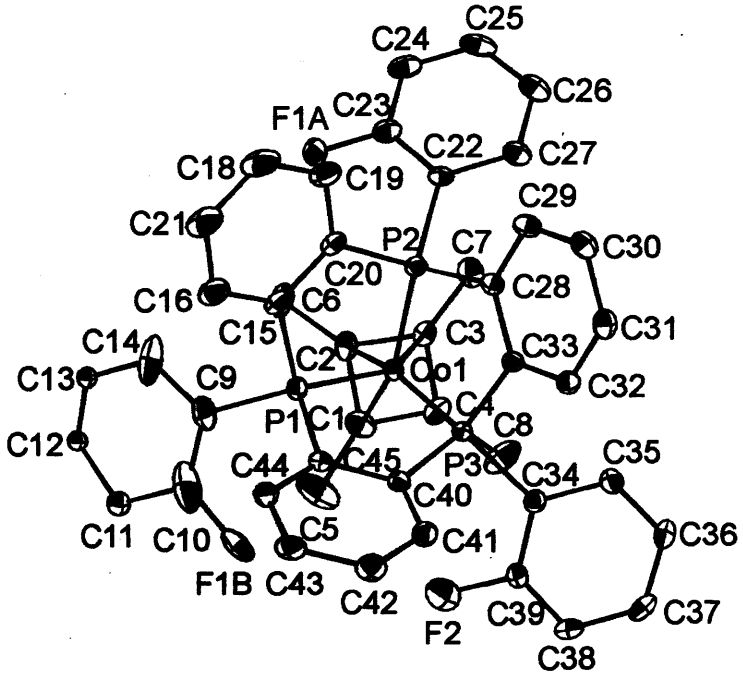

(a)

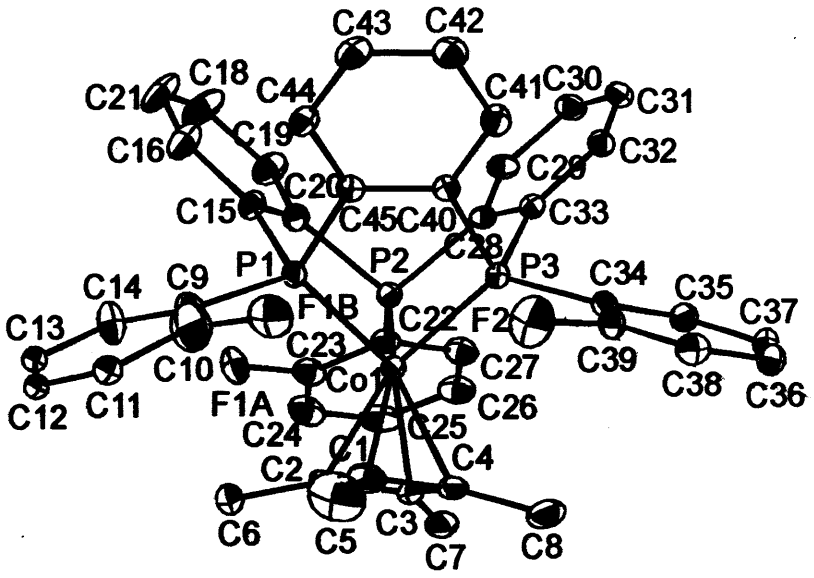

(b)

Selected bond lengths (Å): Co1-C1 2.015(5) Co1-C2 2.016(4) Co1-C3 2.061(4) Co1-C4 2.054(4) Co1-P1 2.1534(12) Co1-P2 2.1615(12) Co1-P3 2.1643(12) **Selected bond angles** (°): P1-Co1-P2 88.10(5) P1-Co1-P3 87.74(4) P2-Co1-P3 88.35(4) C(9)-P(1)-Co(1) 123.13(17) C(15)-P(1)-Co(1) 109.72(15) C(45)-P(1)-Co(1) 109.70(14) C(22)-P(2)-Co(1) 126.71(14) C(28)-P(2)-Co(1) 109.23(14) C(20)-P(2)-Co(1) 108.93(15)

C(34)-P(3)-Co(1) 126.97(14) C(33)-P(3)-Co(1) 109.11(13) C(40)-P(3)-Co(1) 109.16(13)

The structures of **3.4** and **3.5** are quite similar to those of **3.2** and **3.3** respectively. Again both complexes **3.4** and **3.5** have three-legged piano-stool geometries about a pseudooctahedral cobalt centre. The η^4-tetramethylcyclobutadiene ligand coordinates in a facial fashion to the Co(III) centre by occupying three coordination sites. The distances of Co to the plane defined by the cyclobutadiene ring carbons (plane C_4) are 1.773(3) Å in **3.4** and 1.789(3) Å in **3.5**, both of which are larger than that {1.670(10) Å} in **1**.[6] As mentioned before, this is presumably due to the weak π–acceptor/good σ-donor property of CH_3CN ligand in **3.1** allowing for a stronger Co-Cb* interaction,[6] as well as the larger repulsion between the phosphine ligands and Cb*. The Co-N bond length of 1.934(2) Å in **3.4** is comparable to that in **3.2** {1.930(3) Å}, both are less than the average value of 1.950(7) Å in **3.1**. The average Co-P bond length in **3.4** is 2.225(8) Å; the Co-PH_2Ph bond length {2.190(1) Å} in **3.5** is similar to the values between Co and chelate P donors {aver. 2.213(1) Å}. In **3.5**, the dihedral angle between C_4 and P_3 planes is 8.8(1)°, the distance of the Co to P_3 plane centroid is 1.247(1) Å.

Structure **3.6** confirms the formation of the triphosphamacrocycle which sandwiches the Co centre together with the η^4-cyclobutadiene. The macrocycle ligates to the metral centre *via* three fused 5-membered rings as a tridentate crown. The roughly parallel P_3 and C_4 planes have a dihedral angle of 4.1(1)°. The distance of Co to the C_4 plane centroid is 1.762(5) Å, and to the P_3 plane centroid is 1.288(1) Å. The Co-P bond lengths in **3.6** are 2.153(1) Å, 2.161(1) Å, 2.164(1) Å which are significantly shorter than those in **3.5** {aver. 2.215(8) Å}, the complex prior to ring closure. This exemplifies the macrocycle coordination effect leading to strong bonding between the metal centre and the macrocyclic

ligand. This strong bonding is also manifest in the ^{31}P NMR spectrum causing the resonances to be shifted downfield in comparison to **3.5**. The fluorine positions in the structure are disordered and thus it is not possible (from structural data) to identify definitively the two phosphorus atoms bearing the *o*-fluorophenyl substituents. However, two Co-P bond lengths are longer {2.161(1) Å, 2.164(1) Å} than the third {2.153(1) Å}. It is likely that these two longer contacts are to the *o*-fluorophenyl bearing phosphines. This argument is supported by the $^{31}P\{^{1}H\}$ NMR spectrum since an AB_2 pattern is observed where δ A is more deshielded, consistent with a slightly stronger Co-P interaction, and δ B is more shielded with a slightly weaker Co-P interaction due to the electron withdrawing influence of the *o*-fluoro group.

In **3.4**, the *o*-phenylene carbons and two chelating phosphorus atoms are roughly co-planar. This plane and the trigonal plane defined by the two chelating P and Co atoms has a dihedral angle of 10.6(1)°. In **3.5**, the dihedral angle of the corresponding two planes changes to 27.2(1)°. This could be due to a larger replusion between the phenylphosphine and the **dfppb** ligand compared to that between acetonitrile and phenylphosphine in **3.4**. The average corresponding dihedral angle between these planes in **3.6** is 9.5(1)°. In **3.4**, the **dfppb** coordination bite angle is 85.83(3)°, The P···P non-bonded distance is 3.031(1) Å. In **3.5**, this **dfppb** bite angle angle is 86.90(3)°, the other P-Co-P angles are 88.86(3)° and 97.79(3)°, and the P···P non-bonded distance associated with the 5-membered chelate ring is 3.044(1) Å; and the others are significantly longer at 3.102(1) Å and 3.340(1) Å. In **3.6**, the P-Co-P angles of the three fused 5-membered chelate rings are 88.10(5)°, 87.74(4)°, 88.35(4)°, the average P···P distances is 3.000(1) Å.

The methyl groups of cyclobutadiene in **3.6** are displaced out of the C_4 ring plane away from the triphosphamacrocycle as is also observed in complexes **3.2, 3.3, 3.4** and **3.5** this might be presumably due to combination of steric repulsion and electronic factor.[13] The intramolecular repulsion between the Cb* ligand and the terminal phenyl or fluorophenyl group in **3.6** causes the terminal phenyl or fluorophenyl to be bent away from the cobalt atom with the Co-P-C_{exo} (exocyclic phenyl or fluorophenyl group) angles expanded to 123.1(1)°, 126.7(1)°, 126.9(1)° respectively, whereas the Co-P-C_{ring} angles are close to tetrahedral {aver. 109.5(1)°}. It is likely that the two larger Co-P-C_{exo} angles belong to the more sterically demanding fluorophenyl groups, although due to crystallographic disorder, this could not be confirmed structurally.

3.4 Intramolecular C-C bond coupling between phosphine macrocycle and tetramethylcyclobutadiene

Since the fluorine atom is generally a good leaving group for S_NAr reactions and the dehydrofluorination is stoichiometric in base, addition of 2 mol equivalents of strong base to a solution of **3.5** in THF results in removal of two fluorine atoms and **3.6** is formed in almost quantitative yield. With excess base however, two *cis* Cb* ring methyl C-H bonds and the two remaining *o*-aryl C-F bonds were activated which leads to an intramolecular C-C coupling between the cyclobutadienyl ligand and the P_3 macrocycle ligand. The selectivity of the reaction in which **3.6** is formed preferentially to intramolecular C-C coupling indicates the PH protons in **5** are more acidic than the CH protons in the Cb* ligand.

Addition of more than 2 equivalents of $KOBu^t$ to a solution of **3.5** in THF gave rise to the air- and moisture- stable complex **3.7** (*vide supra*). Complex **3.7**, $\{\eta^4$-Me_2C_4-[1,4-bis(2-$CH_2C_6H_4$)-7-C_6H_5-[b,e,h]tribenzo-1,4,7-triphosphacyclononane]-1,2$\}Co^+$, can also be rapidly and almost quantitatively formed by adding $KOBu^t$ to the solution of **3.6** in THF. It is likely that **3.7** was formed *via* C-H bond activation and concomitant intramolecular C-C bond formation by nucleophilic substitution of fluoride and constitutes an unprecedented coupling of a tetramethylcyclobutadienyl ligand with a fluoroaryl phosphine (**Scheme 6**).

Scheme 6: Cb* ring methyl activation and concomitant coupling reaction

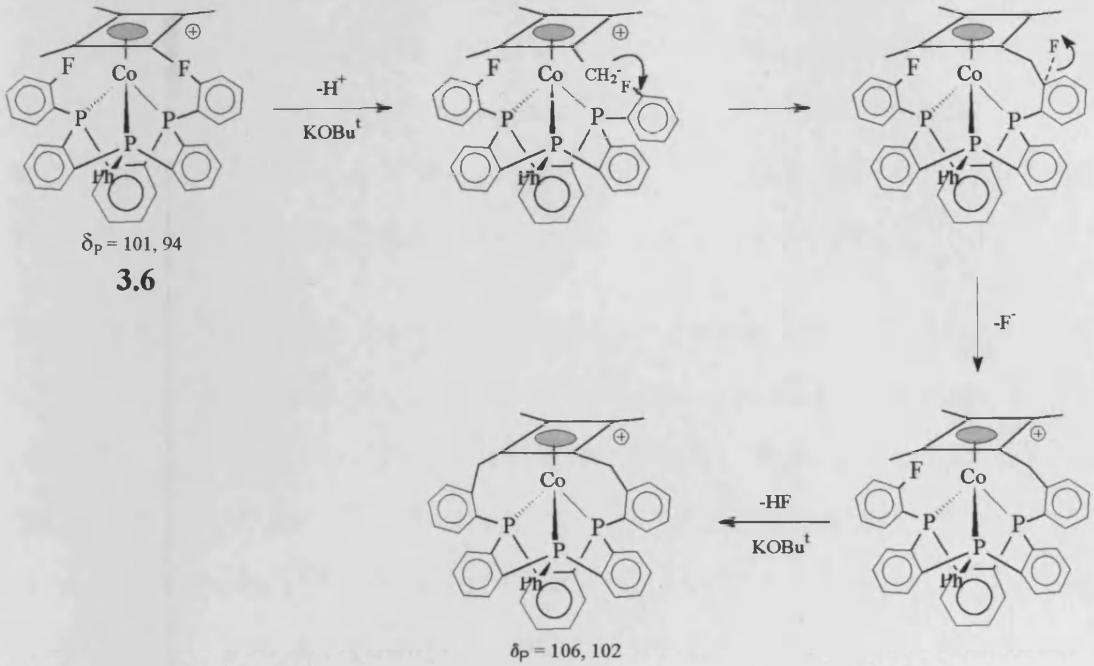

3.6 **3.7** **3.7a**

The mass spectrum of **3.7** showed peaks at 712 (M-2H) and 711 (M-3H) amu. The $^{31}P\{^{1}H\}$ NMR spectrum of complex **3.7** (**Figure 10**) recorded in CD_2Cl_2 shows two resonances shifted downfield relative to **3.6** at δ 106.3 ppm and δ 102.2 ppm with relative intensities 2:1 (A_2B pattern). P-P coupling could not be resolved. The $^{19}F\{^{1}H\}$ NMR spectrum of **3.7** showed solely a doublet at δ -71.6 ppm and δ -74.1 ppm ($^{1}J_{P,F}$ = 710 Hz) due to the PF_6 counter anion. The two methylene protons of the CH_2 bridges are diastereotopic and inequivalent. One appears as a doublet (δ 3.08 ppm) in the ^{1}H NMR spectrum through coupling to its geminal neighbour ($^{2}J_{H,H}$ = 16.8 Hz) while the other is a double of triplets (δ 3.57 ppm) through further coupling to one aromatic proton and a phosphorus. In the $^{13}C\{^{1}H\}$ NMR spectrum, the carbons in the Cb* ring are chemically inequivalent and show two peaks at δ 86.6 ppm and δ 78.3 ppm, a resonance at δ 28.3 ppm is assigned to the methylene carbon and the methyl carbon gives rise to a resonance at δ 9.3 ppm.

Figure 10 $^{31}P\{^{1}H\}$ (**a**) and ^{1}H NMR (**b**) spectra of complex **3.7**

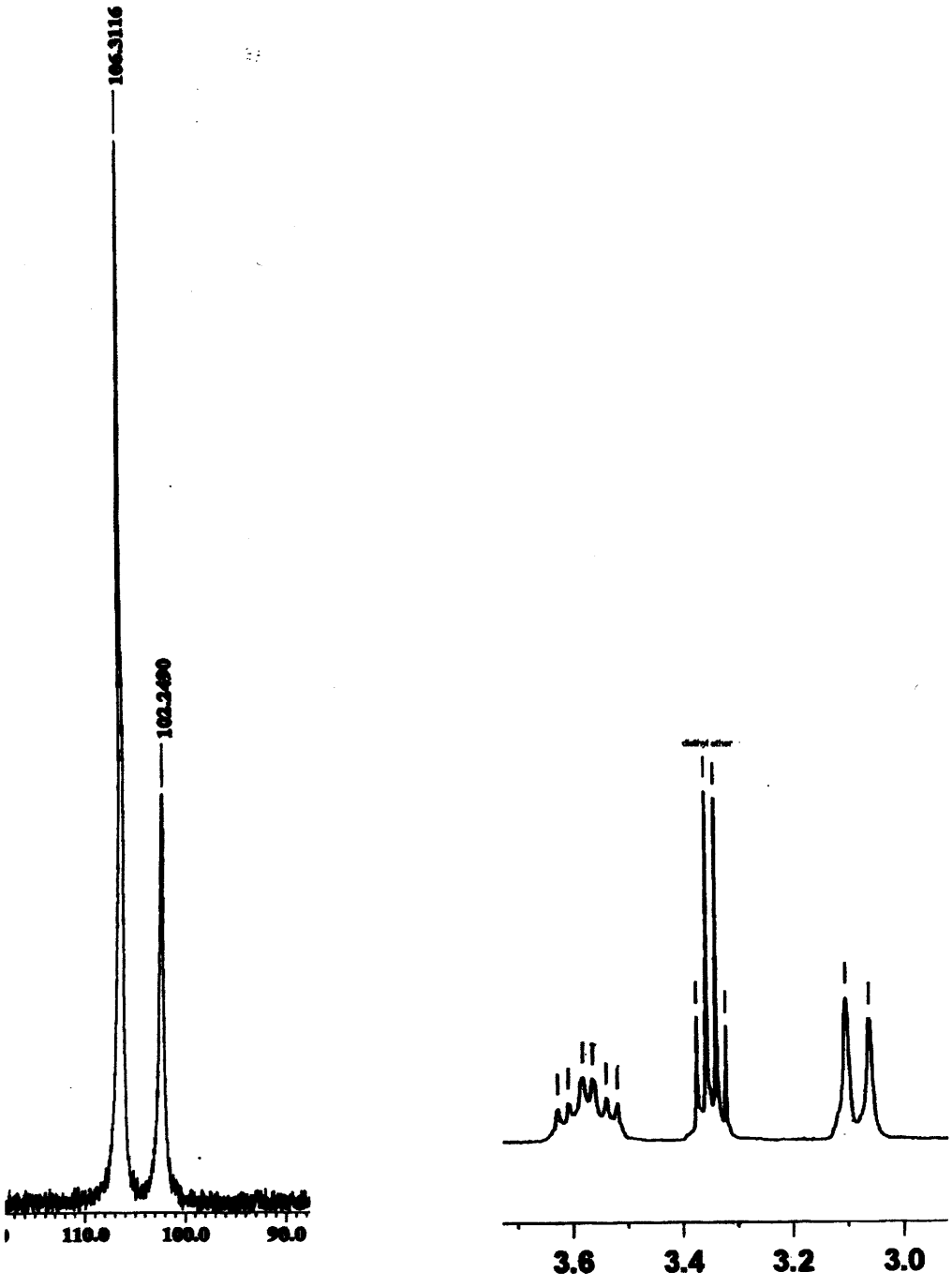

(**a**) (**b**)

The ring methyl C-H bond activation of an η^5-pentamethylcyclopentadienyl ligand and an η^6-arene ligand, followed by intramolecular coupling to the *o*-aryl position of a fluorophenyl phosphine ligand in transition metal complexes has been reported.[14-18]

As far as we know, this is the first example of the ring methyl C-H bond of an η^4-tetramethylcyclobutadienyl ligand, undergoing a similar intramolecular coupling to a phosphine ligand bearing an *o*-fluorophenyl group. The activation of the ring methyl of Cb* provides some opportunities further to investigate the reactions of the activated nucleophile intermediate with other electrophiles in the future.

The precise nature of the ring methyl activation of η^5- C_5Me_5 or η^4-C_4Me_4 or η^6-arene ligands, followed by intramolecular or intermolecular coupling reactions remains speculative. Firstly, there is an unexpected sensitivity of the reactions to the nature of the organometallic base used. In some cases, only $KOBu^t$ was successful, $LiNPr_2$ or other bases are less effective[15,19] and in some of Saunders' cases,[14] no base is necessary. Secondly, in the case of η^5-Cp^*, single or multiple alkylations occur depending upon the metal system.[19] The reaction of **3.6** to give **3.7** can be simply viewed as an overall addition-elimination reaction or a nucleophilic aromatic substitution. We suggest a mechanism similar to that proposed by Saunders[14,16-19] and Hughes[15] where deprotonation of a methyl group on the Cb* ring occurs to form a neutral intermediate bearing a methylene carbanion (**Scheme 6**). The resulting nucleophilic methylene carbon attacks at the *o*-position of the fluorophenyl group resulting in fluorine elimination and the formation of the new C-C bond. The cobalt centre holds the *cis* ring methyl of the Cb* ligand and the *o*-fluorophenyl group of the P_3 macrocycle ligand in close proximity, facilitating the nucleophilic attack. The dehydrofluorinative C-C coupling reaction is fast on the NMR timescale since we could not detect (NMR) or isolate intermediate **3.7a**, even when a deficiency of base was added to the solution of **3.6**.

Complex **3.7** was crystallized as the SbF_6^- salt by anion exchange and characterized by X-ray crystallography (**Figure 11**). The cobalt in **3.7** also has a pseudooctahedral geometry similar to complexes **3.1** to **3.6**. There are however obvious structural differences between **3.7** and the other complexes reported herein. The cobalt centre is encompassed by the two parts of a hybrid triphosphamacrocycle-cyclobutadienyl ligand. The cyclobutadiene part occupies three *fac* coordination sites, the P_3 macrocycle part occupies the other three mutually *cis* sites. Although the two methylene carbon atoms and a ring carbon atom of the cyclobutadiene in **3.7** are disordered, the structure still clearly shows the triphosphamacrocycle linkage to the cyclobutadiene group *via* two *cis* adjacent positions of the cyclobutadiene ring. The hybrid macrocyclic phosphine-cyclobutadiene ligand binds the Co centre strongly acting as a 12 electron formally hexadentate donor. The distance of 1.716(8) Å from Co to the cyclobutadiene ring centroid is shorter than that in **3.6** {1.762(5) Å}. All three Co-P distances in **3.7** become much shorter compared to those in **3.6** after removal of the electron withdrawing fluorine atoms. The two P atoms bearing the *o*-$C_6H_4CH_2$ linkage to the Cb* fragment have Co-P bond lengths of 2.120(1) Å and 2.125(1) Å. The remaining uncoupled P atom has a Co-P bond length of 2.122(1) Å. In **3.7**, the average P-Co-P bite angles are approximately 89.77(7)°, the average P···P distance of 2.996(1) Å is almost identical to that in **3.6** {3.000(1) Å} which reflects the rigidity of the tribenzannulated backbone. The Co-P-C(C1 and C20 on the coupled methylenylphenyl) angles {aver. 119.2(1)°} are smaller than that of the Co-P-C33 {124.4(1)°}. The Co-P-C1 and Co-P-C20 angles are both significantly smaller than those in the uncoupled precusor (**3.6**) due to the constraints imposed as a result of coupling. All the Co-P-$C_{exocyclic\ phenyl}$ angles in **3.7** are larger than those of the backbone Co-P-C_{ring} angles {aver. 108.3(1)°} due to intramolecular repulsion as observed in complex **3.6**.

Figure 11 ORTEP plot (30% probability level) of **3.7** (H atoms and disordered C7B, C11B, C12B, C14B omitted)

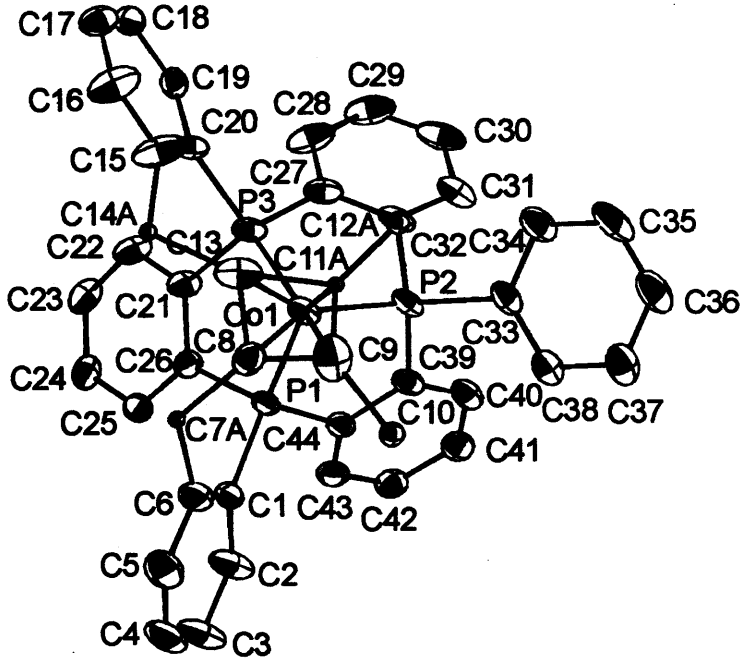

(a)

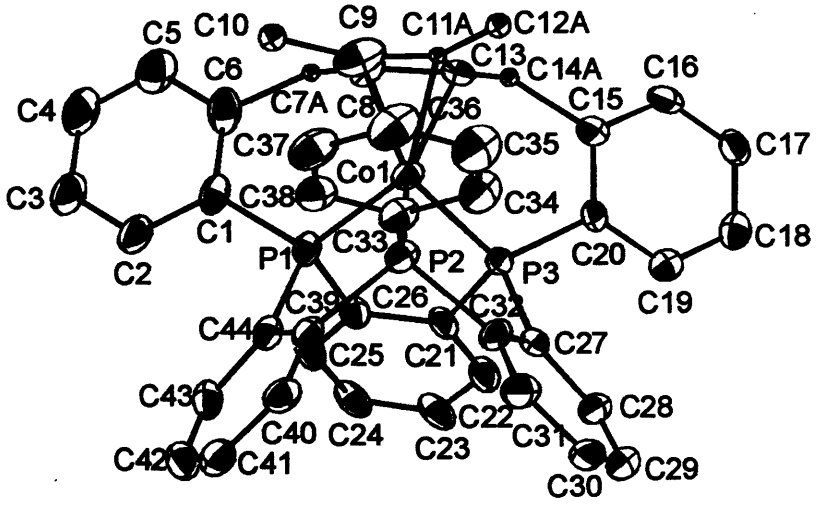

(b)

Selected bond lengths (Å): Co1-P1 2.1200(17) Co1-P2 2.1220(19) Co1-P3 2.1259(18) Co1-C8 1.985(6) Co1-C9 2.000(8) Co1-C11a 1.989(10) Co1-C13 1.994(7) Selected bond angles (°): P1-Co1-P2 90.10(7) P1-Co1-P3 89.37(6) P2-Co1-P3 89.84(7) C(1)-P(1)-Co(1) 120.0(2) C(26)-P(1)-Co(1) 107.70(19) C(44)-P(1)-Co(1) 109.47(19) C(33)-P(2)-Co(1) 124.4(2) C(39)-P(2)-Co(1) 108.3(2) C(32)-P(2)-Co(1) 107.8(2) C(21)-P(3)-Co(1) 107.9(2) C(20)-P(3)-Co(1) 119.2(2) C(27)-P(3)-Co(1) 108.8(2)

3.5 Cyclic Voltammetry

Cyclic voltammetry (CV) gives information about electrochemical process which may be relevant to understanding chemical reactions. By comparison of the redox potentials of the electroactive species obtained from CV, we can get the insight into the influences that various ligands may have upon the metal redox centre and reduction/oxidation resistance of redox active centres. This information could help in the selection of the most suitable reagents to oxidise or to reduce the redox active species. Since we intend to study the liberation of the P_3 macrocycle from complexes **3.6** or **3.7**, by reducing or oxidising the kinetically inert species in order to disrupt the d^6/18 electron configuration of the Co centre and so to form relatively kinetically active intermediates with a d^5/17 or d^7/19 electron configuration. CV measurements were performed in this regard (**Table 1, Figure 12 and Figure 13**).

Table 1 Cyclic voltammetric data for the oxidation of complex **3.6** and **3.7** in CH_3CN[a].

Complex	process	E_p^{ox}(V)	E_p^{red}(V)	ΔE_p(mv)	I_p^{ox}/i_p^{red}
3.6	1	0.407	Irreversible		
	2	0.610	0.535	75	0.93
3.7	1	0.614	0.529	85	0.99

a) Potential is referenced to Cp_2Fe^+/Cp_2Fe; scan rate: 400mv/s; E_p^{ox} = oxidation peak potential; E_p^{red} = reduction peak potential; ΔE_p = separation in reduction and oxidation peak potentials; I_p^{ox} = oxidation peak current; I_p^{red} = reduction peak current

Figure 12 oxidative cyclic voltammogram for complex **3.6**

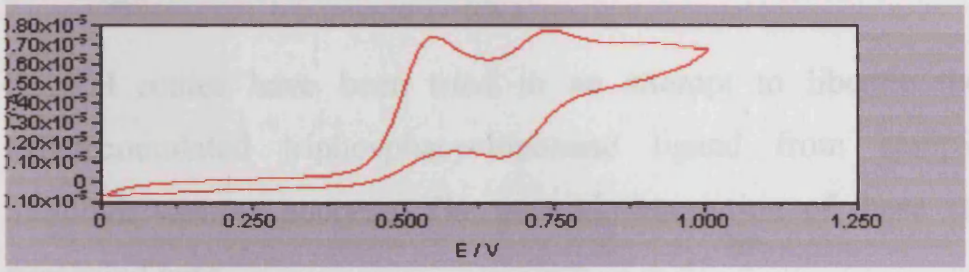

Figure 13 oxidative cyclic voltammogram for complex **3.7**

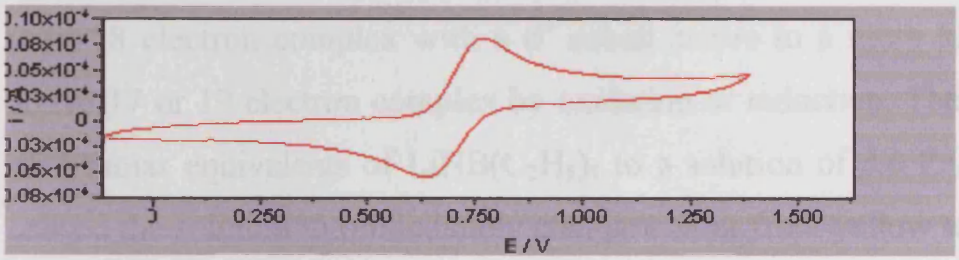

In acetonitrile, both **3.6** and **3.7** show no reduction within the solvent limit (-2.5 V). Thus the P_3 macrocycle ligand/Cb*Co^+ fragment forms a very stable complex against reduction. Complex **3.6** shows two oxidation processes, one irreversible taking place at 0.407 V, another reversible at 0.610 V (*vs* Cp_2Fe^+/Cp_2Fe couple). Complex **3.7** shows one reversible oxidation at 0.614 V (*vs* Cp_2Fe^+/Cp_2Fe couple). The first irreversible oxidation process for **3.6** is explained as a ligand based oxidation and coupled to the chemically irreversible formation of complex **3.7** by electrochemical oxidation. Hence the second oxidation process of **3.6** occurs at the same voltage and has the same shape as complex **3.7** which is assumed to be a metal based single electron oxidation from the 18 electron Co(III) species to a 17 electron Co(IV) species. From the CV, it seems that the reaction of **3.6** with $KOBu^t$ affording **3.7** involves a complicated electron transfer process. Further studies are required in order to distinguish one or two electron process in order to gain mechanistic information of the transformation of **3.6** to **3.7**.

3.6 Ligand liberation studies

Several routes have been tried in an attempt to liberate the 1,4,7-tribenzannulated triphosphacyclononane ligand from complex **3.6**, although without success. The general description of these studies is presented here.

The basic principle for liberation is initially to transform the kinetically inert 18 electron complex with a d^6 cobalt centre to a more kinetically active 17 or 19 electron complex by oxidation or reduction. The addition of 2 molar equivalents of $LiHB(C_2H_5)_3$ to a solution of **3.6**·PF_6 in THF caused the solution to immediately change colour from yellow to red. An intermediate which is soluble in hydrocarbon solvents was isolated and shows a upfield chemical shift in the $^{31}P\{^1H\}$ NMR spectrum compared to **3.6**, no PF_6^- was observed. The gradual degeneration of the intermediate to show a spectrum similar to that of **3.7** however caused us to abandon this course of investigation.

Reductive cleavage of ferrocene to metallic iron and cyclopentadiene by lithium has been reported.[20] Sekiguchi *et al* also reported the synthesis of the cyclobutadiene dianion from CpCocyclobutadiene complexes by reaction with metallic lithium.[21] Thus, reaction of **3.6**·PF_6 in THF solution with metallic lithium was also tried. After stirring overnight, the solution showed no resonance in the $^{31}P\{^1H\}$ NMR spectrum, although. we have not been able to identify any products from this reaction.

Oxidation of **3.6**·PF_6 was carried out in acetonitrile solution with ceric ammonium nitrate. The reaction proceeds quite slowly compared to the Fe analogue. After stirring overnight, the ^{31}P NMR spectrum shows no resonances, presumably due to the formation of a paramagnetic complex.

We have been unable to isolate any identified products during following work.

The attempt to substitute the *otho* fluorine atom in the PC_6H_4F groups by KCN was investigated. Upon heating a solution of **3.6**·PF_6 with excess KCN in phenyl nitrile (160°, >12 h), no reaction was observed.

Gleiter reported cycloaddition reactions of CpCo-stabilized cyclobutadiene derivatives with triple bonded species X≡Y, to yield arenes or pyridines under vigorous conditions.[22] No similar reaction was observed by treating complex **3.6** with phenyl nitrile at 200 °C for more than 12 hours however.

3.7 Conclusions

The lability of acetonitrile ligands of the cationic $[Cb^*Co(NCCH_3)_3]^+$ complex makes the electrophilic Cb^*Co^+ fragment accessible to bisphosphine and monophosphine ligands. By replacing the acetonitrile ligands from $[Cb^*Co(NCCH_3)_3]^+$ sequentially with bisphosphine and monophosphine ligands, the precursor complex, $[Cb^*Co(dfppb)(PH_2Ph)]^+$ (**3.5**) is available which undergoes ring closure to produce a 9-membered 1,4,7-triphosphorus macrocycle complex (**3.6**) with a tribenzannulated backbone *via* intramolecular dehydrofluorinative coupling reactions using $KOBu^t$ as a HF-trapping reagent. This makes the Cb^*Co^+ unit the first alternative non-Fe template for the synthesis of P_3 macrocycles with small ring systems.

Surprisingly, in the presence of $KOBu^t$, the Cb* ring methyl of complex **3.6** undergoes C-H bond activation and concomitant coupling to the *ortho* position of a coordinated PC_6H_4 group. This produces complex **3.7** bearing a 12 electron donor ligand with hybrid phosphine and cyclobutadienyl groups. The significantly shorter Co-P bond lengths in **3.6** and **3.7** suggest a very good ligating behaviour of the P_3 macrocycle to the metal centre that renders corresponding complexes of **3.6** and **3.7** very stable and resistant to reduction (CV).

3.8 Experimental Section

General experimental information: All reactions were performed under nitrogen atmosphere with standard Schlenk glassware, vacuum techniques or Glovebox unless otherwise noted. The solvents were dried and degassed by refluxing over standard drying agents and distilled immediately prior to use. Infrared spectra were recorded on a Perkin Elmer 1600 spectrophotermeter using KBr pellets for solid samples. Mass spectra were carried out on a VG Platform II Fisons mass spectrometer. UV photolyses were carried out using a Hanovia 125 W mercury discharge lamp (254 nm). The NMR spectra were recorded on a Bruker DPX-400 instrument at 400 MHz (^{1}H) and 100 MHz (^{13}C) or a Jeol Lamda Eclipse 300 at 121.65 MHz (^{31}P), 300.52 MHz (^{1}H), 75.57 MHz (^{13}C), 96.42 MHz (^{11}B) and 282.78 MHz (^{19}F). All chemical shifts are quoted in units of δ ppm. ^{1}H and ^{13}C NMR chemical shifts are relative to solvent resonance, ^{31}P chemical shifts are relative to 85% external H_3PO_4 (δ = 0 ppm), ^{11}B chemical shifts are relative to external $BF_3.OEt_2$ (δ = 0 ppm), ^{19}F chemical shifts are relative to external $CFCl_3$ (δ = 0 ppm). Elemental analyses were performed by the Warwick Analytical Service. X-ray diffraction data collection was carried out on a Bruker Kappa CCD diffractometer at 150(2) K with Mo $K\alpha$ irradiation (graphite monochromator). Empirical absorption corrections were performed using equivalent reflections. For the solution and refinement of the structures, the program package SHELXL 97 was employed.[23] H atoms were placed into calculated positions and included in the last cycles of refinement. Complexes **3.2** to **3.6** were crystallised as its PF_6 salts, complex **3.7** as SbF_6 salt. The two F atoms in complex **3.6** are refined and distributed between the three phenyls with a disordered model of 1:0.6:0.4. In complex **3.7**, the positions of two CH_2 carbons, a CH_3 carbon

and a C atom from the Cb* ring are refined isotropically in a disordered mode of 0.6:0.4. Crystal structures and refinement data are collected in **Appendix B** and supplementary CD.

Electrochemical measurements: Cyclic voltammetry was carried out on a Windsor PG system versus an Ag/Ag^+ reference electrode, a glassy-carbon working electrode and a platinum wire as auxiliary electrode. The measurements were recorded on *ca* 1.0 mM solutions of the compounds in acetonitrile (0.1 M Bu_4NPF_6 as supporting electrolyte). 1.0 mM ferrocene solution in the same solvent was used as reference redox couple and all potentials are quoted relative to Fc^+/Fc. Solutions were purged with nitrogen before the measurements. All other chemicals were obtained from commercial sources and where appropriate, dried over molecular sieves and degassed by repeated freeze-thaw cycles.

Materials: $[(C_4Me_4)Co(NCCH_3)_3]PF_6$[1,9] (**3.1**·$PF_6$) and phenyl-phosphine[24] were prepared according to literature methods.

1, 2-bis(dichlorophosphino)benzene[10]

This compound was prepared by a modification of the procedure of Kyba,[12] substituting phosgene by triphosgene. To a solution of 24.4 g (63 mmol) triphosgene in 250 ml dichloromethane was added a solution of 6.7 g (47 mmol) 1,2-diphosphinobenzene at -78 °C. After addition was complete the reaction mixture was left to warm up to room temperature, the solvent was evaporated and the residue distilled in high vacuum (at around 0.1 mmHg, 135 °C) to give a clear liquid, 4.9 g (37%).

1,2-bis(di-2-fluorophenylphosphino)benzene (dfppb)[10]

89 ml of a 2.13 M solution of $LiBu^n$ (0.19 mol) in diethyl ether was diluted with 200ml ether and cooled to -100 °C. To this was added dropwise a solution of 20.6ml (33 g, 0.19 mol) of 2-bromofluorobenzene in 30 ml ether. After the addition was complete the solution was stirred

for 30 minutes and then a solution of 1,2-bis-(dichlorophosphino)benzene (13.2 g, 0.047 mol) in 25 ml ether was added. The mixture was left to stir for 1 h at low temperature and then left to warm up to room temperatue overnight. An aqueous solution of NH_4Cl was added, the organic phase separated and concentrated and the residue crystallized from ethanol. Yield: 33%.

$[(\eta^4\text{-}C_4Me_4)Co(dppe)(NCCH_3)]PF_6$ (3.2·PF_6)

To a solution of $[(C_4Me_4)Co(NCCH_3)_3]PF_6$ (**3.1**·PF_6) (0.10 g, 0.23 mmol) in 20 ml CH_3CN, dppe (0.09 g, 0.23 mmol) was added with stirring. The colour of the deep red solution changed to yellow-brown immediately. The solution showed a resonance at δ 70.2 ppm in the $^{31}P\{^1H\}$ NMR spectrum. The reaction mixture was filtered then concentrated. Orange crystals of **3.2**·PF_6 were obtained by diffusion of diethyl ether vapour into the solution. Yield: 98%.

$[(\eta^4\text{-}C_4Me_4)Co(dppe)(PH_2Ph)]PF_6$ (3.3·PF_6)

To a solution of (**3.2**·PF_6) (0.10 g, 0.12 mmol) in 20ml CH_2Cl_2, phenylphosphine (17mg, 0.15mmol) was added. After stirring for 20 minutes, the ^{31}P NMR spectrum showed two resonances at δ 70.2 ppm and δ -18.6 ppm. The volatiles were then removed in *vacuo*. The solid residue was triturated with petroleum ether then dissolved in CH_2Cl_2, filtered and concentrated. Orange crystals of **3.3**·PF_6 were obtained by diffusion of diethyl ether vapour into the filtrate. $^{31}P\{^1H\}$ ($CDCl_3$): 70.2, -18.6 ($^1J_{H,P}$ = 336 Hz). Yield: 98%.

$[(\eta^4\text{-}C_4Me_4)Co(o\text{-}C_6H_4F)_2PC_6H_4P(o\text{-}C_6H_4F)_2(NCCH_3)]PF_6$ (3.4·PF_6)

To a solution of **3.1**·PF_6 (0.10 g, 0.23 mmol) in 20ml CH_3CN, **dfppb** (0.12 g, 0.23 mmol) was added with stirring. The colour of the red solution changed to orange immediately. $^{31}P\{^1H\}$ NMR spectrum showed

a growth of a resonance at δ 64.3 ppm. The reaction mixture was filtered then concentrated. Orange crystals of **3.4**·PF_6 were obtained by diffusion of diethyl ether vapour into the solution. Yield: 98%. $^{31}P\{^1H\}$ (CD_2Cl_2): 64.3 (dfppb), -143.9 (sep PF_6, $^1J_{P,F}$ = 711 Hz). $^{19}F\{^1H\}$ (CD_2Cl_2): -96.5 (dfppb), -97.1 (dfppb), -73.4(d, PF_6). $^{13}C\{^1H\}$ (CD_2Cl_2): 85.1 (C_4Me_4), 8.2 (C_4Me_4), 1.4 (MeCN). ^1H (CD_2Cl_2): 7.6 to 6.4 (20H, m, H_{aryl}), 0.91 (12H, s, C_4Me_4), 0.79 (3H, s, CH_3CN). IR: 2269 cm^{-1} (CN) Anal. For $C_{40}H_{35}N_1F_{10}P_3Co_1$ (M = 871.56 g mol^{-1}): Calcd (%), C, 55.12; H, 4.05; N, 1.61. Found (%), C, 54.78; H, 4.05; N, 1.51.

[(η^4-C_4Me_4)Co(*o*-C_6H_4F)$_2$PC_6H_4P(*o*-C_6H_4F)$_2$(PH_2Ph)]PF_6 (3.5·PF_6)

To a solution of **3.4**·PF_6 (0.20 g, 0.23 mmol) in 20ml CH_2Cl_2, phenylphosphine (0.03 g 0.27 mmol) in toluene was added. After stirring for 15 minutes, the ^{31}P NMR spectrum showed two resonances at δ 61.7 ppm and δ -19.6 ppm. The reaction mixture was filtered and the solvent removed in *vacuo*. The residue was triturated with diethyl ether to remove excess amount of phenylphosphine and the yellow powder dissolved in CH_2Cl_2 and concentrated. Orange crystals of **3.5**·PF_6 were obtained by diffusion of diethyl ether vapour into the concentrated solution during several days. Yield: 98%. ^{31}P (CD_2Cl_2): 61.7, -19.7 (t, $^1J_{P,H}$ = 336 Hz), -143.8 (sep, PF_6, $^1J_{P,F}$ = 711 Hz). $^{19}F\{^1H\}$ (CD_2Cl_2): -96.3 (dfppb), -97.2(dfppb), -73.3 (d, PF_6). $^{13}C\{^1H\}$ (CD_2Cl_2): 83.7 (C_4Me_4), 6.72 (C_4Me_4). ^1H (CD_2Cl_2): 7.4 to 6.7 (m, 25H, H_{aryl}), 4.0 (dm, 2H, PH, $^1J_{P,H}$ = 336 Hz), 0.86 (s, 12H, C_4Me_4). IR: 2304 cm^{-1} (PH), 2335 cm^{-1} (PH). Anal. for $C_{44}H_{39}F_{10}P_4Co_1$ (M = 940.61 $gmol^{-1}$): Calcd (%), C, 56.19; H, 4.18. Found (%), C, 55.38; H, 4.04.

[η^4-C_4Me_4]Cobalt(III)-1,4-bis(2-fluorophenyl)-7-phenyl-[b,e,h]tri-benzo-1,4,7-triphosphacyclononane hexafluorophosphate (3.6·PF_6)

To a solution of **3.5**·PF_6 (0.27 g, 0.29 mmol) in 20ml THF was added $KOBu^t$ (65 mg, 0.58mmol). The solids were dissolved quickly and the colour of the solution changed immediately from orange to red then back to orange again. After stirring for 15 minutes, the ^{31}P NMR spectrum showed two resonances at δ 102.0 and δ 93.9 ppm with intensities 1:2. The solvent was then removed in *vacuo*. The residue was dissolved in dichloromethane and filtered. The solvent was removed in *vacuo* and replaced by acetonitrile, orange crystals of **3.6**·PF_6·CH_3CN were obtained by diffusion of diethyl ether vapour into the solution. Yield: 95%. $^{31}P\{^1H\}$ (CD_2Cl_2): 100.9 (m), 94.8 (m), -143.0 (sep, PF_6, $^1J_{P,F}$ = 711 Hz). $^{19}F\{^1H\}$: -96.5, -96.8, -97.2, -97.4 (CD_2Cl2_2, -50 ^{0}C); -95.9, -96.3, -96.6 (CD_2Cl_2, 20 ^{0}C); -96.0, -96.1, -96.6, -96.7 (DMSO-D_6, 20 ^{0}C); -96.4, -96.9 (DMSO-D_6, 70 ^{0}C). $^{13}C\{^1H\}$ (CD_2Cl_2): 82.4 (C_4Me_4), 6.2 (C_4Me_4). ^1H (CD_2Cl_2): 7.6 to 7.1 (m, 25H, H_{aryl}), 1.8 (s, 3H, CH_3CN), 0.7 (s, 12H, C_4Me_4). M.S.(APCI): 755(M^+). Anal. for $C_{46}H_{40}N_1F_8P_4Co_1$ (M = 941.65 $gmol^{-1}$): Calcd (%), C, 58.67; H, 4.28; N, 1.49. Found (%), C, 58.59; H, 4.19; N, 1.32.

{η^4, κP, κP, κP-Me_2C_4-[1,4-bis(2-$CH_2C_6H_4$)-7-C_6H_5-[b,e,h]tri-benzo-1,4,7-triphosphacyclononane]-1,2}Co(III) hexafluorophosphate (3.7·PF_6)

To a solution of **3.6**·PF_6 (0.10 g, 0.1 mmol) in 20ml THF was added $KOBu^t$ (24 mg, 0.2 mmol). The solids dissolved quickly and the colour of the solution changed immediately from orange to red, then back to orange. The $^{31}P\{^1H\}$ NMR spectrum showed two new resonances at δ 106 and δ 102 ppm with intensities 2:1. The solvent was removed in *vacuo* and the residue was dissolved in dichloromethane and filtered. The

solvent was removed in *vacuo* and the residue dissolved in acetonitrile. Orange crystals of **3.7**·PF_6 were obtained by vapour diffusion of diethyl ether into the solution. Yield: 95%. $^{31}P\{^1H\}(CD_2Cl_2)$: 106.3 (m), 102.2 (m), -143.1 (sep, PF_6, $^1J_{P,F}$ = 712 Hz). $^{19}F\{^1H\}$ (CD_2Cl_2): -72.9(d, PF_6).$^{13}C\{^1H\}$ (CD_2Cl_2): 84.6 (Cb ring), 78.3 (Cb ring), 26.5 (methene), 7.0 (ring methyl). ^1H (CD_2Cl_2): 7.3 to 8.4 (m, 25H, H_{aryl}), 3.6 (m, 2H, CH_2), 3.08 (d, 2H, CH_2, $^2J_{H,H}$ = 16.8 Hz), 1.08 (s, 6H, Me_2C_4) M.S.(APCI): 712 (M-2H), 711 (M-3H).

References

1. G. E. Herberich, A. R. Kudinov et al, *Eur. J. Inorg. Chem.* **2002**, 2656-2663
2. J. G. Speight, *Lange's Handbook of Chemistry* 16th Ed. McGraw-Hill, New York, 2005.
3. R. Haigh, *Doctoral Thesis*, **2002**, Cardiff University
4. A. Sekiguchi; T. Matsuo; H. Watanbe; *J. Am. Chem. Soc.* **2000**, 122, 5652-5653.
5. C. Schaefer, R. Gleiter, F. Rominger, *Organometallics* **2004**, 23, 2225-2227.
6. (a) A. Efraty, **Chem. Rev.** **1977**, 77, 691. (b) P. M. Maitlis, A. Efraty, M. L. Games, *J. Am. Chem. Soc.* **1965**, 87, 719
7. M. Crocker, M. Green, A. G. Orpen, H.-P. Neumann, C. J. Schaverien, *J. Chem. Soc., Chem. Commun.* **1984**, 1351. (b) M. Crocker, M. Green, K. R. Nagle, A. G. Orpen, H.-P. Neumann, C. J. Schaverien, *Organometallics* **1990**, 9,1422.
8. M. V. Butovskii, U. Englert, G. Herberich, K. Kirchner, U. Koelle, *Organometallics* **2003**, 22, 1989-1991.
9. P. L. Pauson et al, *J. Chem. Soc. Dalton Trans.* **1987**, 2757-2760
10. P. Garrou, *Chem. Rev.*, **1981**, 8, 229.
11. (a) T. Albers, *Doctoral Thesis*, **2001**, Cardiff University. (b) J. Johnstone, *Doctoral Thesis*, **2004**, Cardiff University.
12. E. P. Kyba, M. C. Kerby, S. P. Rines, *Organometallics* **1986**, 5, 1189.
13. E. L. Muetterties, J. R. Bleeke, E. J. Wucherer, *Chem. Rev.* **1982**. 82. 499-525
14. (a) M. J. Atherton, J. H. Hollow, E. G. Hope, A. Karacar, D. R. Russell, G. C. Saunders, *J. Chem. Soc. Chem. Commun.* **1995**, 191-192. (b) M. J. Atherton, K. S. Coleman, J. Fawcett, J. H. Holloway, E. G. Hope, A. Karacar, L. A. Peck, G. C. Saunders, *J. Chem. Soc. Dalton Trans.* **1995**, 24, 4029-38.
15. R. P. Hughes, D. C. Linder, *Organometallics* **1996**, 15, 5678-5686.
16. R. M. Bellabarba, G. C. Saunders, S. Scott, *Inorg. Chem. Commun.* **2002**, 5, 15-18.
17. R. M. Bellabarba, M. Nieuwenhuyzen, G. C. Saunders, *Organometallics* **2002**, 21(26), 5726-5737.
18. R. M. Bellabarba, M. Nieuwenhuyzen, G. C. Saunders, *Organometallics* **2003**, 22(9), 1802-1810.
19. O. V. Gusev, S. Sergeev, I. M. Saez, P. M. Maitlis, *Organometallics*, **1994**, 13, 2059-2065.

20. D. S. Trifan, L. Nicholas, *J. Am. Chem. Soc.* **1957**, 79, 2746-9.

21. A. Sekiguchi, T. Matsuo, H. Watanabe, *J. Am. Chem. Soc.* **2000**, 122, 5652-5653

22. R. Gleiter, D. Kratz, *Angew. Chem. Ed. Int.* **1990**, 29, 276-279.

23. Sheldrick, G. M. SHELXTL97, Program for the refinement of Crystal Structures, University of Goettingen, Germany, **1997**.

24. L. D. Freedman, C. O. Doak, J. Am. Chem. Soc **1952**, 74, 3414.

Chapter 4

Tricarbonylmanganese Template Complexes

Abstract

Sequential substitution reactions of $[(CO)_3Mn(CH_3CN)_3]^+$ (**4.1**) with 1,2-bis(di-2-fluorophenyl)phosphinobenzene (dfppb) and phenylphosphine in CH_2Cl_2 lead to the formation of complexes $[(CO)_3Mn(dfppb)CH_3CN]^+$ (**4.2**) and $[(CO)_3Mn(dfppb)(PH_2Ph)]^+$ (**4.3**) respectively. Treatment of **4.3** with 2 molar equivalents of $KOBu^t$ in THF yields the 9-membered P_3 macrocycle complex, $[(CO)_3Mn\{1,4\text{-bis}(2\text{-fluorophenyl})\text{-}7\text{-phenyl-}[b,e,h]\text{tribenzo-}1,4,7\text{-triphosphacyclononane}\}]^+$ (**4.4**). UV irradiation of **4.4** in benzonitrile at high temperature followed by work-up in air caused the formation of a (syn, anti) macrocycle with two phosphorus donors being oxidized to phosphine oxides and the catalytic transformation of benzonitrile to benzamide resulting in the formation of complex $[(1,4\text{-dioxo-}1,4\text{-bis}(2\text{-fluorophenyl})\text{-}7\text{-phenyl-}[b,e,h]\text{tribenzo-}1,4,7\text{-triphosphacyclononane}\}_2Mn(C_6H_5CONH_2)_2]^{2+}$ (**4.5**) with a Mn(II) center coordinated by 6 O atoms from two macrocycle ligands and two benzamide ligands.

4.1 Introduction

To date, a wide range of 1,4,7-triphosphacyclononane macrocyclic complexes have been synthesized by kinetic template methods using Cp^RFe^+ (R = H, alkyl)[1-5] or Cb^*Co^+ ($Cb^* = \eta^4$-C_4Me_4) (**Chapter 3**) based templates. The methodology, originally developed in our laboratory, is based upon sequentially introducing appropriate phosphine precursors to the template complex followed by an intramolecular ring closing reaction. The template-directed method for the synthesis of P_3 macrocycles has proved highly efficient, straightforward and also occurs with good stereocontrol. The demetallation of the product macrocycle complexes formed by this synthetic methodology remains a significant problem. All the attempts to liberate the free P_3 macrocycles with ring systems smaller than 12-members from their iron or cobalt complexes have been unsuccessful. The difficulty experienced in attempted liberation of the free ligands is presumably linked to these complexes being very robust and this feature no doubt depends upon the ring size of macrocycle (*i.e.* in our case, the 9-membered ring systems appear to optimise stability as might be expected). This also demonstrates the good ligating properties of the P_3 macrocycles with small ring systems and that ligands of this type will have a rich organometallic and coordination chemistry. Thus, the study of other template systems remains an important goal in the search for suitable template systems that may lead to the facile synthesis of these P_3 macrocyclic ligands, but also allow their liberation. In this context, we have continued our study of piano-stool structures containing inert facially capping ligands *trans* to three labile ligands, in the search for alternative templates. We have investigated the substitution and reaction chemistry of these complexes relevant to

phosphorus macrocycle synthesis and we have focused our attention on cationic manganese carbonyls.

As mentioned previously, in all of the template systems investigated to date, the liberation of the free phosphorus macrocycles has only been achieved with the 12-membered, 1,5,9-triphosphacyclododecane and its tertiary phosphine derivatives from the metal carbonyl templates, *fac*-$(CO)_3Cr$ or *fac*-$(CO)_3Mo$, and less efficiently from the η^5-$CpFe^+$ template fragment.[6-9]

The comparison of *fac*-$(CO)_3M$ (M= Cr, Mo), η^5-Cp^RFe^+ and η^4-Cb^*Co^+ based templates indicates why the metal-tricarbonyls are not suitable for the formation of the smaller ring sizes achieved with the Fe and Co templates. Firstly, the spectator ligands in Cp^RFe^+ and Cb^*Co^+ are more sterically bulky than those in *fac*-$(CO)_3Cr$ and *fac*-$(CO)_3Mo$ (Cp^R in Cp^RFe^+, Cb* in Cb^*Co^+, 3 x CO in the carbonyl complexes). Secondly, the phosphine precursor complexes, based on Cp^RFe^+ or Cb^*Co^+, have relatively shorter M-P bond lengths than do the corresponding complexes based on *fac*-$(CO)_3Cr$ or *fac*-$(CO)_3Mo$ due to the smaller radius of Fe and Co in comparison to both Cr or Mo in these complexes. These two factors cause the spectator ligands in Cp^RFe or Cb*Co to push the phosphine precursors into closer proximity and hence facilitate the formation of the smaller 9-membered P_3 macrocycles.

The *fac*-$(CO)_3Mn(CH_3CN)_3^+$ fragment is isoelectronic and structually analogous to *fac*-$(CO)_3Cr$ and *fac*-$(CO)_3Mo$. The cationic Mn(I) centre however has an intrinsically smaller radius than does the neutral metal in the group 6 metal carbonyls (1.27 Å for Mn, 1.28 Å for Cr and 1.39 Å for Mo[10]); this should help facilitate the closure of smaller ring systems. In addition, the $(CO)_3M$ (M = Cr and Mo) templates are the only known for

which liberation of a P3 macrocycle has been reported and the $(CO)_3Mn^+$ system may offer this advantage over the Cp^RFe^+ and Cb^*Co^+ systems.

An alternative manganese complex, (η^5-cyclopentadienyl)$Mn(CO)_3$, has previously been investigated in our group for the template-directed synthesis of P_3 macrocycles. The removal of all the three CO ligands by phosphine precursors however, proved to be difficult and attempts to prepare P_3 macrocycles using this template have failed.[11]

Refluxing $(CO)_5MnBr$ in acetonitrile gives the electrophilic fragment, $[(CO)_3Mn(CH_3CN)_3]^+$ which can be isolated as its PF_6^- salt in high yield.[12] The acetonitrile ligands in this species are labile and can be readily substituted. This feature allows us to develop its chemistry as a template for the synthesis of P_3 macrocycles with small ring systems.

4.2 Synthesis of a tribenzannulated 9-membered triphospha-macrocycles based on *fac*-tricarbonylmanganese templates

Scheme 1 shows the method for the synthesis of *fac*-tricarbonylmanganese(I)-1,4-bis(2-fluorophenyl)-7-phenyl-[b,e,h]tri-benzo-1,4,7-triphosphacyclononane by using the *fac*-$Mn(CO)_3^+$ fragment as a template.

Scheme 1 Synthesis of a manganese complex of tribenzannulated 1,4,7-triphosphacyclo-nonane

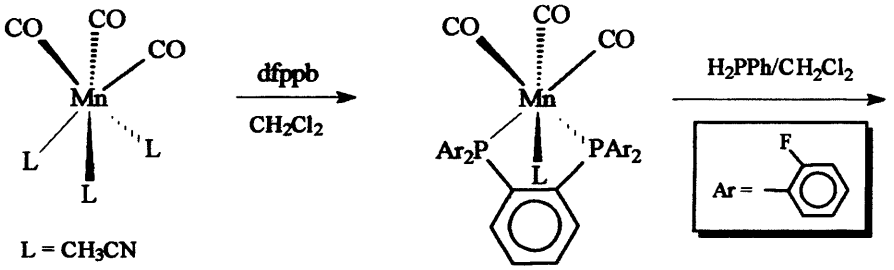

4.1 **4.2**

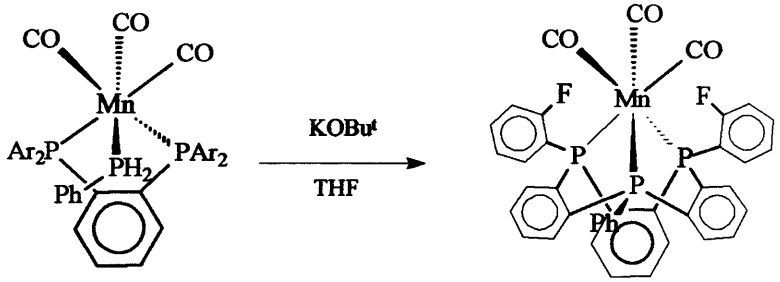

4.3 **4.4**

The strategy is the same as that developed for the synthesis of Fe and Co analogues which has been addressed in Chapter 1 and Chapter 3. The weakly coordinated acetonitrile ligands in $[(CO)_3Mn(CH_3CN)_3]^+$ (**4.1**) act as leaving groups to be sequentially displaced by 1,2-bis(di-2-fluorophenyl)phosphinobenzene (**dfppb**) and phenylphosphine ligands in stoichiometric reactions and affording the bisphosphine-monoacetonitrile complex, **4.2** and bisphosphine-monophosphine complex, **4.3**

respectively. The macrocycle complex, **4.4** was subsequently produced *via* an intramolecular P-C bond ring-closure reaction from **4.3**.

Treatment of $[(CO)_3Mn(CH_3CN)_3]PF_6$ (**4.1**·PF_6) with a molar equivalent of **dfppb** in CH_2Cl_2 produces the orange complex **4.2**, $[(CO)_3Mn(dfppb)CH_3CN]^+$, which was isolated as its PF_6^- salt. No obvious colour change was observed during the reaction. The substitution of CH_3CN ligands from **4.1** by **dfppb** is relatively slow and takes several hours to reach completion. It was found that removal of the volatile components in *vacuo* followed by addition of fresh solvent twice during the reaction facilitated the substitution, resulting in shorter reaction times. To prevent any structural isomerizations of **4.2** at elevated temperature, reactions were performed at room temperature.

The process was monitored by ^{31}P NMR spectroscopy. $^{31}P\{^1H\}$ NMR spectroscopy shows the disappearance of a resonance around δ -34 ppm due to free **dfppb** and the growth of a new resonance at δ 72.9 ppm, which indicates coordinated **dfppb** (**Figure 1**). The starting material (**4.1**·PF_6) was commonly contaminated with other manganese carbonyl species such as $(CO)_3Mn(CH_3CN)_2Br$, and in which case another resonance was observed at δ 59.0 ppm in the $^{31}P\{^1H\}$ NMR spectrum of the product. The product was purified by washing with Et_2O/petrol leaving the less soluble PF_6^- salt of **4.2**. The signal due to the CO resonance in the $^{13}C\{^1H\}$ NMR spectrum was broadened by the influence of the quadrupolar ^{55}Mn nucleus [13] and was observed at δ 215 ppm.

Figure 1 $^{31}P\{^{1}H\}$ NMR spectrum of **4.2** in CD_2Cl_2 at 20 °C.

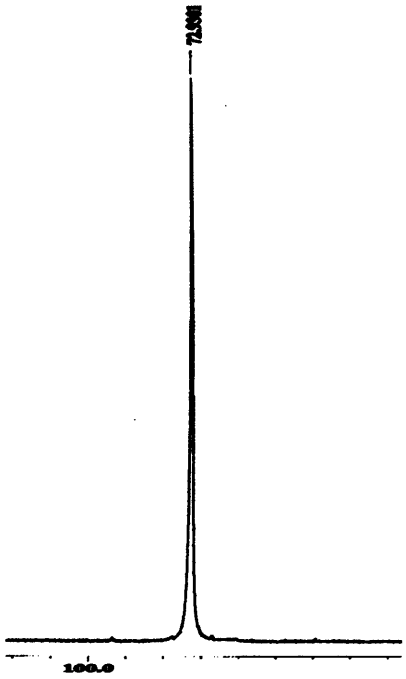

The configuration of **4.2** about the manganese centre can be assigned as *fac,cis-* in which the **dfppb** ligand is *cis* to the CH_3CN ligand and the CO ligands are in a *facial* arrangement. This stereochemistry is confirmed by the ^{31}P NMR and IR spectra. Thus, a single resonance due to coordinated **dfppb** in **4.2** is observed in the $^{31}P\{^{1}H\}$ NMR spectrum suggesting that only one isomer is present in solution. For $(CO_3)Mn(L_2)X$ (L_2, chelated phosphines; X, monodentate ligand) complexes, the CO vibrational frequencies and relative intensities in the IR spectrum are very useful for distinguishing between isomeric metal carbonyl species based on local symmetry of the CO groups.[14] Complex **4.2** has the expected strong $\upsilon_{(CO)}$ absorption bands with approximately equal intensities at 2031(s), 1961(s) and 1915(s) cm^{-1} which supports its *fac,cis-* stereochemistry.[14-16] The absorption band at 2344 cm^{-1} was assigned to $\upsilon_{(CN)}$ of the CH_3CN ligand.

Further displacement of the acetonitrile ligand in **4.2** was achieved by reaction in CH_2Cl_2 with a molar equivalent of phenylphosphine. The substitution reaction progressed quite rapidly and was monitored by

$^{31}P\{^{1}H\}$ spectroscopy. Complex **4.3**, $[(CO)_3Mn(dfppb)(PH_2Ph)]^+$, crystallized as its pale yellow PF_6^- salt in quantitative yield. The IR spectrum of **4.3** shows three CO vibrations at 2037(s), 1974(s), 1964(s) cm^{-1} which indicates a *fac,cis-* geometry as mentioned above; the disappearance of $\upsilon_{(CN)}$ and growth of a new band at 2365 cm^{-1} which assigned to the PH stretching vibration, confirms the replacement of the CH_3CN ligand by a phenylphosphine ligand. The slight increase in $\upsilon_{(CO)}$ upon replacement of CH_3CN by H_2PPh is consistent with H_2PPh being a slightly better π–acid (or poorer σ-base) than CH_3CN. The ^{1}H NMR spectrum of **4.3** shows a broad doublet of PH protons (δ = 4.31 ppm, $^{1}J_{H,P}$ = 360 Hz). The resonances attributed to CO were observed at δ 265 ppm in $^{13}C\{^{1}H\}$ NMR spectrum although these were broadened due to the effect of the ^{55}Mn quadrupolar nucleus as well as coupling to P and were difficult to observe (weak). Again, the signals of coordinated **dfppb** and phenylphosphine in the $^{31}P\{^{1}H\}$ NMR spectrum appear as broad multiplets at δ 72.4 ppm and δ -17.6 ppm respectively (**Figure 2**). The resonances are complicated due to the influence of the ^{55}Mn quadrupolar nucleus superimposed on P-P and P-F coupling.

Figure 2 $^{31}P\{^{1}H\}$ NMR spectrum of **4.3** in CD_2Cl_2 at 20 °C.

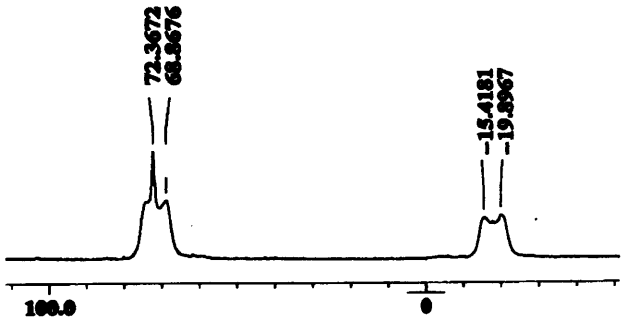

The geometry of **4.3** was further confirmed by its crystal structure which was determined by X-ray diffraction (**Figure 3**). The Mn centre of **4.3** possesses a distorted *fac*-octahedral coordination environment with facial

CO ligands occupying three sites, the **dppb** ligand chelates in the *pseudo*-equatorial plane, and the phenylphosphine resides in the remaining position. The structure of **4.3** bears mirror symmetry, the mirror plane being normal to the plane of the phenyl group of phenylphosphine; it passes through the P-C_{ipso} bond, one CO and the Mn centre. The **dfppb** ligand has relatively longer M-P bond lengths {2.332(1) Å} than does the phenylphosphine ligand {2.322(1) Å}, which may simply be due to the greatly steric demand of the **dfppb** ligand than that of the phenylphosphine ligand although electronic effects may be significant. The electron-withdrawing ability of the fluorine atoms may help to decrease the σ-basicity of **dfppb**. The Mn-C bond length *trans* to the phenylphosphine ligand {1.840(4) Å} is longer than those *trans* to the **dfppb** ligand {1.821(3) Å} suggesting that H_2PPh may be a better π–acid than **dfppb** whereas the Mn-C bond length *trans* to X is shorter than those *trans* to the P atoms of L_2 in the complexes $(CO)_3Mn(L_2)X$ (L_2, chelate phosphines; X, monodentate ligand such as Cl, Br, NCO or PPh_3).[14,17-19] The P-Mn-P angles of 83.61(4)° for the **dfppb** chelate bite in **4.3** is smaller than 90° and is similar to other related 5-membered chelates in $(CO)_3Mn\{C_6H_4(PPh_2)_2\text{-}o\}Cl$ {81.98(6)°}, $(CO)_3Mn\{C_6H_4\text{-}(PH_2)_2\text{-}o\}Cl$ {83.06(6)°} and $(CO)_3Mn(dppe)Br$ {84.14(10)°}.[17]

Figure 3 ORTEP plot (30% probability level) of **4.3** (H atoms on phenyl group omitted).

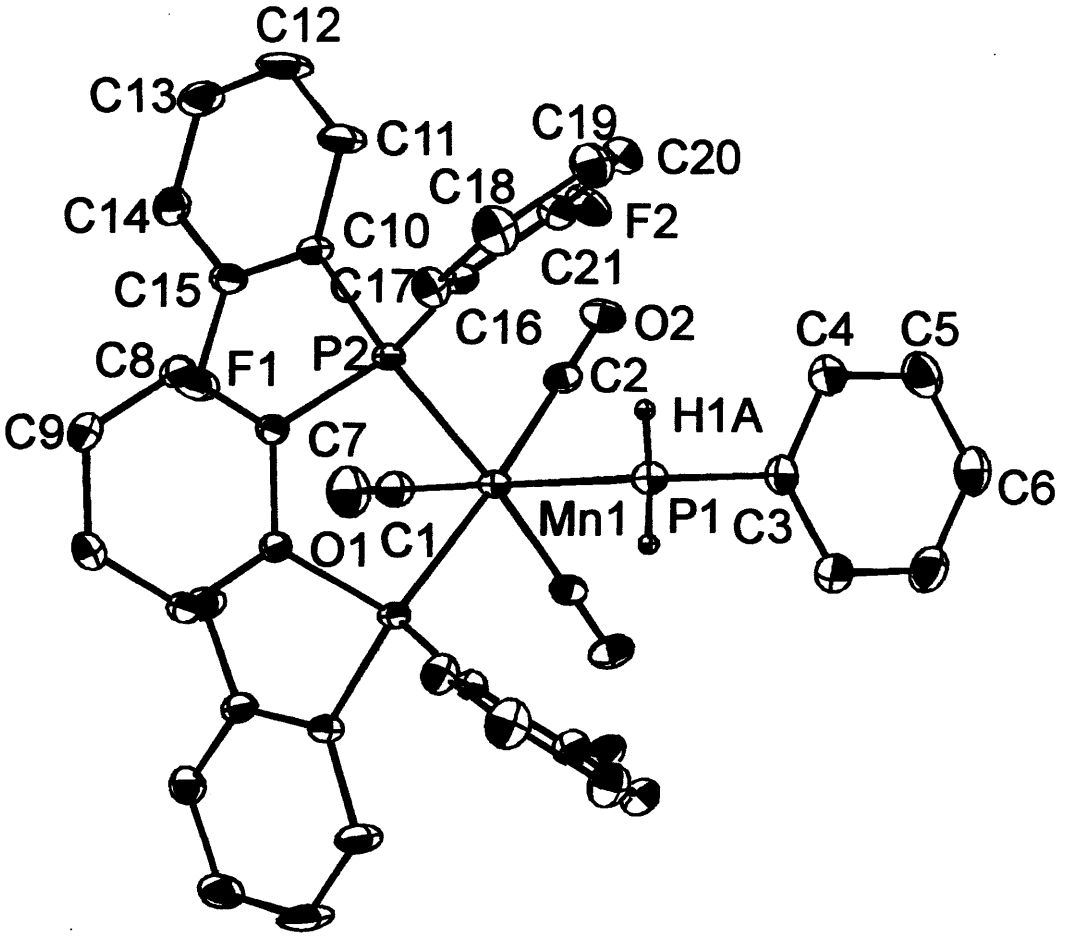

Selected bond distances (Å): C1-Mn1 1.840(4) C2-Mn1 1.821(3) P1-Mn1 2.3221(12) P2-Mn1 2.3328(8) Selected bond angles (°): C2-Mn1-C2#1 92.19(17) C2-Mn1-C1 86.55(13) C2-Mn1-P1 86.19(9) C2-Mn1-P2 92.10(9) C1-Mn1-P1 169.52(14) C1-Mn1-P2 92.93(11) C2#1-Mn1-P2 175.64(9) P1-Mn1-P2 94.88(3) P2#1-Mn1-P2 83.61(4) (#1 x, -y, z)

The cyclization reaction to produce the macrocycle complex, $[(CO)_3Mn\{1,4\text{-bis}(2\text{-fluorophenyl})\text{-}7\text{-phenyl-}[b,e,h]\text{tribenzo-}1,4,7\text{-triphosphacyclononane}\}]^+$ (**4.4**), was carried out by addition of 2 molar equivalents of $KOBu^t$ to a solution of **4.3**·PF_6 in anhydrous THF, resulting in a rapid change of colour from yellow to red within a minute. The solution subsequently changed colour to pale yellow and the less soluble complex, **4.4**·PF_6 precipitated out as an off-white powder. Complex **4.4**·PF_6 is obtained as an air-stable solid although in solution a colour change (from colourless to pale yellow) was noticed in the presence of air and an unidentified species was observed in the ^{19}F (s, -δ 102 ppm) and $^{31}P\{^1H\}$ (δ 28.4 ppm) NMR spectra. **4.4**·BPh_4 was obtained by anion exchange in order to enhance the solubility of the cation in common organic solvents. This salt was used for micro-analysis. It is reasonable to propose that the mechanism of ring closure is similar to that for the synthesis of the Fe and Co tribenzannulated 1,4,7-[9]ane-P_3 macrocyclic analogues. The process involves deprotonation of phenylphosphine by base to produce a coordinated phosphide nucleophile, followed by intramolecular nucleophilic aromatic substitution of the *ortho* fluorine atom in the fluorophenyl group within the coordination sphere of manganese. Although the Mn-P bond lenghs in complex **4.3** are expected to be relatively longer than the Fe-P and Co-P bond lengths in analogous Cp^RFe and Cb*Co complexes, the less-restricted rotation of the -C_6H_4F group around the P-C_{ipso} bond (due to the lower bulk of the CO and perhaps an electrostatic attraction between the F atom and the phosphide lone pair) allows the nucleophile and electrophile to orientate in close proximity to favour the cyclisation reaction. The yield of **4.4** is sensitive to the amount of $KOBu^t$ used. With excess $KOBu^t$, the **dppb** ligand in **4.3** may be displaced from the Mn

centre. Under these conditions, the free ligand was observed by $^{31}P\{^{1}H\}$ NMR spectroscopy.

Complex **4.4** was characterized by spectroscopic and analytical methods. The IR spectrum shows three bands due to $\upsilon_{(CO)}$ {2030(s), 1974(s,), 1962(s) cm^{-1}} indicating the *fac-* configuration. The P_3 macrocycle ligand should have an excellent ligating ability and be a stronger σ-donor than the combination of **dfppb** and H_2PPh ligands in **4.3**. This would cause the metal centre in the macrocycle complex to be more electron rich than that in **4.3**. This renders a slight reduction in $\upsilon_{(CO)}$ in **4.4** in comparison to that in **4.3**. The molecular ion (m/z = 728 amu) was observed in the mass spectrum. The disappearance of resonances due to the coordinated **dfppb** and phenylphosphine ligands in **4.3** and the growth of resonances significantly shifted downfield in the $^{31}P\{^{1}H\}$ NMR spectrum (**Figure 4**), suggests the formation of the macrocycle. The resonance in the $^{31}P\{^{1}H\}$ spectrum (δ 109 ppm) is complex due to P-P and P-F coupling and quadrupolar broadening which cause the superimposition of multiplets due to the two unique sets of P atoms in the macrocycle with an A_2B resonance pattern. The single resonance of **4.4** in the $^{19}F\{^{1}H\}$ NMR spectrum (δ -96.4 ppm) indicates rapid rotation of fluorophenyl groups around the P-C_{exo} bonds and relatively little steric hindrance between the CO ligands and the fluorophenyl group.

Figure 4 $^{31}P\{^{1}H\}$ NMR spectrum of **4.4** in CD_3NO_2 at 20 °C.

The crystal structure of **4.4** is presented in **Figure 5** which shows the tribenzannulated 1,4,7-[9]ane-P_3 ligand binding the Mn centre *via* three fused 5-membered chelate rings with three *trans* (to P) CO ligands making up the distorted octahedral configuration around the Mn centre. The Mn-P bond lengths in **4.4** {2.259(1) Å, 2.258(1) Å, 2.261(1) Å} are significantly shorter than those in the acyclic **4.3** {aver. 2.327(1) Å} and in the {1,5,9-[12]ane-P_3Et_3}$Mn(CO)_2Br$[20] complex {2.327(2) Å, 2.243(2) Å, 2.331(2) Å}. In the example of 1,5,9-[12]ane-P_3Et_3, the Mn-P bonds are associated with 6-membered chelate rings. The relatively short Mn-P distances in **4.4** indicate the good ligating capability of the 9-membered P_3 macrocycle. The non-bonded P...P distances of 3.019(15) Å, 3.024(15) Å and 3.030(15) Å in **4.4** are comparable to those in the tribenzannulated macrocycle Co analogues {**3.6** in chapter 3, aver.

3.000(12) Å} but are slightly longer than those in the iron complex, $[Cp^{R}Fe(1,4,7\text{-}[9]aneP_3\text{-}Et_3)]^+$ {aver. 2.969(3) Å}, which has an aliphatic backbone.[21] The slightly longer non-bonded P...P distances in aromatic macrocycle complexes (**4.4** and **3.6**) may be due to the rigidity of the phenylene backbone functions. The P-Mn-P angles of 83.79(5)°, 83.96(5)° and 84.23(5)° are smaller than those in the Co macrocycle complex, **3.6** {88.10(5)°, 87.74(4)°, 88.35(4)°}, which is expected due to Mn(I) having a larger radius than Co(III) hence a longer Mn-P bond length than Co-P bond length. The P-Mn-P angles in the more restricted 5-membered rings in **4.4** are also smaller than those in the 6-membered chelate rings in $\{1\text{-}5,9\text{-}[12]ane\text{-}P_3Et_3\}Mn(CO)_2Br$ {aver. 93.81(7)°}.[20] The average value of 119.2(1)° for the Mn-P-C_{exo} (exocyclic phenyl or fluophenyl group) angles indicates steric repulsion between the terminal phenyl or fluorophenyl groups and the CO spectator ligands. The Mn-P-C_{exo} angles are however considerably smaller than those in the Co analogue {**3.6**, aver. 125.60(17)°} indicating that the corresponding repulsion in **4.4** is weaker than that in **3.6** which bears a much bulkier tetramethylcyclobutadienyl ligand.

Figure 5 ORTEP plot (30% probability level) of **4.4** (H atoms omitted)

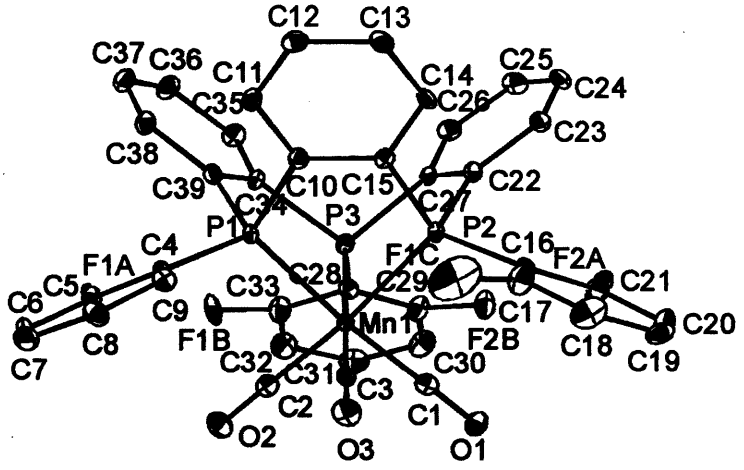

(a)

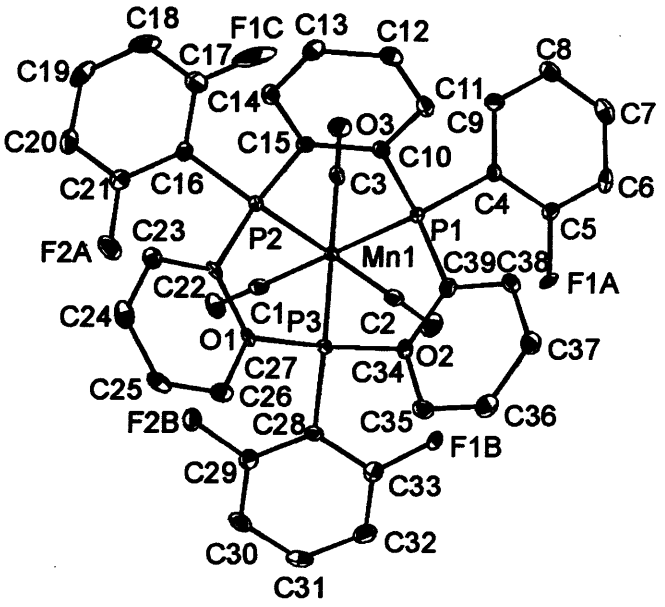

(b)

Selected bond distances (Å): Mn1-C3 1.825(6) Mn1-C2 1.832(6) Mn1-C1 1.837(6) Mn1-P2 2.2583(15) Mn1-P1 2.2590(15) Mn1-P3 2.2616(15) Selected bond angles (°): C(3)-Mn(1)-C(2) 93.6(2) C(3)-Mn(1)-C(1) 92.5(2) C(2)-Mn(1)-C(1) 92.2(2) C(3)-Mn(1)-P(2) 90.95(16) C(2)-Mn(1)-P(2) 174.09(17) C(1)-Mn(1)-P(2) 91.32(17) C(3)-Mn(1)-P(1) 91.18(17) C(2)-Mn(1)-P(1) 91.97(18) C(1)-Mn(1)-P(1) 174.25(18) P(2)-Mn(1)-P(1) 84.21(5) C(3)-Mn(1)-P(3) 173.15(17) C(2)-Mn(1)-P(3) 91.34(17) C(1)-Mn(1)-P(3) 91.99(17) P(2)-Mn(1)-P(3) 83.78(5) P(1)-Mn(1)-P(3) 83.95(5) C(4)-P(1)-Mn(1) 119.33(17) C(10)-P(1)-Mn(1) 110.15(18) C(39)-P(1)-Mn(1) 110.09(19) C(16)-P(2)-Mn(1) 119.10(18) C(15)-P(2)-Mn(1) 109.89(18) C(22)-P(2)-Mn(1) 110.30(18) C(28)-P(3)-Mn(1) 119.22(17) C(27)-P(3)-Mn(1) 110.15(18) C(34)-P(3)-Mn(1) 109.73(19)

4.3 Preliminary reaction studies towards macrocyclic ligand liberation

A series of reactions involving metal oxidation, CO abstraction and fluorine atom substitution of **4.4** have been surveyed in order to explore macrocyclic ligand liberation methods. Preliminary results show that the $(CO)_3Mn^+$ fragment is not as stable as the Cp^RFe^+ and Cb^*Co^+ fragments. Complex **4.4** is susceptible to nucleophilic attack and strong bases such as $KOBu^t$. The CO ligand can be removed by CO abstraction reagents such as Me_3NO.[22] Variations of the macrocycle may be available by nucleophilic aromatic substitution at the *ortho* position of the *exo* fluorophenyl group by hydride reagents and other nucleophiles. The oxidation of the d^6 Mn(I) centre to higher oxidation states is also possible under mild conditions.[23] All these present an opportunity for the liberation of the P_3 macrocycle and for future exploration of its coordination and/or catalytic chemistry. Interestingly, UV irradiation of **4.4** in benzonitrile at high temperature for 3 hours, followed by work-up in air, gives rise to a new complex, $[(1,4\text{-dioxo-}1,4\text{-bis}(2\text{-}FC_6H_4)\text{-}7\text{-}C_6H_5\text{-}[b,e,h]\text{tribenzo-}1,4,7\text{-triphosphacyclononane})_2Mn(C_6H_5CONH_2)_2]^{2+}$ **(4.5)**, which was isolated as a minor product (**Scheme 2**).

Scheme 2 liberation of P_3 macrocycle by photolysis and oxidation

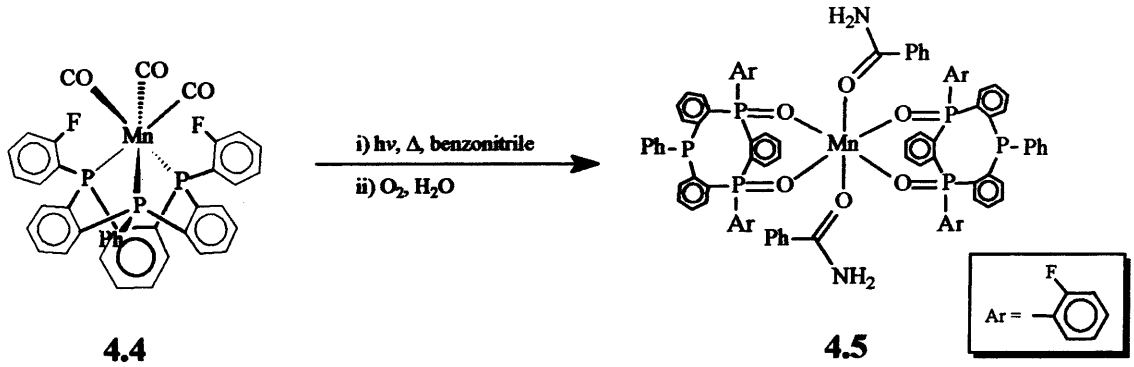

4.4 **4.5**

Complex **4.5** was crystallized as its SbF_6^- salt and characterized by X-ray diffraction (**Figure 6**). The cation bears an octahedral Mn(II) centre located on a crystallographic inversion centre with a MnO_6 environment. The CO ligands in **4.4** have clearly been removed. Two P atoms of each triphosphamacrocycle in **4.4** have been oxidised to phosphine oxides which are coordinated to the Mn atom in a *cis* arrangement through the O donors. It is reasonable to assume that the two P atoms which bear electron-withdrawing fluorophenyl groups were oxidised although the positions of these two F atoms could not be unequivocally located as they were disordered in the crystal structure and refined in partial occupancies (0.8, 0.7, 0.5) attached to all three phenyl substitutents. All the P=O oxygens lie in the equatorial plane. The third P atom is uncoordinated and is inverted relative to the others two, presumably due to the high temperature during the reaction, although oxidation of the other two phosphines may cause this inversion depending upon the mechanism of oxidation. The resultant conformation at the three P atoms is *syn, anti*. Surprisingly, two benzamide ligands are also coordinated to the Mn centre *via* the O donors; they occupy the axial positions.

It is not clear what mechanism operates during this reaction, or what kind of intermediates are involved during the reaction. The reaction which yielded **4.5** however is important in that it clearly indicates that the P_3 macrocycle ligand has been liberated during the reaction. In this study, it appears that these manganese complexes show catalytic activity for the hydration of benzonitrile to benzamide.[24] A trace of water present in the system is presumably responsible for the promoting this transformation.

Figure 6 ORTEP plot (30% probability level) of **4.5** (H atoms on phenyl group omitted).

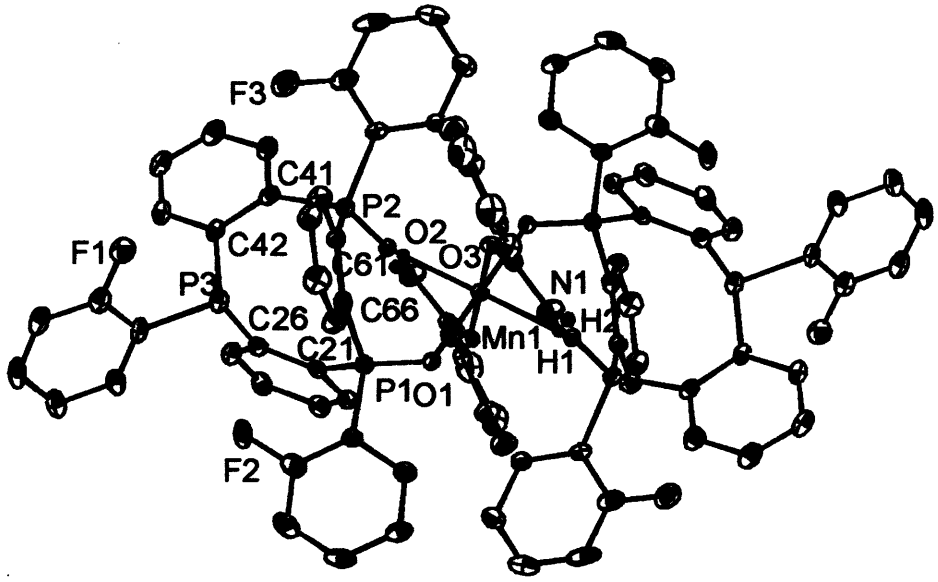

(a)

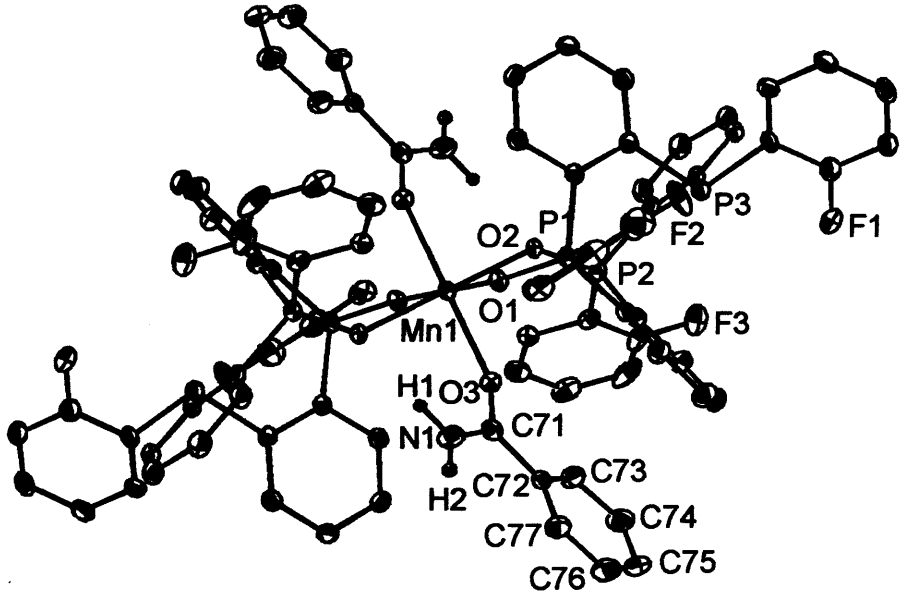

(b)

Selected bond distances (Å): Mn1-O1 2.106(2) Mn1-O2 2.246(2) Mn1-O3 2.154(3) O3-C71 1.250(4) N1-C71 1.322(5) Selected bond angles (°): O1#1-Mn1-O1 180.0(3) O1#1-Mn1-O3 92.38(10) O1-Mn1-O3 87.62(10) O1-Mn1-O3#1 92.38(10) O3-Mn1-O3#1 180.0(2) O1-Mn1-O2#1 94.49(9) O3-Mn1-O2#1 91.62(9) O1-Mn1-O2 85.51(9) O3-Mn1-O2 88.38(9) O2#1-Mn1-O2 180.0(2) (#1 -x, -y, -z)

4.4 Conclusions and Prospects

For the first time, the carbonyl manganese complex, *fac*-$(CO)_3Mn^+$ has been successfully used as a template to synthesize a 9-membered P_3 macrocycle, $(CO)_3$Mn-1,4-bis(2-fluorophenyl)-7-phenyl-[b,e,h]tribenzo-1,4,7-triphosphacyclononane (**4.4**). The work is of interest since it may be easier to labilise the Mn (than the Fe or Co in previously studied templates) and hence to liberate the macrocycle ligand. Preliminary experiments show that complex **4.4** undergoes very interesting reactions towards the liberation of the macrocycle ligand.

For the Cp^RFe^+, Cb^*Co^+ and $(CO)_3Mn^+$ templates, the strategy for the synthesis of 9-membered P_3 macrocycles with tribenzannulated backbones by an intramolecular dehydrofluorination works well. In contrast to the Fe system, the Co and Mn systems seem to be less suitable for the synthesis of other P_3 macrocycle derivatives with small ring systems and aliphatic backbones. The template-directed method is based on substituting labile acetonitrile ligands with a suitable diphosphine followed by introduction of a complementary monophosphine to the metal centre in the first stage. The limitations of this method arise from the different ability of appropriate phosphines to form reasonably stable complexes with the template metal, and also to substitute acetonitrile. Thus to extend the chemistry of the Cb^*Co^+ and *fac*-$(CO)_3Mn^+$ fragments as more versatile templates for the synthesis other P_3 macocycle derivatives with small ring systems remains a challenging task.

4.5 Experimental Section

For general experimental information see **Chapter 2** and **3**.

Materials: $[(CO)_3Mn(CH_3CN)_3]PF_6$[12] and phenylphosphine[25] were prepared according to literature methods.

X-ray crystallography: Complex **4.3** was crystallised as its PF_6^- salt. Both of complex **4.4** and **4.5** were crystallised as SbF_6^- salts. The two F atoms of fluorophenyl group in **4.4** are refined and distributed in five *ortho* positions of three phenyls with disordered model of approximately occupancy factor of 0.64:0.22:0.14:0.56:0.44 for F1A, F1B, F1C, F2A and F2B respectively. Crystal structure and refinement data are collected in **Appendix C** and supplementary CD.

$[(CO)_3Mn\{(o\text{-}C_6H_4F)_2PC_6H_4P(o\text{-}C_6H_4F)_2\}(CH_3CN)]PF_6$ (4.2·PF_6)

To a solution of $[(CO)_3Mn(CH_3CN)_3]PF_6$(**4.1**·PF_6) (0.15 g, 0.368 mmol) in 20ml CH_2Cl_2, **dfppb** (0.19g, 0.368 mmol) was added with stirring. After 2 hours, the solvent was evaporated in *vacuo*. Then 20ml CH_2Cl_2 was added and stirring continued for another 2 hours. The $^{31}P\{^1H\}$ NMR spectrum showed the growth of a resonance due to coordinated **dfppb** at δ 72.9 ppm. All the volatiles were removed in *vacuo*, and the solid residue washed with Et_2O/petrol and then dissolved in CH_2Cl_2, followed by filtration and concentration. Orange crystals of **4.2**·PF_6 were obtained by diffusion of diethyl ether vapour into the solution. Yield: 98%. $^{31}P\{^1H\}$ (CD_2Cl_2): 72.9(dfppb), -144.1(sep, PF_6, $^1J_{P,F}$ = 711 Hz). $^{19}F\{^1H\}$ (CD_2Cl_2): -94.5 (s, dfppb), -95.0 (s, dfppb), -73.1(d, PF_6). $^{13}C\{^1H\}$ (CD_2Cl_2): 215 (CO, weak and broad), 2.4 (MeCN). ^1H (CD_2Cl_2): 7.6 to 6.4 (20H, m, H_{aryl}), 1.15 (3H, s, CH_3CN). IR: 2344 (w, CN), 2031 (s, CO), 1961 (s, CO), 1915 (s, CO)

$[(CO)_3Mn\{(o\text{-}C_6H_4F)_2PC_6H_4P(o\text{-}C_6H_4F)_2\}(PH_2Ph)]PF_6$ (4.3·PF_6)

To a solution of **4.2**·PF_6 (0.20g, 0.22mmol) in 20ml CH_2Cl_2, phenylphosphine (0.03g, 0.27mmol) in toluene was added. After stirring for 15 minutes, $^{31}P\{^1H\}$ NMR spectrum showed the growth of a broad resonance of coordinated phenylphosphine at δ –17.6 ppm. The resonance for coordinated dfppb became very broad at δ 72.4 ppm. Then the reaction mixture was filtered. The solvent was removed in *vacuo* and the residue was triturated with diethyl ether to remove excess amount of phenylphosphine. The yellow powder was then dissolved in CH_2Cl_2 and concentrated. Yellow crystals of **4.3**·PF_6 were obtained by diffusion of diethyl ether vapour into the solution. Yield: 98%. $^{31}P\{^1H\}$ (CD_2Cl_2): 72.4 (dfppb), -17.6 (dfppb), -143.3 (sep, PF_6, $^1J_{P,F}$ = 710 Hz). $^{19}F\{^1H\}$ (CD_2Cl_2): -93.2 (s, dfppb), -94.4 (s, dfppb), -73.2(d, PF_6). $^{13}C\{^1H\}$ (CD_2Cl_2): 265 (CO, very weak). ^1H (CD_2Cl_2): 7.4 to 6.7 (m, 25H, H_{aryl}), 4.31 (d, 2H, PH, $^1J_{P,H}$ = 360 Hz). IR: 2365 (s, PH), 2037 (s, CO), 1974 (s, CO), 1964 (s, CO). M.S.(APCI): 767.9 (M^+)

$(CO)_3$Mn-1,4-bis(2-fluorophenyl)-7-phenyl-[b,e,h]tribenzo-1,4,7-triphosphacyclononane hexafluorophosphate (4.4·PF_6)

To a solution of **4.3**·PF_6 (0.27 g, 0.29 mmol) in 30ml THF was added $KOBu^t$ (65 mg, 0.58mmol). The colour of the solution changed over approximately 1 minute from yellow to red then to very pale yellow with the formation of a white precipitate. After filtering, the white precipitate was dissolved in CH_2Cl_2 and a $^{31}P\{^1H\}$ NMR spectrum showed a broad complex multiplet significantly shifted downfield at δ 109 ppm. **4.4**·BPh_4 was collected by anion exchange from its PF_6^- salt in THF to enhance the solubility. Single crystals for X-ray analysis ware obtained as its SbF_6^- salt. Yield: more than 80%. $^{31}P\{^1H\}$ (CD_3NO_2): 109 (m, broad), -144.7 (sep, $^1J_{P,F}$ = 712 Hz). $^{13}C\{^1H\}$ (CD_2Cl_2): 251 (CO, very weak). ^{19}F

(CD_2Cl_2): -96.4 (s, fluorophenyl), -73.4 (d, PF_6). ^1H {CD_2Cl_2}: 7.6 to 7.1 (m, H_{aryl}). IR (KBr): 2030 (s, CO), 1974 (s, CO), 1962 (s, CO). M.S.(APCI) : 728.0 (M^+). Anal. Calcd for $C_{63}H_{45}B_1F_2Mn_1O_3P_3$ (**4.4**·BPh_4, M = 1046.71 gmol^{-1}): C, 72.29; H, 4.33. Found: C, 72.08; H, 4.23.

[$(CO)_3$Mn{1,4-dioxo-1,4-bis(2-fluorophenyl)-7-phenyl-[b,e,h]tri-benzo-1,4,7-triphosphacyclononane}]SbF_6 (4.5·SbF_6)

A solution of **4.4**·SbF_6 (40 mg, 0.04 mmol) in 20 ml benzonitrile was irradiated with UV light at 180 °C for 3 hour. The colour of the solution changed from colourless to red. Mass and $^{31}P\{^1H\}$ NMR spectra indicated that **4.4** still existed as the major component in the solution. The solvent was removed in *vacuo* and the residue was dissolved in CH_3CN. Colourless crystals of **4.5**·SbF_6 were obtained by evaporation of the solvent slowly in open air.

References

1. P. G. Edwards; M. L. Whatton; R. Haigh, *Organometallics* **2000**, 19(14), 2652-2654.
2. P. G. Edwards; P. D. Newman; D. E. Hibbs, *Angew. Chem. Int. Ed.* **2000**, 39(15), 2722-2724.
3. R. Haigh, *Doctoral Thesis*, **2002**, Cardiff University
4. T. Albers, *Doctoral Thesis*, **2001**, Cardiff University
5. J. Johnstone, *Doctoral Thesis*, **2004**, Cardiff University
6. S. J. Coles; P. G. Edwards; J. S. Fleming; Hursthouse, B. Michael; S. S. Liyanage, *Chem. Commun.* **1996**, (3), 293-4.
7. P. G. Edwards; J. S. Fleming; S. S. Liyanage, *Inorg. Chem.* **1996**, 35(16), 4563-4568.
8. P. G. Edwards; J. S. Fleming; S. S. Liyanage, *Dalton Trans.*, **1997**, (2), 193-197.
9. A. J. Price; P. G. Edwards, *Chem. Commun.* **2000** (11), 899-900.
10. J. G. Speight, *Lange's Handbook of Chemistry* 16th Ed. McGraw-Hill, New York 2005.
11. R. Haigh, *Doctoral Tthesis* **2002**, Cardiff University
12. R. H. Reimann; E. Singleton, *J. Organomet. Chem.*, 59, C24-C26, **1973**
13. D. Rentsch; R. Hany; W. von Philipsborn, *Magnetic Resourance in Chemistry*, vol. 35, 832-838, **1997**
14. M. A. Beckett et al, *J. Organomet. Chem.*, 688, 174-180, **2003**
15. G. A. Carriedo, V. Riera, *J. Organomet. Chem.*, 205, 371-379, **1981**
16. R. J. Angelici; F. Basolo; A. J. Poe, *J. Am. Chem. Soc.* 85(15), 2215-19, **1963**.
17. S. J. A. Pope, G. Reid, *J. Chem. Soc., Dalton Trans.*, 1615-1621, **1999**
18. S. K. Mandal; D. M. Ho; M. Orchin, *Polyhedron*, 11(16), 2055-2063, **1992**
19. T. M. Becker; J. A. Krause-Bauer; C. L. Homrighausen; M. Orchin, *Polyhedron*, 18, 2563-2571, **1999**.
20. R. J. Baker; P. G. Edwards; J. Gracia-Mora; F. Ingold; K. M. A. Malik, *Dalton Trans.* **2002**, (21), 3985-3992.
21. P. G. Edwards; P. D. Newman; K. M. A. Malik, *Angew. Chem. Int. Ed.* **2000**, 39(16), 2922-2924.
22. M. O. Albers; N. J. Coville, *Coord. Chem. Rev.*, 53, 227-259, **1984**.

23. R. H. Reimann; E. Singleton, *J. Chem. Soc, Dalton Trans*, 808-813, **1974**

24. Wai Kit Fung; X. Huang; M. L. Man; S. M. Ng; M. Y. Hung; Z. Lin; C. Po. Lau, *J. Am. Chem. Soc.* **2003**, 125(38), 11539-11544.

25. L. D. Freedman; C. O. Doak, *J. Am. Chem. Soc* **1952**, 74, 3414.

Appendix A

Crystal data and structure refinement for complexes in Chapter 2

Complex	**2.1**·2BF_4	**2.2**·2BF_4·CH_3CN	**2.3**·2BF_4	**2.4**·2BF_4·CH_3CN	**2.5**·2BF4
Empirical formula	C22H31N9B2F8Fe1	C36H34N10B2F8Fe1	C22H31N9B2F8Co1	C36H34N10B2F8Co1	C32H54N2B2F8P4Fe1
M, g mol^{-1}	651.03	836.20	654.11	839.28	820.12
Crystal system	Trigonal	Monoclinic	Trigonal	Monoclinic	Monoclinic
Space group	P-3	P2(1)/n	P-3	P2(1)/n	P2(1)/n
a, Å	11.3020(7)	12.3614(2)	11.3359(5)	12.3345(2)	10.3691(3)
b, Å	11.3020(7)	16.4253(3)	11.3359(5)	16.3676(3)	11.8290(3)
c, Å	13.3820(6)	19.3493(4)	13.2939(6)	19.3388(4)	16.2524(4)
β, °		92.5822(10)		92.6709(6)	92.2681(16)
Z	2	4	2	4	2
V, $Å^3$	1480.34	3924.69(13)	1479.43(11)	3899.99(12)	1991.89(9)
D_{calcd}, g cm^{-3}	1.427	1.415	1.435	1.429	1.367
μ, mm^{-1}	0.586	0.463	0.656	0.520	0.602
Crystal size (mm^3)	0.23 x 0.19 x 0.17	0.20 x 0.18 x 0.16	0.12 x 0.10 x 0.08	0.22 x 0.18 x 0.08	0.26 x 0.22 x 0.18
Reflections collected	6874	31085	6424	61192	18584
Unique reflections (R_{int})	1931(0.0559)	7718(0.0809)	2255(0.0520)	7619(0.1291)	4542(0.0676)
Max./min.transmission	0.9273/0.9018	0.9295/ 0.9130	0.9494/0.9254	0.9596/ 0.8943	0.8994/0.8592
Goodness-of-fit on F^2	1.094	1.053	1.080	1.029	0.997
R values [$I < 2\sigma(I_0)$]	$R1$ = 0.0716 $wR2$ = 0.2048	$R1$ = 0.0574 $wR2$ = 0.1336	$R1$ = 0.0752 $wR2$ = 0.2329	$R1$ = 0.0495 $wR2$ = 0.1130	$R1$ = 0.0608 $wR2$ = 0.1738
R values, all data	$R1$ = 0.0923 $wR2$ = 0.2231	$R1$ = 0.0812 $wR2$ = 0.1462	$R1$ = 0.1098 $wR2$ = 0.2515	$R1$ = 0.0668 $wR2$ = 0.1225	$R1$ = 0.0866 $wR2$ = 0.1838

*Atomic coordinates, equivalent isotropic displacement parameters, bond lengths and bond angles for all the complexes are collected in the supplementary CD.

Appendix B

Crystal data and structure refinement for complexes in Chapter 3

Complex	**3.2**·PF_6	**3.3**·PF_6	**3.4**·PF_6	**3.5**·PF_6	**3.6**·PF_6·CH_3CN	**3.7**·SbF_6·0.5CH_3CN
Empirical formula	C36H39Col F6N1P3	C40H43Col F6P4	C40H35Col F10N1P3	C44H39Col F10P4	C46H40Col F8N1P4	C45H36.5 Col F6N0.5P3Sb1
M, g mol^{-1}	751.52	820.55	871.53	940.56	941.60	971.88
Crystal system	Monoclinic	Monoclinic	Orthorhombic	Triclinic	Monoclinic	Monoclinic
Space group	P 21/c	P 21/c	P cab	P -1	P 21/c	C 2/c
a, Å	11.3864(3)	13.3220(2)	11.3359(5)	10.9766(2)	14.5081(3)	29.757(5)
b, Å	16.8174(4)	19.5100(4)	11.3359(5)	13.7217(3)	14.9988(3)	14.137(5)
c, Å	18.6870(4)	14.5130(3)	13.2939(6)	13.8448(3)	19.7361(4)	19.573(5)
α, °			15.9700(2)	84.052(1)		
β, °	104.2732(10)	96.3780(12)	24.4817(3)	75.647(1)	100.0900(10)	96.818(5)
γ, °			19.5063(3)	79.706(1)		
Z	4	4	8	2	4	8
V, Å^3	3467.91(14)	3748.76(12)	7626.43(18)	1983.81(7)	4228.23(15)	8176(4)
D_{calcd}, g cm^{-3}	1.439	1.454	1.518	1.575	1.479	1.579
μ, mm^{-1}	0.693	0.688	0.656	0.675	0.628	1.245
Crystal size (mm^3)	0.40, 0.35, 0.30	0.35, 0.25, 0.23	0.35, 0.20, 0.15	0.35, 0.30, 0.15	0.20, 0.20, 0.20	0.25, 0.10, 0.10
Reflections collected	30795	42415	94367	29619	40958	62879
Unique reflections (R_{int})	7921(0.0930)	8574(0.1104)	8722(0.1228)	9034(0.0810)	9481(0.0991)	9339(0.1234)
Max./min. transmission	0.962/0.686	0.936/0.829	0.9080/ 0.7980	0.9055/0.7980	0.998/0.843	0.8856/0.7461
Goodness-of-fit on F^2	1.062	1.032	1.041	1.050	1.021	1.031
R values [$I < 2\sigma(I_0)$]	$R1$ = 0.0560 $wR2$ = 0.1229	$R1$ = 0.0479 $wR2$ = 0.1064	$R1$ = 0.0463 $wR2$ = 0.0961	$R1$ = 0.0467 $wR2$ = 0.0972	$R1$ = 0.0697 $wR2$ = 0.1477	$R1$ = 0.0820 $wR2$ = 0.1940
R values, All data	$R1$ = 0.0886 $wR2$ = 0.1359	$R1$ = 0.0839 $wR2$ = 0.1210	$R1$ = 0.1087 $wR2$ = 0.1166	$R1$ = 0.0794 $wR2$ = 0.1093	$R1$ = 0.1242 $wR2$ = 0.1695	$R1$ = 0.1149 $wR2$ = 0.2163

*Atomic coordinates, equivalent isotropic displacement parameters, bond lengths and bond angles for all the complexes are collected in the supplementary CD.

Appendix C

Crystal data and structure refinement for complexes in Chapter 4

Complex	4.3·PF_6	4.4·SbF_6·2CH_3CN	4.5·2SbF_6·2CH_3CN
Empirical formula	C39H27F10Mn1O3P4	C43H31F8Mn1N2O3P3Sb1	C90H70F16Mn1N4O6P6Sb2
M, g mol^{-1}	912.43	1045.30	2091.76
Crystal system	Orthorhombic	Triclinic	Triclinic
Space group	C cmb	P -1	P -1
a, Å	18.2370(2)	9.0240(2)	13.1630(2)
b, Å	21.3400(3)	15.6510(3)	14.2040(3)
c, Å	19.5450(3)	15.9190(4)	14.8460(3)
α, °		75.1480(10)	111.1180(10)
β, °		80.1430(10)	115.5180(10)
γ, °		77.2800(10)	97.725(2)
Z	8	2	1
V, Å^3	7606.48(18)	2104.11(8)	2194.06(7)
D_{calcd}, g cm^{-3}	1.594	1.650	1.583
μ, mm^{-1}	0.603	1.134	0.925
Crystal size (mm^3)	0.32 x 0.25 x 0.20	0.25 x 0.10 x 0.05	0.23 x 0.23 x 0.20
Reflections collected	53306	32820	32132
Unique reflections (R_{int})	3995(0.0781)	8594(0.1244)	10016(0.0774)
Max./min. transmission	0.8888/0.8303	0.9455/0.7647	0.8324/0.8107
Goodness-of-fit on F^2	1.014	1.081	1.034
R values [$I < 2\sigma(I_0)$]	$R1$ = 0.0447 $wR2$ = 0.1088	$R1$ = 0.0605 $wR2$ = 0.1482	$R1$ = 0.0542 $wR2$ = 0.1036
R values, all data	$R1$ = 0.0550 $wR2$ = 0.1145	$R1$ = 0.0901 $wR2$ = 0.1629	$R1$ = 0.1044 $wR2$ = 0.1204

*Atomic coordinates, equivalent isotropic displacement parameters, bond lengths and bond angles for all the complexes are collected in the supplementary CD.

Acknowledgements

This thesis was completed under the supervision of Prof. Peter G. Edwards. I sincerely appreciate his instructions, not only on chemistry but English and other aspects, and financial support throughout the three years study.

Grateful thanks are also due to Dr Paul D. Newman for valuable advice and assistance on daily laboratory work and proof-checking.

I would also like to thank Dr Angelo J. Amoroso for his help in electrochemistry and kind encouragements in 6 monthly interviews with Dr Ian A. Fallis. I thank Dr Abdul Malik and Dr Li-ling Ooi for crystallography, Prof. Andrew Harrison (University of Edinburgh) for magnetic susceptibility measurements, John for help with the safety issues, Rob for technical assistance on NMR spectroscopy, Sham and Robin for the Mass spectra, Gary and Stephen for organizing the chemicals, Alun for checking the pump and not least, Ricky for making the glassware.

Thanks to all my colleagues in Lab. 2.91 during the memorable three years including Andy, Dongmei, Julia, Eli, Becky, Adam, Kate, Chris, Sultan, Dan, Martie, Abdulla, Sudantha, Rajika, Gayani, Thusith, Peter, Andrea and Mark.